



Norwegian University of  
Science and Technology

# Characterization of Early Triassic Griesbachian intervals from wellbore cores 6611/09-U-01 and 6611/09-U-02 in the Helgeland basin, offshore Mid- Norway

**Karen Margrete Lie Christensen**

Natural Resources Management

Submission date: June 2018

Supervisor: Arve Næss, IGP

Co-supervisor: Maarten Felix, IGB

Norwegian University of Science and Technology  
Department of Geoscience and Petroleum



## Abstract

Cores 6611/09-U-01 and 6611/09-U-02 from the Helgeland basin cover a 750-metre-thick succession of marine sandstone, turbidites and shales. The upper 400 metres of the drilled cores are dated as the lower Triassic and referred to as the Griesbachian interval. The Griesbachian interval is the focus of interest in this thesis.

Sedimentological analyses from the Griesbachian interval in core 6611/09-U-01 and 6611/09-U-02 were used to identify the variability of lithofacies, depositional elements and the depositional environment at the time of deposition. A sedimentological description was made, and 24 thin sections were analyzed. 6 lithofacies and 4 facies associations were made based on the observations from the sedimentological log and the thin sections. From the lithofacies interpreted, 4 facies associations were described all with different depositional processes: debris flow, turbidity current, transitional flow and hemipelagic settling.

Evaporitic intervals were observed in both core 6611/09-U-01 and 6611/09-U-02. Three models are proposed for interpreting the depositional process of the gypsum interval: sabkha environment, transportation and recrystallization. Based on thin sections and core observations the most favoured model with recrystallization of evaporitic sediment is proposed.

Statistical analysis based on observed thicknesses of facies association beds in core 6611/09-U-01 and 6611/09-U-02 were performed to look at the thickness distributions through the core. Correlation of core 6611/09-U-01 and 6611/09-U-02 with regards to the evaporitic gypsum and a conceptual depositional model were carried out based on the sedimentological description, the facies associations interpretation and the statistical analysis. The conceptual depositional model for the Helgeland basin was proposed by a small-scale submarine fan system stacked in an aggradation pattern with sediment input by several feeder channels from east to west.

The result of this study is an integrated data analysis and facies model which represents the paleoenvironment within the deposition of the Griesbachian interval in the Helgeland Basin.

## Acknowledgements

I would like to express my gratitude to my main supervisor Arve Næss. Without his open mind to discuss various interpretations, keen eye and patient to guide me through this challenge, this thesis would not have been possible. Thank you for taking me through a fun and challenging period and for including me in two of Equinor's trips to Stavanger and Dora.

I will also direct a big thank to my co-supervisor Maarten Felix for challenging me in sedimentological interpretation and for reading correction on my thesis. To Atle Mørk for guidance with the cores and for preparation of thin sections and to Mai-Britt Mørk for guidance of thin section analysis.

Last but not least I will thank my partner Alexander Strand for being there for me through this chapter of my life.

Trondheim, June 2018

Karen Christensen

## Table of content

Abstract .....	1
Acknowledgements .....	2
List of figures .....	5
1 Introduction.....	10
1.1 Aim of study .....	11
1.2 Study Area .....	12
1.2.1 Previous work.....	13
1.3 Methodology.....	14
1.3.1 Sedimentological core description .....	14
1.3.2 Thin sections .....	16
1.3.3 Correlation.....	17
2 Geological Framework.....	18
2.1 Structural framework of Mid-Norway.....	18
2.1.1 Early Phanerozoic .....	18
2.1.2 Carboniferous .....	18
2.1.3 Permian.....	20
2.1.4 Triassic .....	22
2.1.5 Jurassic .....	23
2.1.6 Cretaceous .....	24
2.1.7 Cenozoic.....	24
2.2 The Trøndelag Platform - Helgeland Basin.....	25
2.2.1 Permian deposits .....	26
2.2.2 Triassic deposits .....	26
2.3 Flow Processes and definitions.....	28
2.3.1 Turbidity currents .....	28
2.3.2 Debris flow .....	30
2.3.3 Transitional flows.....	31
2.3.4 Pelagic and hemipelagic deposition .....	32
2.4 Submarine fan models .....	33
3 Petrography .....	35
3.1 Introduction .....	35
3.1.1 Sandstone lithology .....	36

3.1.2	Siltstone and clay lithology .....	36
3.1.3	Matrix lithology.....	36
3.1.4	Gypsum lithology .....	37
4	Facies description and interpretation .....	40
4.1	Lithofacies .....	40
4.1.1	Clean fining up sandstone (Sst1).....	40
4.1.2	Fining up sandstone with mud clasts (Sst2).....	41
4.1.3	Fining up sandstone with current ripples (Sst3).....	41
4.1.4	Unsorted sandstone (Ds1) .....	42
4.1.5	Patchy sandstone (Ds2) .....	42
4.1.6	Laminated mudstone (Mm/Fa5).....	43
4.2	Facies associations.....	50
4.2.1	Debrite facies association (Fa1) .....	50
4.2.2	Turbidite facies association (Fa2) .....	54
4.2.3	Transitional facies association (Fa3).....	57
4.2.4	Heterolithic facies association (Fa4) .....	60
5	Depositional model .....	64
5.1	Introduction .....	64
5.2	Thickness variations .....	64
5.2.1	6611/09-U-01 .....	65
5.2.2	6611/09-U-02 .....	70
5.3	Correlation .....	74
5.3.1	Interpretation of gypsum .....	74
5.3.2	Correlation based on facies associations .....	78
5.3.3	Correlation based on the sedimentary logs.....	80
5.4	Conceptual model .....	83
5.4.1	Deep-marine system .....	84
5.4.2	Conceptual model for the Helgeland basin .....	86
6	Conclusions.....	89
7	References.....	91
8	Appendix.....	94

## List of figures

Figure 1.1: Main structural elements in NW65 offshore Mid-Norway retrieved from NPD, 2014.....	11
Figure 1.2: Left: Stratigraphic map of the eastern Mid-Norwegian Sea with the Trøndelag Platform and Helgeland Basin. Shallow stratigraphic boreholes 6611/09-U-01 and 6611/09-U-02 in red. Right: Sedimentological log of the Griesbachian interval with a 60-metre overlap. Modified from Bugge et al. (2002). .....	12
Figure 1.3: Classification regarding the degree of sorting (Compton, 1962). .....	16
Figure 1.4: Terminology of degree of rounding of detrital grains (Powers, 1953).....	16
Figure 2.1: Regional paleogeography of the Norwegian Sea during the Early Carboniferous. Red area shows parallel basins. Modified from Ramberg (2008).....	19
Figure 2.2: Regional paleogeography and the most important sediment types during the Mid Carboniferous. The highlighted region in red shows the area of interest. Modified from Ramberg (2008).....	20
Figure 2.3: Regional paleogeography during Late Permian. Highlighted in red is the area of interest. Modified from Ramberg (2008) .....	21
Figure 2.4: Schematic illustration of the Late Permian- Early Triassic basin between Norway and Greenland. Modified from Bugge et al. (2002).....	21
Figure 2.5: Regional paleogeography during Triassic. (A) Middle Triassic. (B) Late Triassic. (C) Latest Triassic. Modified from (Ramberg, 2008). .....	22
Figure 2.6: Structural elements of the Norwegian sea during the Jurassic (Ramberg, 2008)..	23
Figure 2.7: Interpreted seismic line containing the locations of the two boreholes. As seen on the seismic the deposits of the Helgeland basin dip towards the NW. From Bugge et al. (2002). .....	25
Figure 2.8: Sedimentological log of the Griesbachian interval from core 6611/09-U-01 and 6611/09-U-02. Bugge et al., (2002). .....	27
Figure 2.9: Schematic illustration of a turbidity current. Modified from Meiburg and Kneller (2010). .....	28
Figure 2.10: Turbidite deposition, retrieved from Allen (1985) .....	29
Figure 2.11: Debris deposit. From Stow (1985).....	30
Figure 2.12: Sandy debris flow process. By Allen. (1985). .....	30
Figure 2.13. Transitional flow process by Felix and Peakall (2006). .....	31

Figure 2.14: Principal features of a stepped deep-water system. Two mechanisms to generate accommodation on the slope are shown: generation of a slope step due to tectonic faulting and above a scar of a mass transport complex (MTC). From Spsychala et al. (2015). ..... 33

Figure 3.1: Thin section from a coarse sandstone dominated by quartz with some feldspar showing secondary porosity. Thin section taken from Core 6611/09-U-01 at depth 195.83m. The blue arrow show the upright way. Left: Microscope photo in cross-polarized light. Right: Microscope photo in plane-polarized light..... 37

Figure 3.2: Thin section from an interpreted heterolith facies association taken from Core 6611/09-U-01 at depth 128.79m. The heterolith facies association shown here is composed of fined grained sand on top and silt at base. The blue arrow show the upright way. Left: Microscope photo in cross-polarized light. Right: Microscope photo in plane-polarized light. .... 38

Figure 3.3: Thin section from a transitional facies association with a laminated sole pointing up, interpreted as Facies association 3a. The blue arrow show the upright way. The thin section is taken from core 6611/09-U-01, at depth 50.7m. Left: Microscope photo in cross-polarized light. Right: Microscope photo in plane-polarized light. .... 38

Figure 3.4: Thin section from a mixed sandstone/matrix interpreted as Facies association 1. The thin section is taken from core 6611/09-U-02, at depth 42.42m. The blue arrow show the upright way. Left: Microscope photo in cross-polarized light. Right: Microscope photo in plane-polarized light..... 39

Figure 3.5: Thin section from a gypsum bed interpreted as Facies association 4b. the layer is composed of two beds shown by the orange arrow. The blue arrow show the upright way. The thin section is taken from core 6611/09-U-01, at depth 64.45m. Left: Microscope photo in cross-polarized light. Right: Microscope photo in plane-polarized light. .... 39

Figure 4.1: Lithofacies clean fining up sandstone (Sst1). The red lines indicates base and top of the lithofacies. A) Clean medium coarse sandstone fining up into fine sand from core 6611/09-U-01. B) Coarse sandstone fining up into medium sandstone from core 6611/09-U-02. .... 44

Figure 4.2: Fining up sandstone with clasts (Sst2). The red lines indicates base and top of the lithofacies. A) Clean medium coarse sandstone fining up into fine sand with mud clast at top, from core 6611/09-U-01. B) Coarse sandstone fining up into medium sandstone from core 6611/09-U-02. Horizontally aligned mud clasts in middle and on top. .... 45

Figure 4.3: Fining up sandstone with current ripples (Sst3). The red lines indicates base and top of the lithofacies. A) Fine sandstone in horizontal lamination at base and current ripples



at top from core 6611/09-U-02. B) Very fine sandstone with lamination at base and current ripples at top from core 6611/09-U-01.....	46
Figure 4.4: Unsorted sandstone (Ds1). The red lines indicates base and top of the lithofacies.	
A) Mixed sandstone and mud with significant shearing, from core 6611/09-U-01. B) Coarse sandstone and mud in chaotic mix with shearing and sand patches from core 6611/09-U-02.47	
Figure 4.5: Patchy sandstone (Ds2). The red lines indicates base and top of the lithofacies.	
A) Medium coarse sandstone fining up into fine sand with sand patches at top, from core 6611/09-U-01. B) Coarse sandstone fining up into medium sandstone with sand patches through the bed, from core 6611/09-U-02.....	48
Figure 4.6: Laminated mudstone (Mm). The red lines indicates base and top of the lithofacies.	
A) Dark black mudstone in cm thick layers from core 6611/09-U-02. B) Grey cm thick layers of mudstone from core 6611/09-U-01.....	49
Figure 4.7: Histogram showing thickness distribution of Fa1, core 6611/09-U-01.....	51
Figure 4.8: Histogram showing thickness distribution of Fa1, core 6611/09-U-02.....	51
Figure 4.9: Debrite facies association. The red lines indicates base and top (if observed) of lithofacies. A) Debrite with significant mud shearing and clasts (Core 6611/09-U-01) B) Debrite with unsorted matrix and mud streaks (Core 6611/09-U-01).....	53
Figure 4.10: Histogram showing thickness distribution of Fa2, core 6611/09-U-01.....	54
Figure 4.11: Histogram showing thickness distribution of Fa2, core 6611/09-U-02.....	55
Figure 4.12: Turbidite facies association. The red lines indicates base and top (if observed) of lithofacies. A) Fining up turbidite from medium to very fine sand (Core 6611/09-U-02, depth 17.1m). B) Fining up turbidite from conglomerate to medium coarse sand (Core 6611/09-U-02, depth 275.0m). C) Fining up turbidite from fine sand to very-fine sand (Core 6611/09-U-01, depth 103.65m).....	56
Figure 4.13: Histogram showing thickness distribution of Fa3, core 6611/09-U-01.....	57
Figure 4.14: Histogram showing thickness distribution of Fa3, core 6611/09-U-02.....	58
Figure 4.15: Transitional facies association. The red lines indicates base and top (if observed) of lithofacies. A) transitional facies association with a thin turbidite base, overlain by a patchy sandstone (Core 6611/09-U-01, depth 50-7m). B) Fining up turbidite overlain by debrite without mud on top (Core 6611/09-U-01, depth 22.2m). C) Fining up turbidite overlain by debrite and mud (Core 6611/09-U-02, depth 131.5m).....	59
Figure 4.16: Histogram showing thickness distribution of Fa4, core 6611/09-U-01.....	61
Figure 4.17: Histogram showing thickness distribution of Fa4, core 6611/09-U-02.....	61

Figure 4.18: Heterolithic facies association. The red lines indicates base and top (if observed) of lithofacies. A) Thin bedded sand, silt, clay and gypsum (Core 6611/09-U-02, depth 64.3m). B) Thick bedded sand, silt and clay (Core 6611/09-U-02, depth 129.65m). C) Thin bedded sand, silt and clay (Core 6611/09-U-02, depth 131.4m). ..... 63

Figure 5.1: Left: Histogram showing number of observations for depth intervals of 13m for Fa1- Core 6611/09-U-01. Right: Scatter plot showing thickness variation vs depth for Fa1- Core 6611/09-U-01. .... 65

Figure 5.2: Left: Histogram showing number of observations for depth intervals of 13m for Fa2- Core 6611/09-U-01. Right: Scatter plot showing thickness variation vs depth for Fa2- Core 6611/09-U-0. .... 66

Figure 5.3: Left: Histogram showing number of observations for depth intervals of 13m for Fa3- Core 6611/09-U-01. Right: Scatter plot showing thickness variation vs depth for Fa3- Core 6611/09-U-01. .... 66

Figure 5.4: Left: Histogram showing number of observations for depth intervals of 13m for Fa4- Core 6611/09-U-01. Right: Scatter plot showing thickness variation vs depth for Fa4- Core 6611/09-U-01. .... 67

Figure 5.5: Left: Histogram showing number of observations for depth intervals of 13m for lithofacies Mm- Core 6611/09-U-01. Right: Scatter plot showing thickness variation vs depth for lithofacies Mm- Core 6611/09-U-01 ..... 67

Figure 5.6: Distributions of facies associations through core 6611/09-U-01 calculated as percentages of each facies association. .... 69

Figure 5.7: Left: Histogram showing number of observations for depth intervals of 13m for Fa1- Core 6611/09-U-02. Right: Scatter plot showing thickness variation vs depth for Fa1- Core 6611/09-U-02. .... 70

Figure 5.8: Left: Histogram showing number of observations for depth intervals of 13m for Fa2- Core 6611/09-U-02. Right: Scatter plot showing thickness variation vs depth for Fa2- Core 6611/09-U-02. .... 70

Figure 5.9: Left: Histogram showing number of observations for depth intervals of 13m for Fa3- Core 6611/09-U-02. Right: Scatter plot showing thickness variation vs depth for Fa3- Core 6611/09-U-02. .... 71

Figure 5.10: Left: Histogram showing number of observations for depth intervals of 13m for Fa4- Core 6611/09-U-02. Right: Scatter plot showing thickness variation vs depth for Fa4- Core 6611/09-U-02. .... 71

Figure 5.11: Left: Histogram showing number of observations for depth intervals of 13m for Fa5- Core 6611/09-U-02. Right: Scatter plot showing thickness variation vs depth for Fa5- Core 6611/09-U-02. ....	72
Figure 5.12: Distributions of facies associations through core 6611/09-U-02 calculated as percentages of each facies association. ....	73
Figure 5.13: Core photos of core 6611/09-U-01 with gypsum intervals in red. ....	76
Figure 5.14: Core photo of core 6611/09-U-02 with gypsum interval marked in red. ....	77
Figure 5.15: Correlation of core 6611/09-U-01 and 6611/09-U-02 based on the percentage of each facies association observed. ....	79
Figure 5.16: Correlation of core 6611/09-U-01 and 6611/09-U-02 based on interpreted facies associations. Scale 1:500. Black lines show correlation lines.....	81
Figure 5.17: Correlation based on sedimentological log. Area in red show sedimentological log in scale 1:100.....	82
Figure 5.18:Schematic model of a deep-marine system, Modified from Meiburg and Kneller (2010). ....	84
Figure 5.19: Different turbidite deposits with interpreted depositional environment. From Pickering et al. (2016). ....	85
Figure 5.21: Vertical section of interpreted stacking pattern from core 6611/09-U-01 and 6611/09-U-01 on a 1:100 scale. Red box shows outlined area. ....	87
Figure 5.20:Vertical section of interpreted stacking pattern from core 6611/09-U-01 and 6611/09-U-01 on a 1:500 scale. ....	87
Figure 5.22: Illustration of a proposed conceptual depositional model for the Helgeland basin. Well 6611/09-U-01 and 6611/09-U-02 indicated with black. Red line indicates vertical section.....	88

# 1 Introduction

The Trøndelag platform is situated in the Norwegian Sea area and is one of the major structural elements off central Norway. It includes the Helgeland Basin, Frøya High, Froan Basin, Ylvingen Fault zone and Vega high (Figure 1.1). IKU (now SINTEF Petroleum Research) drilled the two wells 6611/09-U-01 and 6611/09-U-02 in 1992 as part of the shallow stratigraphic drilling project from 1982 to 1993. The project mapped parts of the Norwegian continental shelf using shallow stratigraphic drilling to investigate outbound stratigraphic units on the seabed where the core material was untouched sediment. They also used high-resolution shallow seismic and by drilling two wells at a short distance from each other they could examine the extent of the stratigraphy and facies development for a possible correlation (Bugge et al., 2002). In those two wells, cored intervals include Permian-Triassic succession measuring more than 750 m thick stratigraphy with oil-stained sandstone and mudstone with source rock potential correlatable to the oil prone Ravnefjeld formation on East-Greenland (Bugge et al., 2002). The investigated interval in this master thesis is lower Triassic, Griesbachian of approximately 460m of drilled cores. Not many studies from this area have been published in the open literature, and there still are many aspects regarding the Permian-Triassic development in this area that have not been addressed. Therefore, there is a motivation for working scientifically with Triassic and Permian deposits as there are few core samples from these intervals. Petroleum industry applications include new play models and improved knowledge about the Permian- Triassic depositional systems, so this study was conducted to get a better understanding of the sedimentology from Permian-Triassic in the Helgeland Basin.

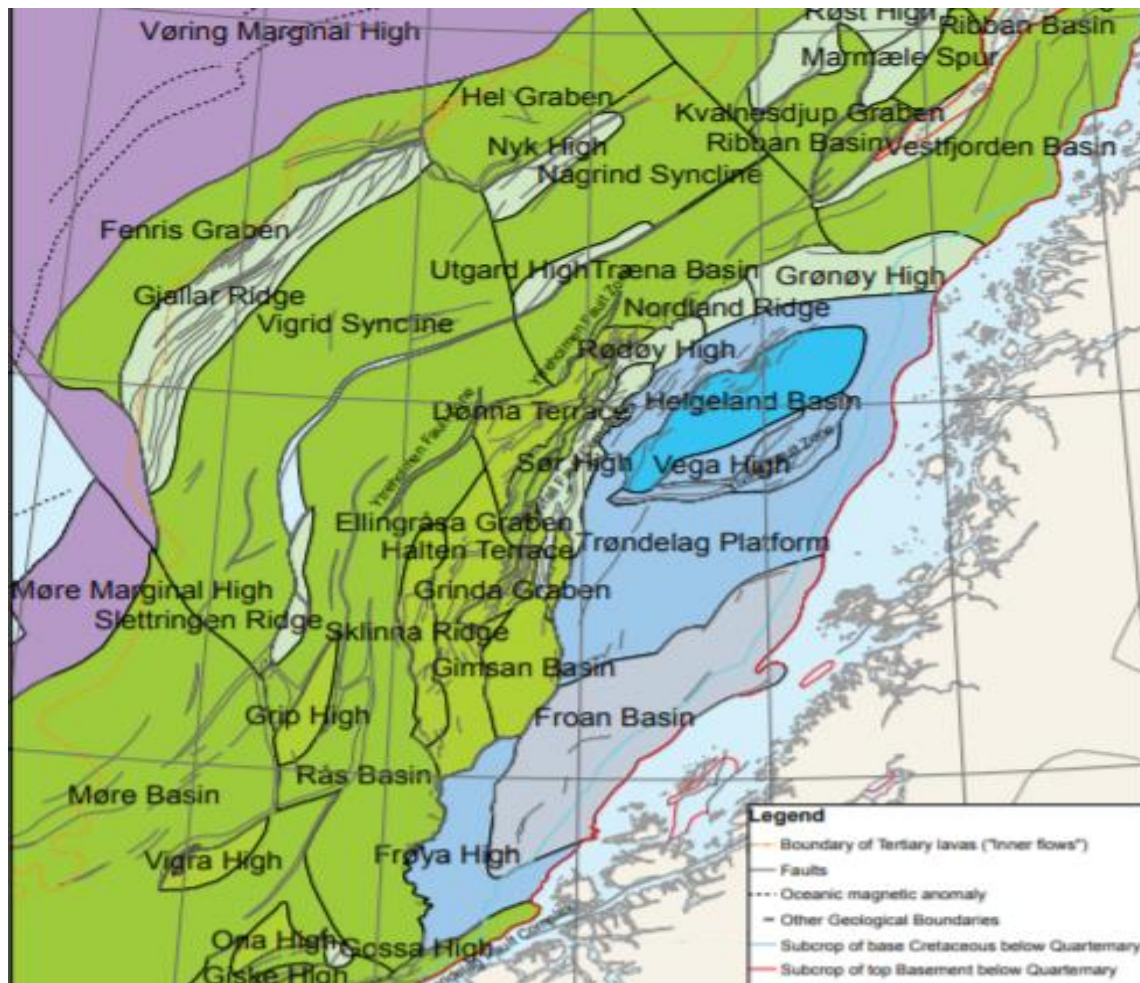


Figure 1.1: Main structural elements in NW65 offshore Mid-Norway retrieved from NPD, 2014.

## 1.1 Aim of study

Objective: the objective of this work is the development and discussion of a conceptual depositional model for the Griesbachian interval in core 6611/09-U-01 and 6611/09-U-02.

The aim for this thesis was to provide a detailed sedimentological analysis of wells 6611/09-U-01 and 6611/09-U-02 in the Helgeland basin. A sedimentological approach with lithofacies and facies associations has been chosen to provide a better understanding of the sedimentological and geological processes at the time of deposition. The major focus was to provide a conceptual depositional model for the Griesbachian interval in the Helgeland Basin. This objective was achieved by detailed core logging and qualitative analysis of the sedimentological variations in the Griesbachian.

## 1.2 Study Area

The study area for this thesis is situated in the Norwegian Sea on the passive continental margin offshore mid-Norway and is referred to as the Helgeland Basin. The Helgeland Basin is part of the Trøndelag platform situated east of the Halten Terrace and the Nordland Ridge. Well locations for the cores 6611/09-U-01 and 6611/09-U-02 are shown in Figure 1.2.

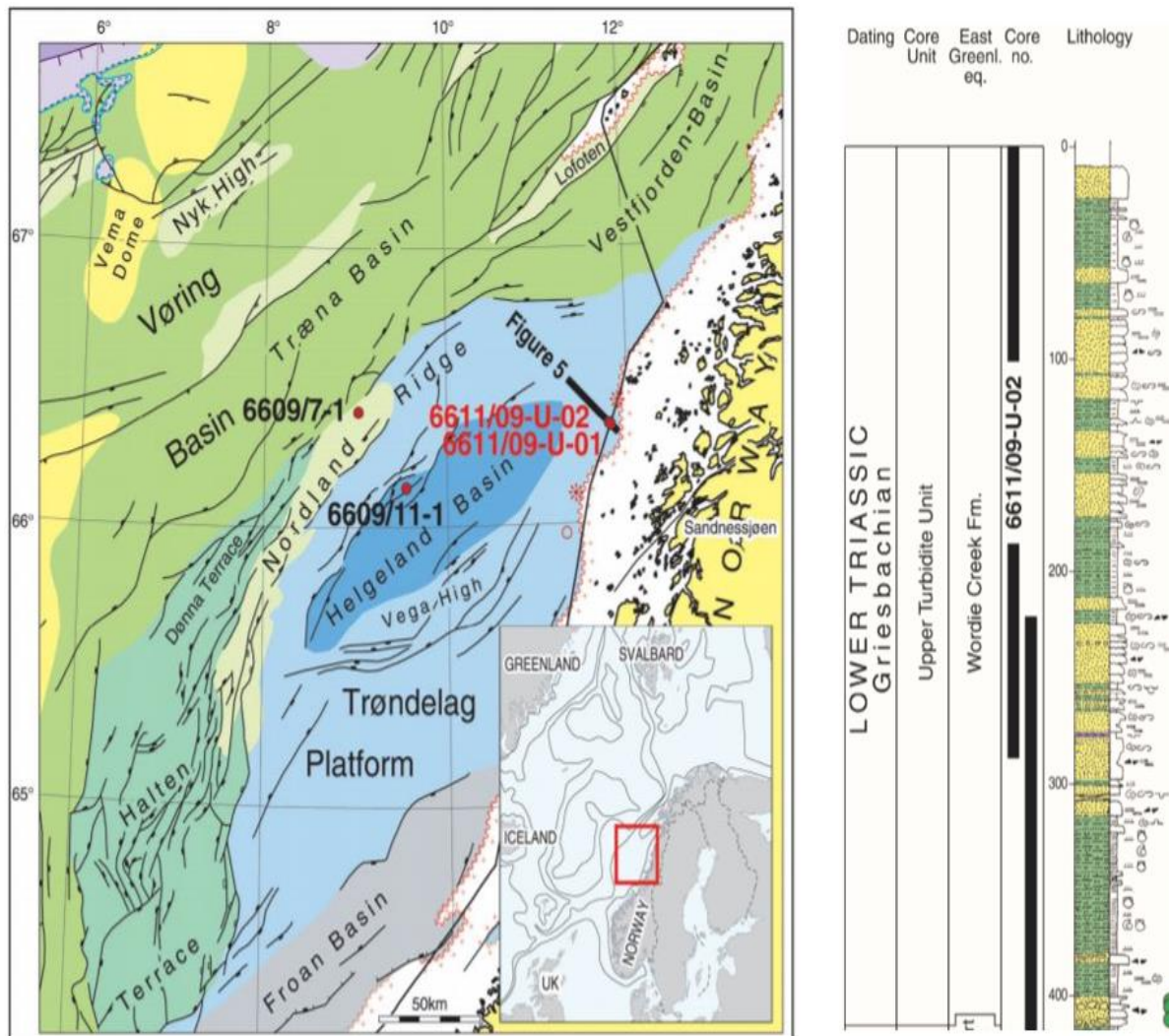


Figure 1.2: Left: Stratigraphic map of the eastern Mid-Norwegian Sea with the Trøndelag Platform and Helgeland Basin. Shallow stratigraphic boreholes 6611/09-U-01 and 6611/09-U-02 in red. Right: Sedimentological log of the Griesbachian interval with a 60-metre overlap. Modified from Bugge et al. (2002).

### 1.2.1 Previous work

The 6611/09-U-01 and 6611/09-U-2 wells are documented in Bugge et al. (2002). A brief description of the lower Triassic interval is included. The paper defines interpreted sedimentary intervals and shows a sedimentary log and the gamma-ray, sonic and neutron readings. Reservoir quality, provenance, dating, source potential and correlation are also discussed in brief discussion.

Two other publications address aspects of the Permian-Triassic succession from the two wells.

Müller et al. (2005) address the basin infill history and paleogeography on the Mid-Norwegian shelf. A new sedimentological subdivision of the Triassic succession on the Mid-Norwegian shelf is suggested, based on a detailed facies analysis of cores like the 6611/09-U-01 and 6611/09-U-02 cores. Müller et al. (2005) integrate seismic interpretation with facies analysis for discussion of the timing of tectonic events and their influence on sedimentary architecture. Investigation of the tectonic sedimentary history of the Mid-Norwegian shelf and East-Greenland is discussed to make an overall model of the basin infill history and paleogeography of the region in Permian-Triassic time.

Hochuli et al. (2010) focus on the palynological record from the Mid-Norwegian with focus on cores 6611/09-U-01 and -02. Hochuli et al. (2010) interpreted the Upper Permian section as equivalent to the Schuchert Dal Formation based on palynomorphs while the Wordie Creek formation could be assigned to the Early Triassic (Griesbachian). Data from the Griesbachian show that in some areas, various plant assemblages survived the Permian-Triassic mass extinction. From the cores 6611/09-U-01 and -02 Hochuli et al (2010) only found minor changes in the palynological assemblage from Permian to Triassic with disappearance of Vittatina (group of Pteridosperm pollen) and appearance of the Aratrisporites group. Analysis from the Griesbachian succession shows distinct changes in varying abundance of cavate spores and bisaccata pollen interpreted as reflecting variations in humidity.

### 1.3 Methodology

This study is based on the following data:

- Sedimentological core descriptions of wells 6611/09-U-01 and 6611/09-U-02
- Petrographic descriptions of selected thin sections from various facies
- Official published core photos from the Norwegian Petroleum Directorate
- Earlier published papers

#### 1.3.1 Sedimentological core description

The core description took place at Dora core storage facilities with core logging and thickness measurements. The two wells 6611/09-U-01 and 6611/09-U-02 have cored intervals of 560m and 280m respectively with a 60-metre stratigraphic overlap between 220m and 280m in the two cores as seen in Figure 1.2. The cores were described from the display cores at a 1:20 scale with sedimentary description containing textures, bed contacts, trace fossils and other observations noted on the log. A summary log at scale 1:200 was redrawn from the 1:20 log for overview and a summary log at a scale 1:500 was redrawn from the 1:200 log for correlation.

Data from the core description are presented in the section on facies and facies associations, and the redrawn 1:20 and 1:200 sedimentological logs are presented in appendix 1 and appendix 2. Photos used to illustrate the interpreted facies and environments are taken from the NPD database ([www.npd.no](http://www.npd.no)) supplemented with the author's own photos taken with a high-resolution digital camera. Thickness measurements were analysed and applied to study trends in thicknesses from the bottom to the top. This is limited to a interval from 180m – 280m for well 6611/09-U-02 and from 220m – 320m for well 6611/09-U-01. Results are presented in section 6: Thickness measurements.

A number of lithofacies definitions is given in the literature. In this thesis the definition by Walker (2006) is adopted where the lithofacies or facies is characterised by specific distinguishing features such as grain size or sedimentary structures, and it can be used for interpretation of depositional environment or processes (Walker, 2006). Based on Walker (2006), facies is a term that can be used in both a descriptive and interpretive sense. In this thesis the lithofacies is applied as a descriptive term in which one or more depositional processes are inferred.



Lithofacies or facies are gathered into a facies association (FA). A facies association is thought to be a genetically linked group of facies interpreted to have been deposited by one flow in the same environment (Walker, 2006). Since a facies association is a group of several individual facies they may be stacked vertically or interbedded randomly. Johannes Walther stated in 1894 that the vertical sequence of rocks could be used to interpret the environments and make a reasonable assumption to those environments used to be next to each other. In this thesis Walther's Law is taken into consideration when grouping the facies into facies associations by looking at the stacking pattern, the interpreted facies and other sedimentological core observations.

The facies described and presented in this thesis are primarily based on lithology, sedimentary structures, textures and colour variations. Due to lack of trace fossils, fossils is not taken into consideration when interpreting facies.

#### *1.3.1.1 Uncertainties and sources of error*

Interpretations of the depositional environment and depositional processes are based on the description of the cores and will therefore be prone to individual interpretations and uncertainties associated with these. When core 6611/09-U-01 and 6611/09-U-02 were cut in two, the one half were prepared with lack and used as a display core, while the other half were boxed away without any preparation. The prepared display cores are lacquered which makes it difficult to observe the true grain size and to feel the texture. In some places the cores are broken, missing or destroyed during cutting which makes it impossible to interpret the area. The unprepared core cut are boxed and stored away so these have been retrieved only for specific occasions and not for the whole core.

Beyond challenges related to poor core quality there will always be some degree of uncertainty in sedimentological core interpretation. During core logging, interpretation of the different facies has been challenging because many facies are similar and often grade into each other. In cases where distinction of facies has been specifically challenging, these have been marked in the log with two facies. In the statistical analysis (described in section 4.2 and 5) some decisions must be taken as only one facies can be used.

### 1.3.2 Thin sections

A total of 11 thin sections from the 6611/09-U-01 core and 20 thin sections from the 6611/09-U-02 core were used to analyse the mineralogy and diagenetic processes observed in the cores and to support the lithofacies description. All the thin section were studied under plane polarized light (ppl) and cross polarized light (xpl), to observe mineralogy, lithology, structures, average grain size, grain shape and sorting. The degree of sorting was decided based on the classification scheme of Compton (1962) (Figure 1.3) while the degree of rounding of detrital grains was described with terminology developed by Powers (1953) (Figure 1.4). Photos used to illustrate the facies were taken through the microscope lens using a high-resolution camera. Thin section observations are described in appendix 3.

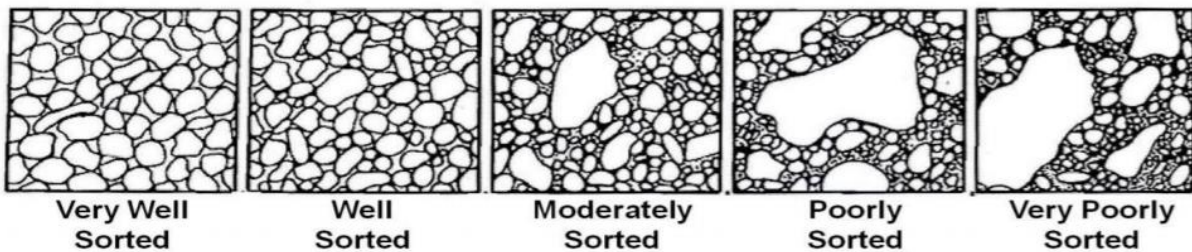


Figure 1.3: Classification regarding the degree of sorting (Compton, 1962).

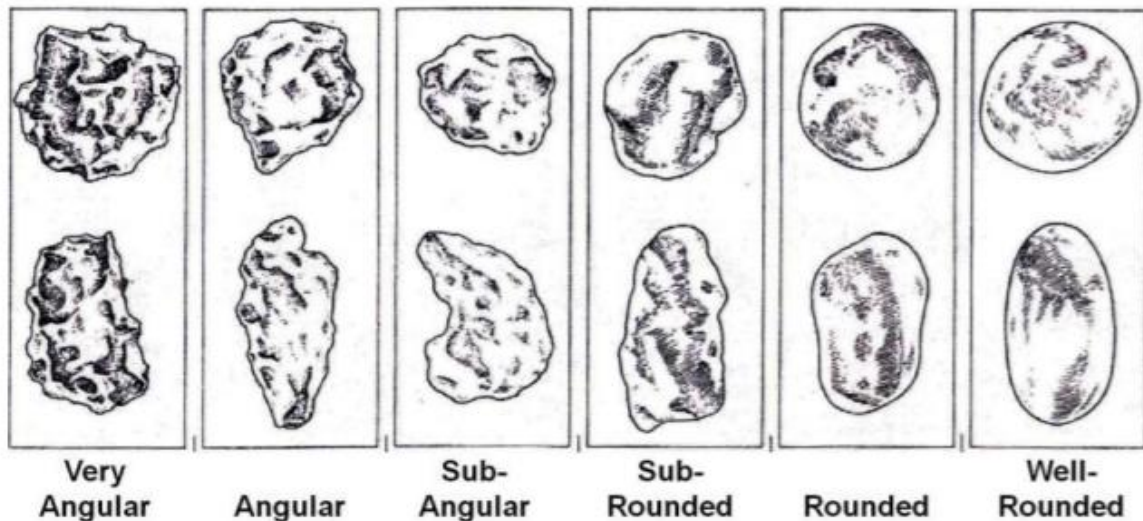


Figure 1.4: Terminology of degree of rounding of detrital grains (Powers, 1953)

### 1.3.3 Correlation

The two IKU wells drilled in 1992 from the Helgeland Basin were drilled 1200 metres apart with an overlap of 60 metres. The correlation was done by comparing the 1:200 sedimentary logs and the cores for marker events and trends. In addition, statistical analysis of thickness variations was used for supporting the proposed correlation. A gypsum interval only occurring once in both cores is of special interest and is presented in further detail in the correlation section. In this thesis the correlation is based on lithostratigraphy where the classification of rock type is based on the mineralogy and the relation to rocks above and below.

## 2 Geological Framework

### 2.1 Structural framework of Mid-Norway

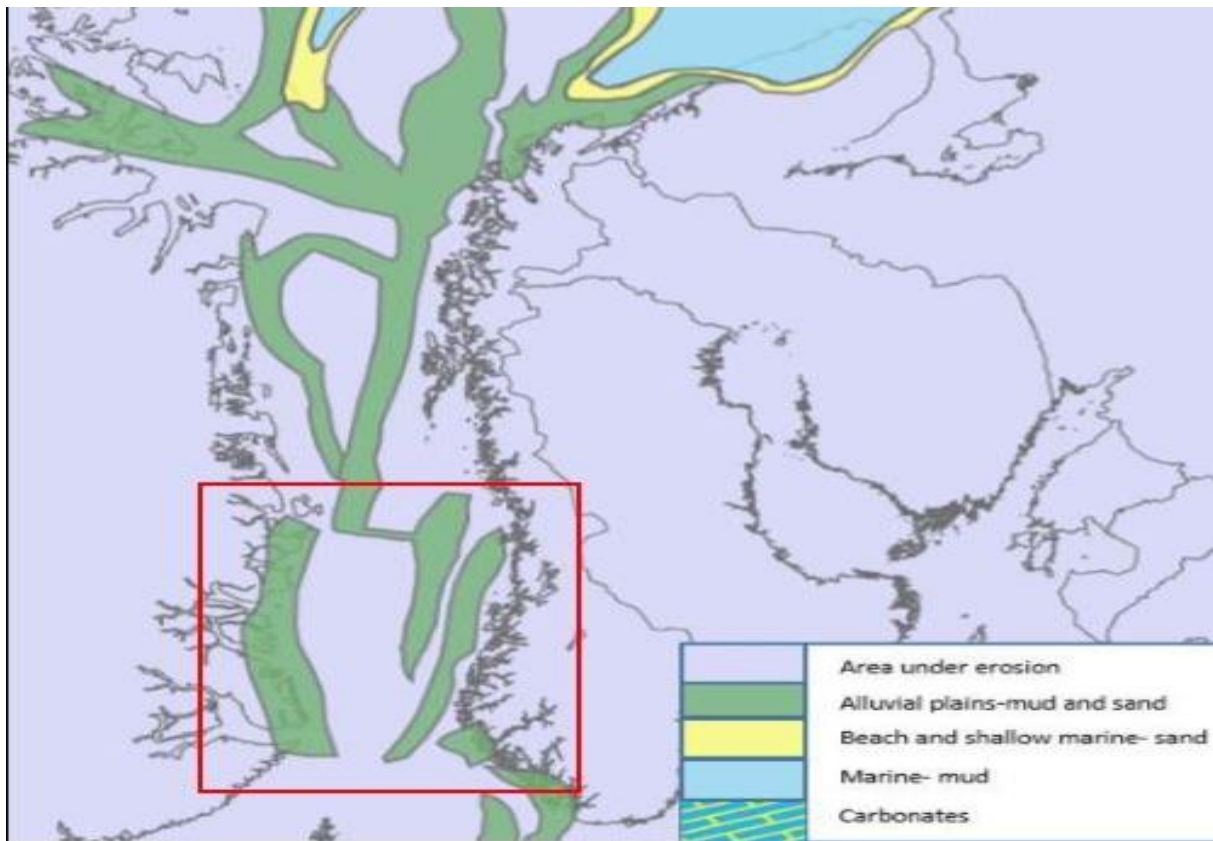
The Norwegian continental shelf extends from the central North Sea in the south to the Arctic Ocean north of Svalbard in the north and covers most of the continental margin of the Norwegian continental shelf from 62°N to 69°30' N (Brekke et al., 2001, Blystad et al., 1995). From the Early Devonian to the Eocene, the Norwegian continental shelf went from a phase of plate convergence and growth of continents to several phases dominated by tectonic rifting and continental break-up (Brekke et al., 2001).

#### 2.1.1 Early Phanerozoic

After several million years of continental collision and closing of the Iapetus ocean, the Caledonian Orogeny reached its climax during the Silurian- Early Devonian time, when the tectonism changed from compressional to extensional. The collisional climax affected the mountain belt with collapse, thinning of the lithosphere and, subsequently, repeated rifting (Mosar et al., 2002). The change in the tectonic stress led to the formation of small parallel basins (Ramberg, 2008).

#### 2.1.2 Carboniferous

Very little information is available from the Carboniferous on the shelf offshore Mid-Norway, but what is known is derived from shallow boreholes and correlation from exposures of East Greenland which at this time was situated close to Norway (Ramberg, 2008). During the Devonian period several areas were affected by uplift due to the compressional tectonics. These areas underwent intense erosion in the Early Carboniferous, which resulted in the filling of parallel basins (Figure 2.2) with Devonian sediments.



*Figure 2.1: Regional paleogeography of the Norwegian Sea during the Early Carboniferous. Red area shows parallel basins. Modified from Ramberg (2008).*

In the Mid-Carboniferous there is an abrupt climate change from humid to arid conditions, giving deposition of desert sand on the Trøndelag platform (Figure 2.2). These conditions continued into the Early Permian and affected the whole Norwegian Sea with erosion and removal of substantial amounts of strata from Devonian to Cambro-Silurian times in uplifted

areas. A deep seismic reflector observed in data from the Trøndelag Platform is believed to represent a major unconformity of Early-Mid-Triassic age. Correlation from the Norwegian Sea to East-Greenland suggests the age of the reflector to be Mid-Permian. The reflector can be interpreted as a period of deep erosion (Brekke & Riis, 1987; Bugge et al., 2002).

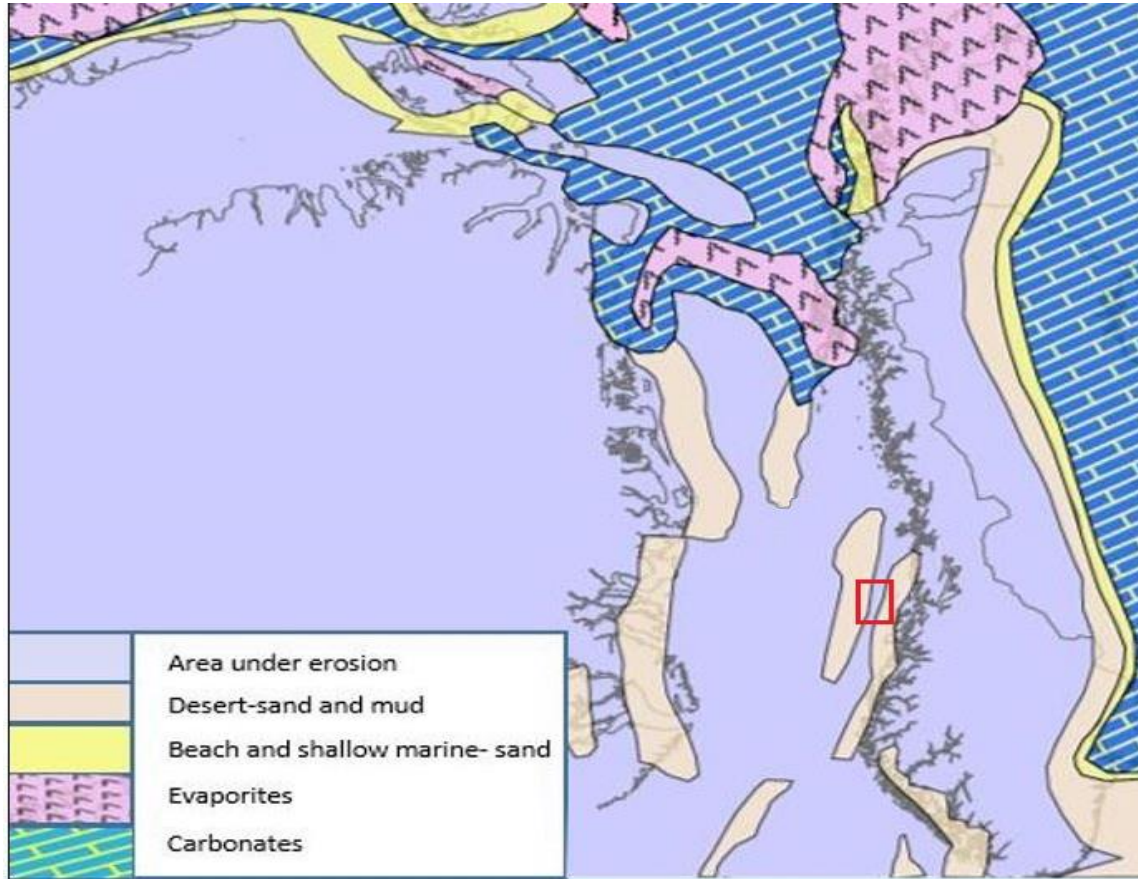


Figure 2.2: Regional paleogeography and the most important sediment types during the Mid Carboniferous. The highlighted region in red shows the area of interest. Modified from Ramberg (2008).

### 2.1.3 Permian

The major unconformity of Early-Mid-Triassic age can be correlated from East-Greenland mid-Permian time. The unconformity underwent faulting during the Late Permian, and a seaway in the present Norwegian Sea started to open.

During the Late Carboniferous to Early Permian a period of extensive tectonics started. Examples of this are found in East-Greenland where the tectonics lead to formation of half-grabens bounded by listric, basement-involved normal faults (Bugge et al., 2002; Bukovics and Ziegler, 1985).

There is no physical evidence from the Norwegian Sea, but Bukovics and Ziegler (1985) presumed that the Norwegian continental margin also experienced subsidence of half-grabens that became sites for accumulation of clastic sediment and carbonates (Figure 2.3).

The Permian crustal extension and subsidence continued into the Triassic, resulting in the creation of deep marine rift basins filled with marine sand and mud (Figure 2.4) (Nøttvedt et al., 2008).

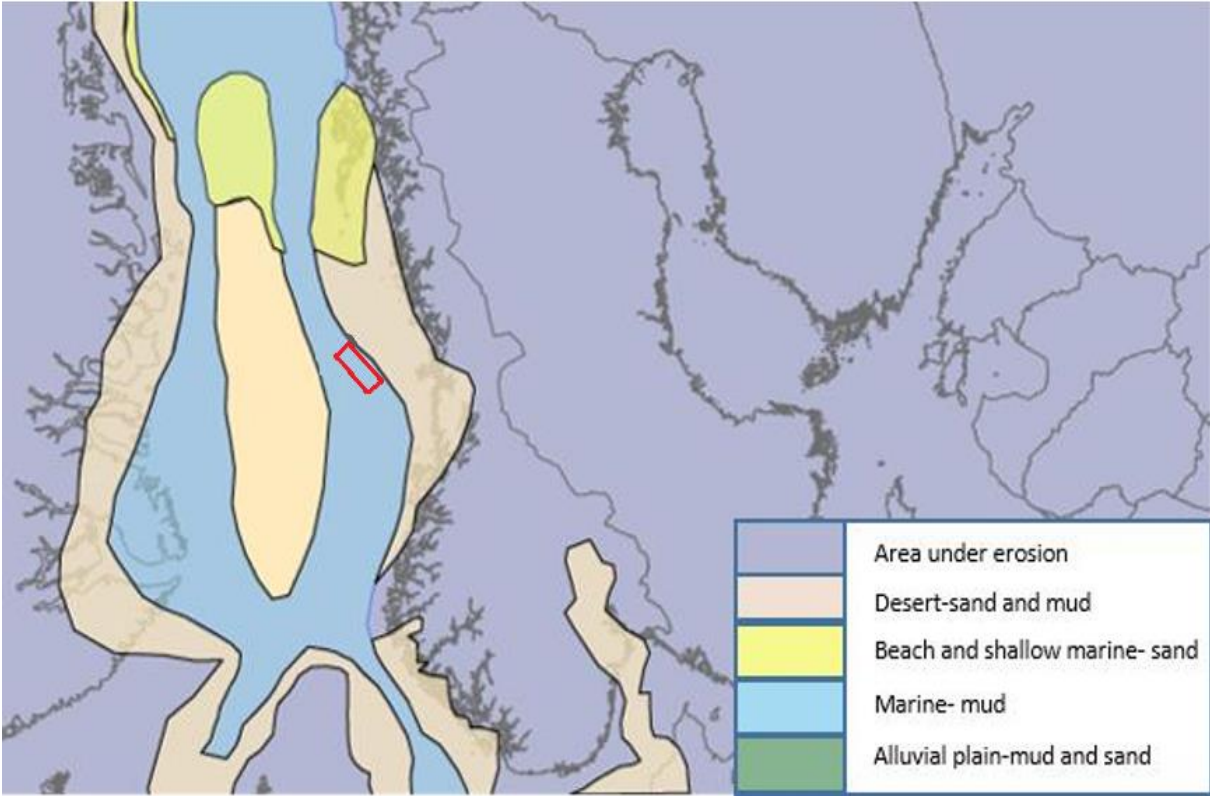
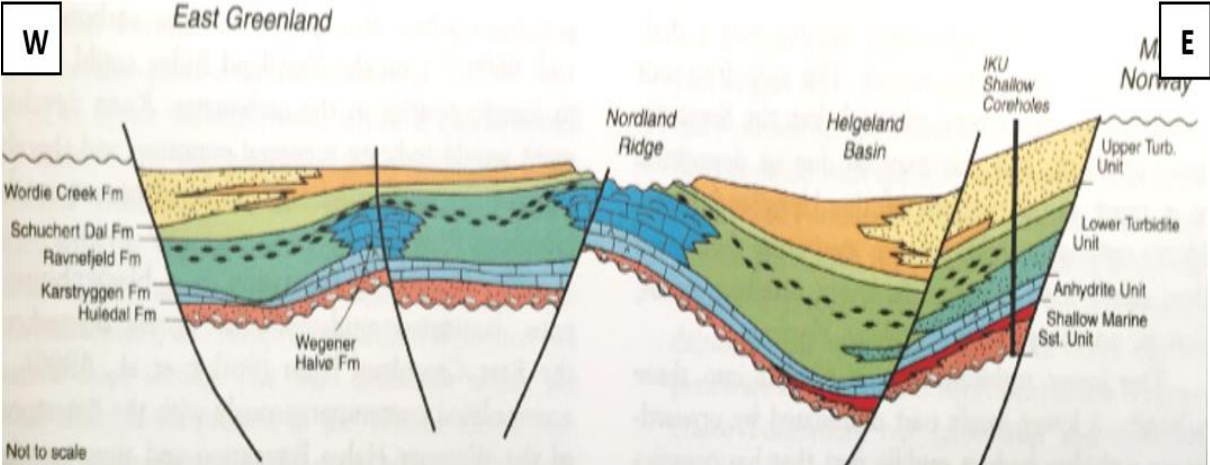


Figure 2.3: Regional paleogeography during Late Permian. Highlighted in red is the area of interest. Modified from Ramberg (2008)



Norway and Greenland. Modified from Bugge et al. (2002).

### 2.1.4 Triassic

The active rifting that started in the Permian lasted to the Early Triassic and ended in a deep rift basin between Norway and Greenland, marking the onset of the breakup of Pangaea (Nøttvedt et al., 2008). The active rifting also influenced the Helgeland Basin with subsidence of the basin (Brekke et al., 2001; Gowers and Lunde, 1984; Ramberg, 2008). The subsidence of the basin led to the development of the Helgeland Basin as an embayment with restricted water entry and deposition mainly by marine silts and clay, but also as thin turbiditic sands on the basin floor (Bugge et al., 2002). The Triassic sediments within the Trøndelag platform consist of a thick succession of continental red beds interbedded with two evaporite layers. The two evaporitic layers are interpreted as evidence for a marine transgression in the Mid-Triassic which were developed during later rifting episodes (Blystad et al., 1995; Bugge et al., 2002; Bukovics and Ziegler, 1985; Riis et al., 2014). Entering the earliest middle Triassic, the rift zone became less active and most of the marine basins became filled up with sediment, and broad alluvial plains were formed (Figure 2.5A). In the Middle to Late Triassic there was a new period of rifting, subsequently generating a new erosional unconformity. This rifting was more pronounced in the north and associated with an NNE fault trend east of the Frøya High and in the Froan Basin. At the same time the old Permian- Triassic rift basins became affected by subsidence which resulted in the Trøndelag Platform and the Halten terrace becoming parts of a large NS-trending subsiding basin (Brekke et al., 2001; Nøttvedt et al., 2008; Riis et al., 2014). During the Late Triassic the sea flooded the alluvial plains from the middle Triassic and a coastal and shallow marine environment appeared (Figure 2.5B).

At the same time the old Permian- Triassic rift basins became affected by subsidence which resulted in the Trøndelag Platform and the Halten terrace becoming parts of a large NS-trending subsiding basin (Brekke et al., 2001; Nøttvedt et al., 2008; Riis et al., 2014). During the Late Triassic the sea flooded the alluvial plains from the middle Triassic and a coastal and shallow marine environment appeared (Figure 2.5B).

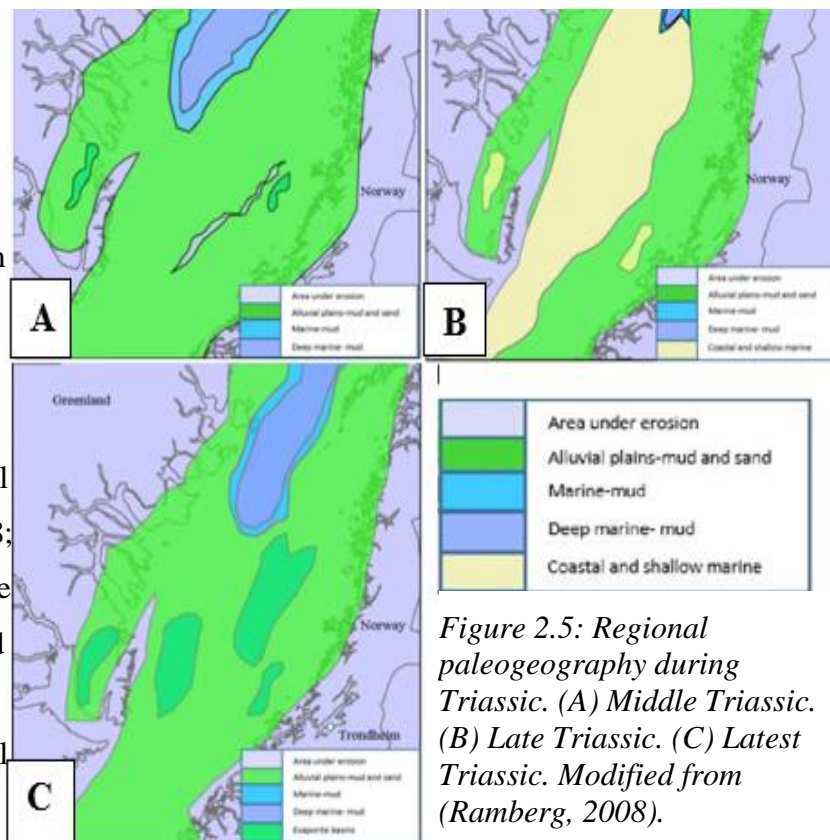


Figure 2.5: Regional paleogeography during Triassic. (A) Middle Triassic. (B) Late Triassic. (C) Latest Triassic. Modified from (Ramberg, 2008).



### 2.1.5 Jurassic

During the Early Jurassic the Norwegian Sea area was almost totally dominated by humid swamplands which resulted in a succession of fluvial to shallow marine mudstone and sandstone. Even though most of the sediment packages were thin, continued subsidence as a consequence of the Permian-Triassic rifting gave rise to sediment thicknesses up to 1000 metres above the rift axis (Nøttvedt et al., 2008; Ramberg, 2008). In the Mid-Jurassic tectonic rifting started again, and this led to several rifting episodes, which lasted into the Cretaceous (Riis et al., 2014). The rifting led to extension, faulting and thinning of the upper crust, but also affected the basement in several ways. In the Møre and Vøring basins the basement was uplifted, the Nordland Ridge and Frøya High were also sites of uplift while the Helgeland Basin subsided (Riis et al., 2014). The Halten Terrace and Trøndelag Platform to the east of uplifted Møre and Vøring basin, Nordland Ridge and the Frøya High were little affected by the tectonics in this rifting phase while the Helgeland Basin continued to subside into the Late Jurassic (Riis et al., 2014).

From the late Jurassic to the Early Cretaceous the earlier uplifted areas started to subside. This subsidence led to the creation of a complex system of structural highs and lows that restricted the evolving seaway between the Boreal Ocean in the northwest and the Tethyan Ocean in the southeast (Brekke et al., 2001). Figure 2.6 shows the structural map of the Mid-Norwegian sea with a Trøndelag Platform High and a subsided Helgeland Basin.

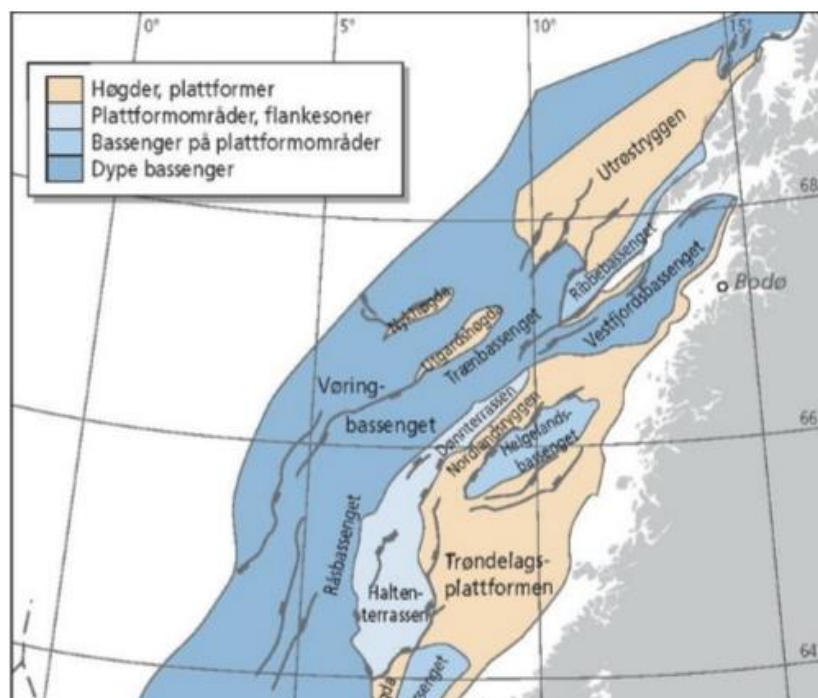


Figure 2.6: Structural elements of the Norwegian sea during the Jurassic (Ramberg, 2008).

### 2.1.6 Cretaceous

During the Early Cretaceous the rifting of the Norwegian Sea continued with a complex development of the region, which Gowers & Lunde (1984) divided into three major phases:

1. Berriasian-Valangian: gradual subsidence of the Helgeland Basins due to an active fault on the eastern Nordland Ridge.
2. Valangian-Barremian: a flexure zone developed along the Rødøy High due to subsidence.
3. Aptian-Albian: the region underwent extensive transgression, which submerged most of the highs and halted erosion.

In the Mid-Cretaceous the active rift gradually decreased, and the Halten Terrace and Trøndelag Platform subsided, which led to an almost open seaway between the Boreal Ocean and the Tethyan Ocean (Bukovics and Ziegler, 1985). According to Bukovics and Ziegler (1985) the subsidence of the Norwegian Sea was a result of a gradual cooling affecting the whole Mid-Norwegian offshore area. At the same time, the sea level experienced a global rise and, together with the subsidence activity, water flooded the former rift system (Bukovics and Ziegler, 1985).

### 2.1.7 Cenozoic

During the Late Cretaceous to early Palaeogene the last important rifting event took place with the final splitting of the Norwegian-Greenland continental plate and development of oceanic crust (Ramberg, 2008). This splitting caused an isostatic rebound during the Paleocene with a regional uplift of the Norwegian continental shelf and subaerial exposure resulting in increased sediment transport (Ramberg, 2008).

## 2.2 The Trøndelag Platform - Helgeland Basin

The Trøndelag platform is situated in the Mid-Norwegian Sea between 63°N-65°50'N and 6°20'E-12°E and covers an area of more than 50.000km<sup>2</sup> (Blystad et al., 1995). The Helgeland basin where the two cores were drilled is a depression in the northern part of the Trøndelag platform between 66°25'N-65°40'N and 11°E-8°40'E. The basin is approximately 150km long and 70km wide and is divided into two equal sub-basins by a saddle. The Helgeland basin was formed in the Early Cretaceous by a normal fault in the northwest downwarping in the south-east (Blystad et al., 1995). The basin experienced subsidence during the Cretaceous and was tilted towards the northwest like the rest of the Trøndelag platform during the Pliocene uplift of mainland Norway (Figure 2.7).

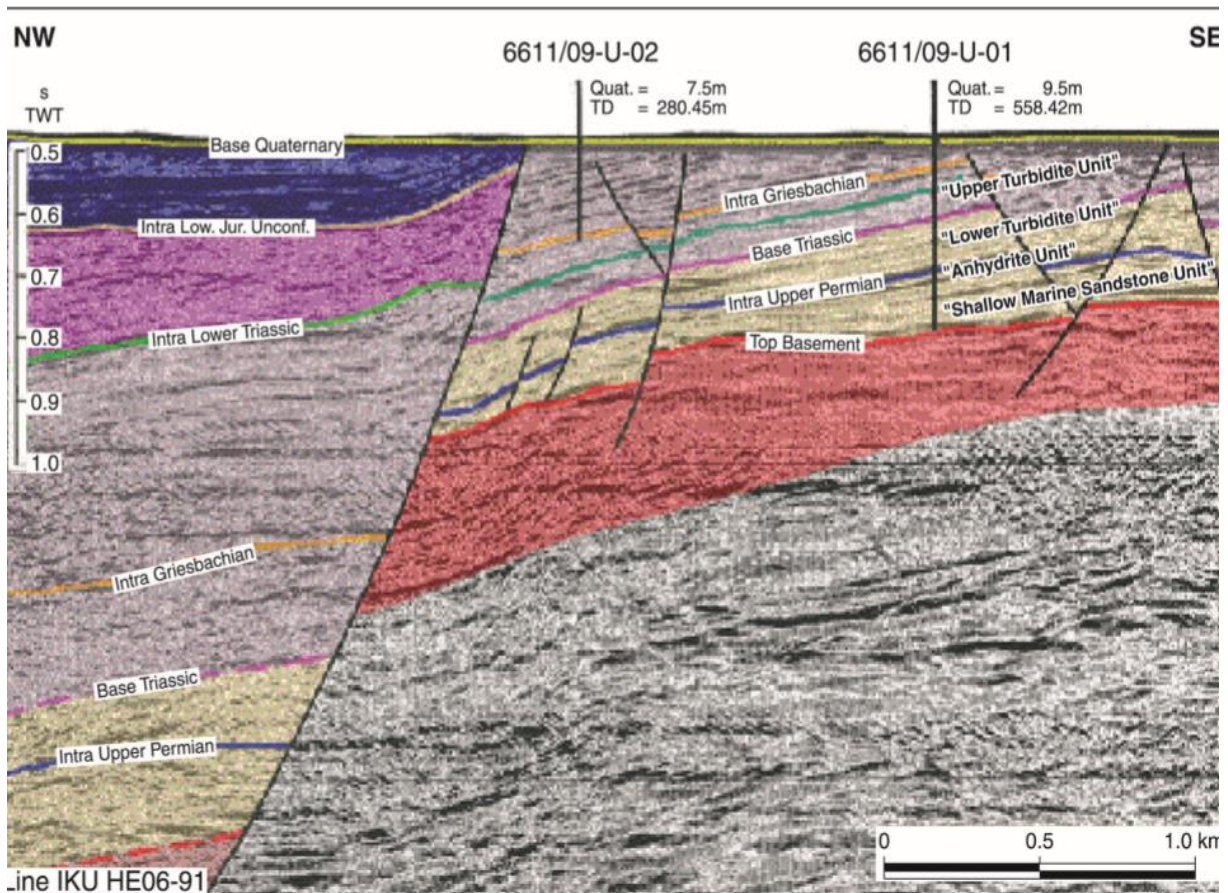


Figure 2.7: Interpreted seismic line containing the locations of the two boreholes. As seen on the seismic the deposits of the Helgeland basin dip towards the NW. From Bugge et al. (2002).

### 2.2.1 Permian deposits

During the Permian, the Norwegian continental landmass was situated within the northern tropical zone with a hot, dry climate for most of the period, and by the end of the Permian the great mass extinction occurred (Ramberg, 2008; Hochuli et al., 2010). Until the Late Permian, the marine and terrestrial life was rich, but an abrupt shift led to mass extinction of approximately 90% of marine animals and 80% of land animals and plants (Ramberg, 2008). Hochuli et al. (2010) investigated the changes in the marine and terrestrial life after the mass extinction and found only minor changes in the palynology from core 6611/09-U-01 and 6611/09-U-02. The Permian interval in the core is significantly bioturbated while the Triassic intervals only show rare signs of bioturbation and fossils, but with significant interbedded coal seams.

Bugge et al. (2002) subdivided the Late Permian unit into three parts: the lower Shallow Marine Sandstone unit, the Anhydrite Unit and the Lower Turbidite Unit. The Shallow Marine Sandstone unit is 174.5 m thick and is characterized as a series of massive, bioturbated sandstone units on top of a metamorphic basement. The lowermost part is described as red in colour and slowly changes upward to a greyish colour (Bugge et al., 2002). On top of the Shallow Marine Sandstone unit a 15.5m thick Anhydrite Unit is present. This unit is characterized by anhydrite beds within laminated siltstone (Bugge et al., 2002). The Lower Turbidite Unit of 166m thickness represents the youngest part of the Permian succession. The Lower Turbidite Unit has been described as a series of 1-2m thick fining upward sandstone beds with variably bioturbated, dark-grey siltstone layers. In the upper part of the unit there are two organic-rich, non-bioturbated, dark-grey siltstone/mudstone (Bugge et al., 2002).

### 2.2.2 Triassic deposits

The Triassic is characterized by relatively similar climatic conditions as the Late Permian with a hot, dry climate, but extensive plate movements led to a progressively more humid climate and altered conditions for life on earth (Ramberg, 2008).

In the earliest Triassic the Norwegian landmass was situated at the border of the temperate sub-tropical zone between 25 and 40 degrees north of the equator. This location favoured the hot dry climate which promoted intense weathering and oxidation with gravel, sand and red-coloured mud deposited in continental and marine basins (Ramberg, 2008; Bugge et al., 2002).

During the Triassic, the Norwegian landmass drifted towards the north and in the Late Triassic the climate became more humid with denser vegetation on land, increased chemical weathering and increased production of clay minerals, and quartz sand (Ramberg, 2008).

According to Bugge et al. (2002), the Triassic period is represented by the unit interpreted as the Upper Turbidite Unit. The Upper Turbidite Unit comprises the upper 190m of core 6611/09-U-01 and the entire 270m of core 6611/09-U-02, including a stratigraphic overlap of 60m (Figure 2.8). The Upper Turbidite Unit has been described as a series of fining-upwards sandstone beds with thicknesses from 0.5 to 1.5 metres, interbedded with heterolithic, siltstone and mud (Bugge et al., 2002). Minor, centimetre-thick gypsum layers occur in a 10m interval within the 60 metres stratigraphic overlap and have been interpreted as due to evaporation of saltwater in a closed basin with hot climate (Bugge et al., 2002; Ramberg, 2008).

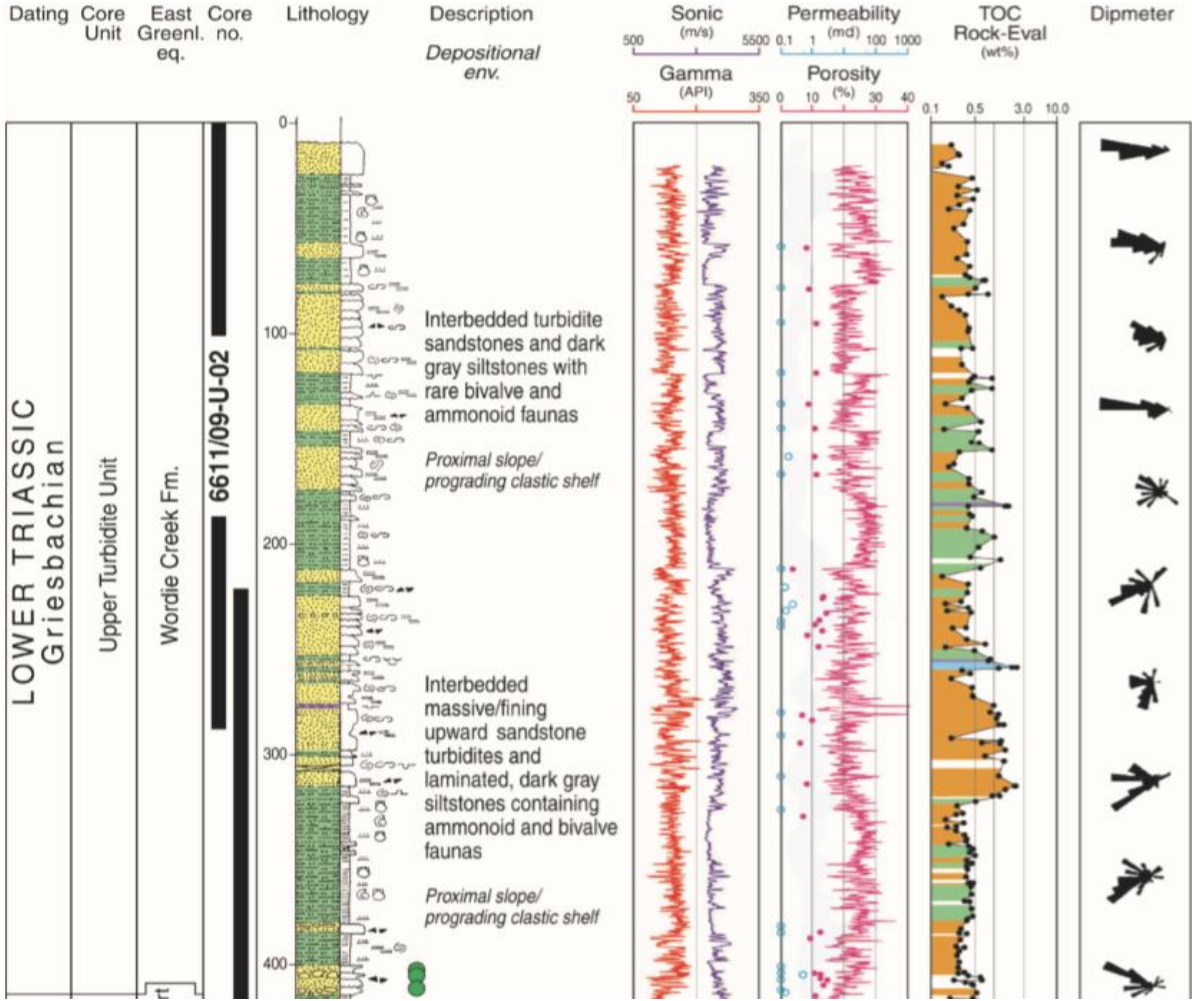


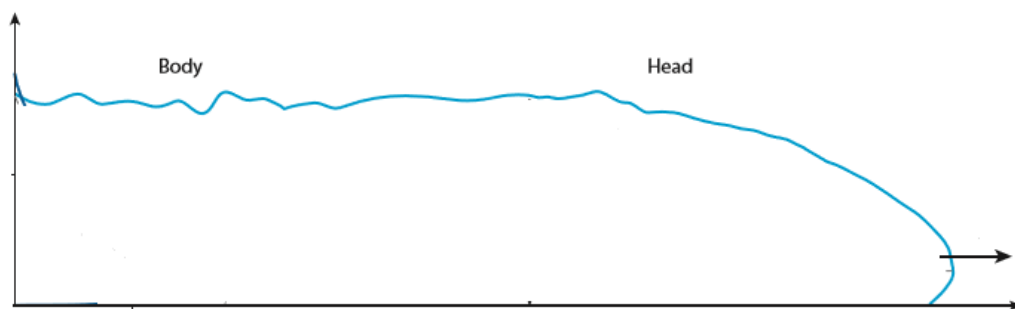
Figure 2.8: Sedimentological log of the Griesbachian interval from core 6611/09-U-01 and 6611/09-U-02. Bugge et al., (2002).

## 2.3 Flow Processes and definitions

Sediment gravity flow processes are processes in subaqueous environments which transport, erode and deposit sediment. A sediment gravity flow can be defined as a mixture of fluid and sediment where the mass is driven by the gravity and can also be referred to as gravity flows, sediment flows, density flows and mass flows. In this thesis rock intervals deposited mainly by three sediment gravity flows will be investigated and discussed. These are turbidity currents, transitional flows and debris flows. Pelagic and hemipelagic deposition will also be included as a depositional processes in the deep marine environment.

### 2.3.1 Turbidity currents

Turbidity currents are an important mechanism of sediment transport as they move coarse-grained material from the margins to the interiors of basins. Turbidity currents form one class of sediment gravity flows and are defined as “particle-laden gravity-driven underflows in which the particles are largely or wholly suspended by fluid turbulence (Meiburg and Kneller, 2010). Turbidity currents can be triggered by several processes. The three most common include i) triggered by submarine failures such as slumps or slides, ii) hyperpycnal flows related to rivers with high concentration of sediments, and iii) initiation by storm-induced waves (Meiburg and Kneller, 2010). The turbidity current consists of sediment-laden, turbid water that travels downslope and the flow consist of a head, body and tail (Figure 2.9). As the sediment gravity flow accelerates downslope, it scours the bottom, entraining fluid from above and sediment from below (Meiburg and Kneller, 2010).



*Figure 2.9: Schematic illustration of a turbidity current. Modified from Meiburg and Kneller (2010).*

When the sediment drops out of suspension or the bedload transport ceases, it forms a turbidite deposit. Coarse turbidites are formed from turbulent high-density turbidity currents close to the source (proximal) with fast fallout of grains from suspension, while fine grained turbidites are formed by low-density turbidite currents further from the source (distal) which can keep the grains in suspension for a longer time.

In 1962, Arnold H. Bouma classified the turbidites in a five-division scheme (A-E) later called the Bouma sequence (Figure 2.10). The Bouma sequence is a set of sedimentary structures typically preserved in sand or silt-mud facies. From base to top, Bouma divided the turbidite into: (Ta) massive to graded sand with load cast and irregular base, (Tb) plane-parallel laminated sand, (Tc) cross-laminated sand and silt, (Td) parallel-laminated sand to silt, and (Te) laminated to homogeneous mud. (Mulder and Hüneke., 2014).

The coarse, proximal turbidites consist of thick beds of coarse-grained material over scoured bases while the intermediate grained turbidites often display the Bouma sequence.

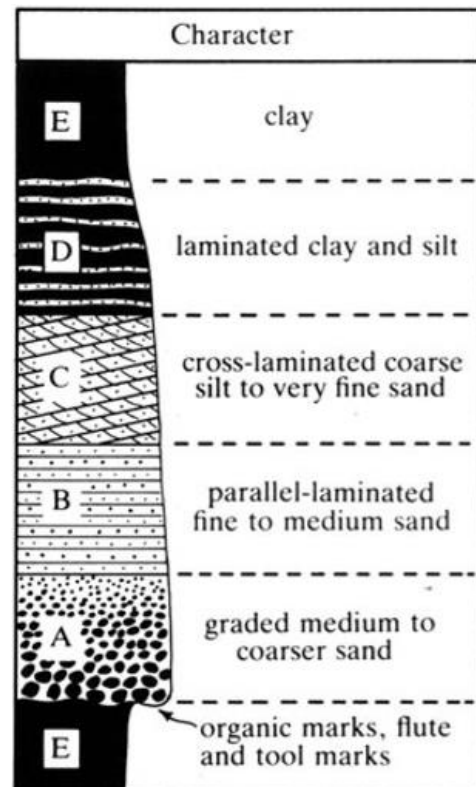


Figure 2.10: Turbidite deposition, retrieved from Allen (1985)

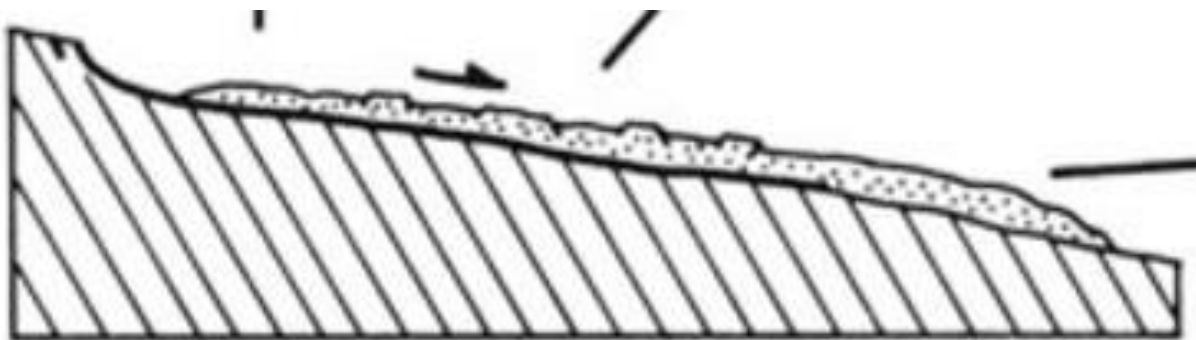
### 2.3.2 Debris flow

A debris flow is a gravity-induced mass movement that originates when poorly sorted rock and soil debris are mobilized from slopes and channels by saturation of dry or moist soils, water loss to the dry ground below or saturation of fissured muddy sediments either on the land or beneath water (Allen., 1985). Essential conditions for most debris flows include an abundant source of unconsolidated coarse or fine-grained sediments and steep slopes greater than 15-20° (Costa, 1984). Most debris flows are channelized deposits resulting in a long and narrow form, but they can transform into lobed sheets where they spread over open ground. Debris flows generally move at low speed as a plug with little or no transformation (Figure 2.12) (Allen., 1985).

When a debris flow deposits, it is called a debrite. A debrite is a poorly-sorted mixture of different lithologies with grain sizes ranging from mud to larger boulder-sized clasts. The concentration of mud is sufficiently abundant to form a matrix supporting the coarser elements. The deposit is often structureless and disorganized as seen in Figure 2.11.



*Figure 2.11: Debris deposit. From as Stow (1985).*



*Figure 2.12: Sandy debris flow process. By Allen. (1985).*



### 2.3.3 Transitional flows

In a transformation from a dense, sediment rich, laminar debris flow to a less dense, watery turbulent flow, there are different flow stages leading to various types of deposits (Felix and Peakall, 2006; Kane & Pontén, 2012; Southern et al., 2017). Transformation of debris flows occurs through a series of processes including erosion of the dense mass, breaking up the dense underflow, breaking of internal waves and turbulent mixing. Felix and Peakall (2006) proposed a transformation model from debris to turbidite showing the different steps in the transformation (Figure 2.13):

1. In a debris flow with high density and viscosity there is no dilution or erosion and the flow is a complete plug flow with little or no movement
2. For a debris flow with slightly less viscosity, the material is in motion with some erosion of the mass forming a turbid cloud. Sediment can be kept in suspension on top of the dense mass, while the dense bottom part is still a plug.
3. The mass still has quite high density and viscosity but is now deformable. In between the dense bottom layer and the overlying turbid cloud, waves are forming creating increased roughness which leads to more erosion and a larger turbid cloud.
4. If the waves in between the bottom layer and the turbid cloud increases to an amplitude equal to the flow thickness, the flow splits up and the stiff bottom plug gets separated. This leads to small coherent parts forming small debris blocks at base with a turbulent top.
5. If the stiffness of the initial debris flow is lower than the present stiffness, the individual broken blocks will start deforming and the waves will start breaking. This leads to an almost complete mixing of the dense bottom part with some blocks unmixed.
6. Fully mixed turbidite flow.

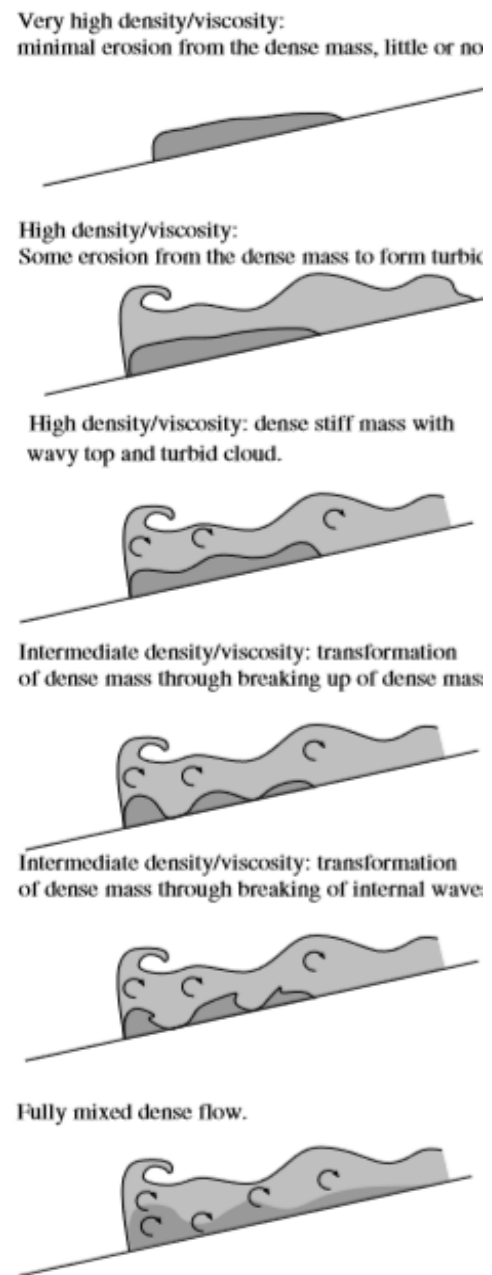


Figure 2.13. Transitional flow process by Felix and Peakall (2006).

A transitional deposit can have a wide spectrum of combination based on where in the transformation from the debris it is and if the plug is broken, and on the mixing of the flow.

#### 2.3.4 Pelagic and hemipelagic deposition

Pelagic and hemipelagic deposits are characterized by fine-grained sediment without significantly structures. The deposits are typically for low-energy environments such as deep-sea plains, closed shelves and fast deep subsiding basins (Garrison, 1990).

Deep-sea sediments commonly contain a mixture of terrigenous and biogenic components, but the proportions of these components vary greatly. Hemipelagic sediment is composed mostly of terrigenous silt and clay where at least 25% of the grains is terrigenous, volcanic or is derived from shallow-marine sediments. The pelagic sediments commonly contain less than 25% of grains from terrigenous, volcanic origin (Einsele, 2013; Stow, 1985).

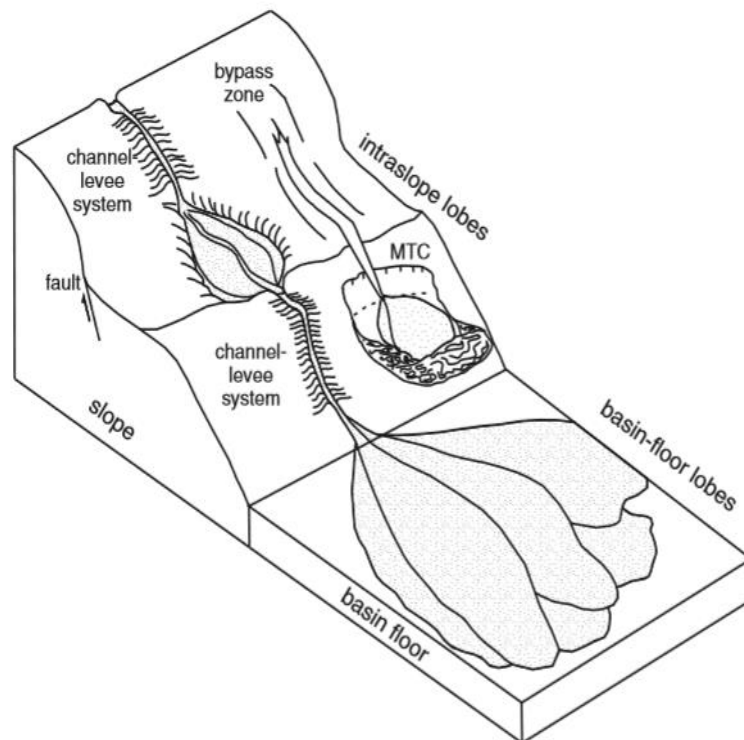
Pelagic sediments are typical for deep ocean settings, with little or no input from the continents but with minor contributors of biogenic material, aeolian dust and volcanic ash. The hemipelagic sediments accumulate in continental margin or shelf settings often with significant amounts of continental-derived detritus and a mix of fine-grained siliciclastic and biogenic material (Einsele, 2013). Because of the added continental sediments for hemipelagic deposits, sedimentation rates are higher than for pelagic deposits (Stow, 1985; Garrison, 1990; Einsele, 2013).

## 2.4 Submarine fan models

A submarine fan is a deposit at the base of a slope formed as a cone. The deposit consists of mostly turbidite beds where turbidity currents have travelled into deep water through a submarine canyon from a source area and have deposited the sediment they carried.

Since the first published model of a submarine fan many models have been proposed.

Advances in understanding deep water environments in the last decades have resulted in that many of the previously used models were now not that relevant (Pickering et al., 2016). One of the major problems in choosing a model is that there is no general model that is applicable to describe all deep-water systems because of different data sets, scales and terminologies of fan components.



*Figure 2.14: Principal features of a stepped deep-water system. Two mechanisms to generate accommodation on the slope are shown: generation of a slope step due to tectonic faulting and above a scar of a mass transport complex (MTC). From Sychala et al. (2015).*

The three basic elements of a submarine fan are: canyons, channels and lobes (Figure 2.14) (Pickering et al., 2016). A submarine canyon is a steep-sided valley often with a V-shaped profile that incises into the continental shelf and slope. Submarine canyons serve as major conduits for sediment transport from land to the deep-sea environment and are accumulation sites for deposits like turbidites, slumps, debrites and hemipelagic material (Shanmugam, 2016).

Submarine channels are recognized by thinning and fining upward cycles and with erosive bases and often rip-up clasts (Mutti and Ricci Lucchi, 1978; Shanmugam and Moiola, 1988). The dimensions of submarine channels vary in length from several km up to several thousands of km and in width from several km up to 20km.

The term lobe was proposed by Mutti and Ricci Lucchi (1978) for an ancient fan with characteristics such as thickening upwards cycles, coarse to fine sandstone, laterally continuous beds, bed thickness of 3-14m and development near mouths of submarine fan channels. However, the validity of Mutti and Ricci Lucchi's (1978) lobe term is questioned due to observations of vertical aggradation rather than basinward progradation and thin thickening up sequences. In general, both an aggradation and a progradation can be responsible for a lobe formation (Shanmugam and Moiola, 1988).

There are 26 well known submarine fan models published in literature, where the primary characterization factor is based on lobe types. The basic problem is that some models are derived from the ancient record and some are derived from the modern (present-day deep-water system) record (Shanmugam, 2016). Instead of looking at the submarine fan model the interpretation of discrete fan element like channels, levees and lobes are presented and discussed in Chapter 5: Conceptual model.

### 3 Petrography

#### 3.1 Introduction

The thin sections investigated consist of 11 samples from core 6611/09-U-01 and 15 samples from core 6611/09-U-02. Details of the thin sections are presented in Appendix section 8.1 and the positions of the thin sections are indicated on the sedimentary logs in Appendix 8.3-8.8. All the photos used in this section is taken by a high-resolution camera, and the diameter of the pictures are 50mm. Though the petrography of the Helgeland Basin is not a central part of this master theses a brief description is still presented for the three main lithologies. The lithofacies and facies associations used in table 1 and figures will be presented in section 4.1: Lithofacies and section 4.2: Facies association

Depth	Lithofacies	Depth	Lithofacies
15.14	Sst1	12.1	Sst2
50.7	Sst3 and Ds1	13.69	Sst1
64.45	Gypsum	21.95	Sst1
115.67	Mm and Sst3	37.94	Sst3
128.79	Mm and Sst3	42.42	Ds1
190.19	Sst1 and Sst3	76.64	Sst1
190.68	Sst1	77.54	Sst1
192.67	Sst1	80.35	Sst1
193.42	Sst1	93.75	Sst1
195.83	Sst1	95.21	Sst1
200.95	Sst1	117.22	Sst1
		224.07	Sst1
		230.42	Sst1
		236.52	Sst1
		279.71	Sst1

*Table 1: Left: Thin sections from core 6611/09-U-01 which show the depth they are taken from and the interpreted lithofacies. Right: Thin sections from core 6611/09-U-02 which show the depth they are taken from and the interpreted lithofacies*

### 3.1.1 Sandstone lithology

Twenty of the thin sections were collected from sandstone beds with a wide range in grain size and colour (Figure 3.1). The samples show a grain size distribution from very coarse-grained to very fine-grained sandstone. All the sandstone samples are quartz, feldspar and mica rich with some clay mineral matrix between the grains. The sorting of the framework minerals is poor to very poor with grain rounding dominated by angular to sub-rounded grains. The quartz grains include both monocrystalline and polycrystalline types and comprise about 70-90 % of the clastic framework minerals. Quartz grains displaying either undulating extinction or distinct extinction are found in the thin sections. The feldspar content is estimated to be 10-20 % of the framework minerals and comprises plagioclase, alkali feldspar and perthites. Some feldspar grains show secondary porosity. The mica comprises about 2-5% of the clastic framework and is dominated by biotite grains. Other observed minerals include thin muscovite flakes, carbonate grains, garnet and pyrite.

The clastic mineral content of the sandstone beds is interpreted to be derived from a crystalline source like a granite, granodiorite or quartz diorite. The poor sorting and rounding can be interpreted as short transportation time and rapid deposition. Some ductile grains are significantly transformed, and the occurrence of garnet shows an immature composition (M. B. Mørk, 2018, pers.comm.)

### 3.1.2 Siltstone and clay lithology

Two of the thin sections are from siltstone and clay lithologies. The siltstone sample is poorly sorted with angular to sub-rounded grains. Grains are very tightly packed with very little porosity. The homogenous clay is observed as clay fractions and some organic matter (coal), interpreted to originate from the settling of fine particles through the water column, hemipelagic mud. The thin silt laminae are interpreted as the upper silt/clay laminae, Td division of the Bouma sequence deposited by highly dilute turbidity currents. Figure 3.2 and Figure 3.3 show a layer of silt with poor sorting and tight packing. In Figure 3.3 it is also possible to see some horizontal lamination in the upper part.

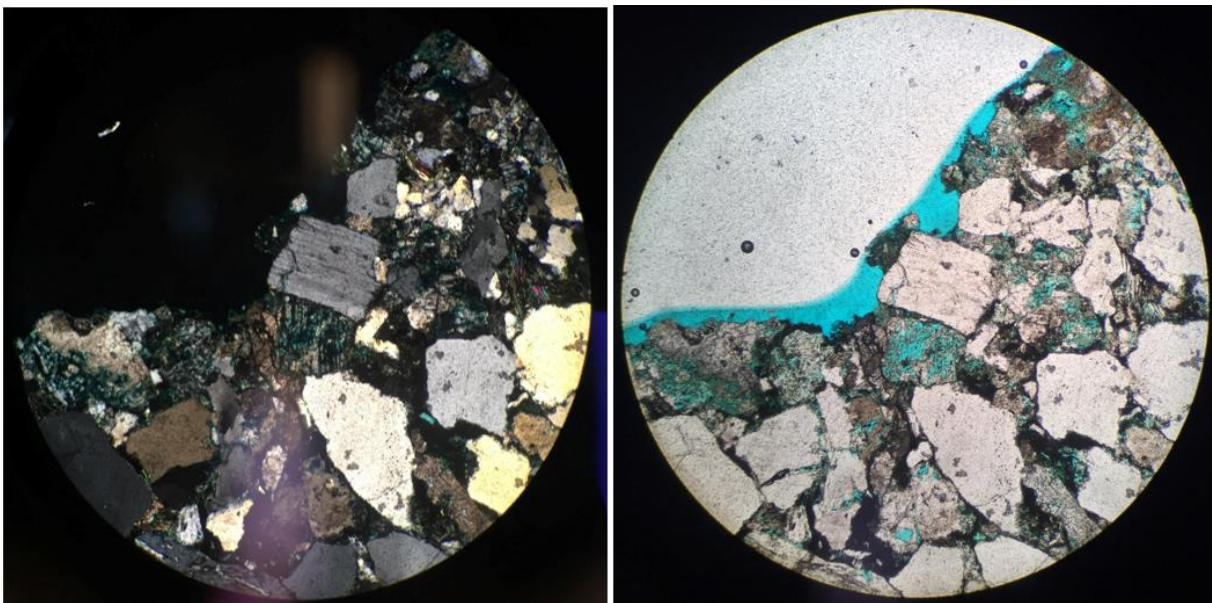
### 3.1.3 Matrix lithology

In several of the thin sections there is matrix in between framework grains. The matrix consists of a great amount of mica, carbonate, clay minerals and transformed grains (quartz, mica, feldspar). The matrix grain size is small (1mm-3mm) with angular to sub-rounded form and many of the grains are broken. There is little to no porosity.

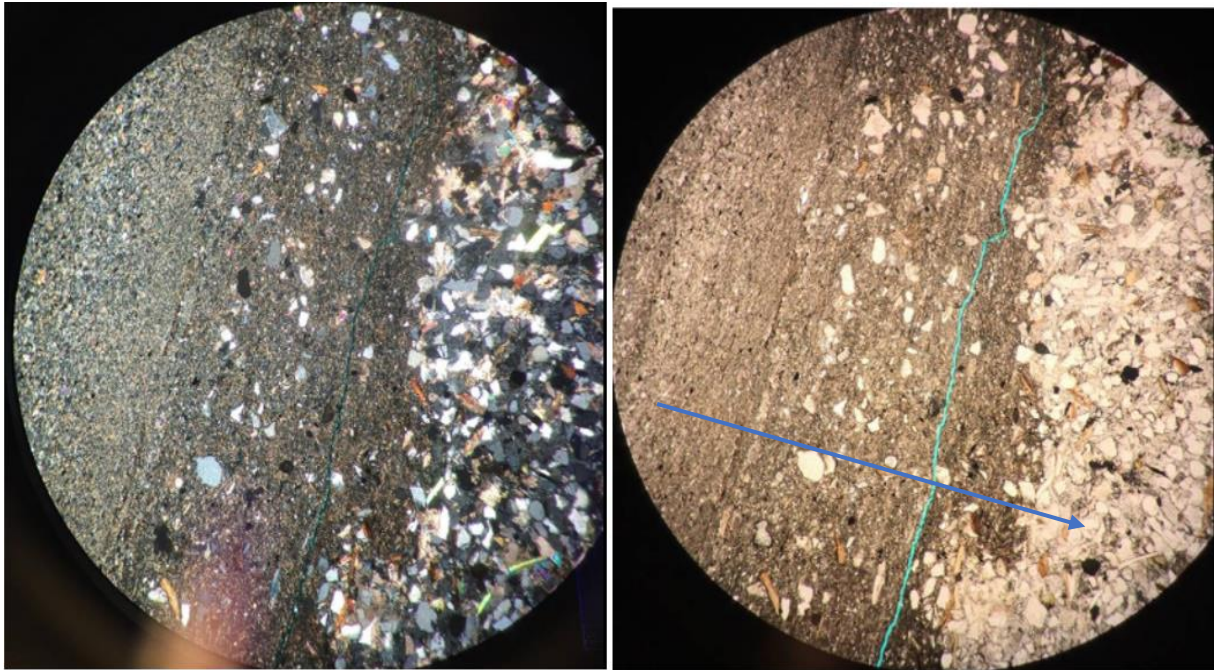
Figure 3.4 shows a chaotic mixture of framework grains in a very fine matrix. It is possible to see some broken grains in the matrix, but the major proportion is mica and carbonate.

#### 3.1.4 Gypsum lithology

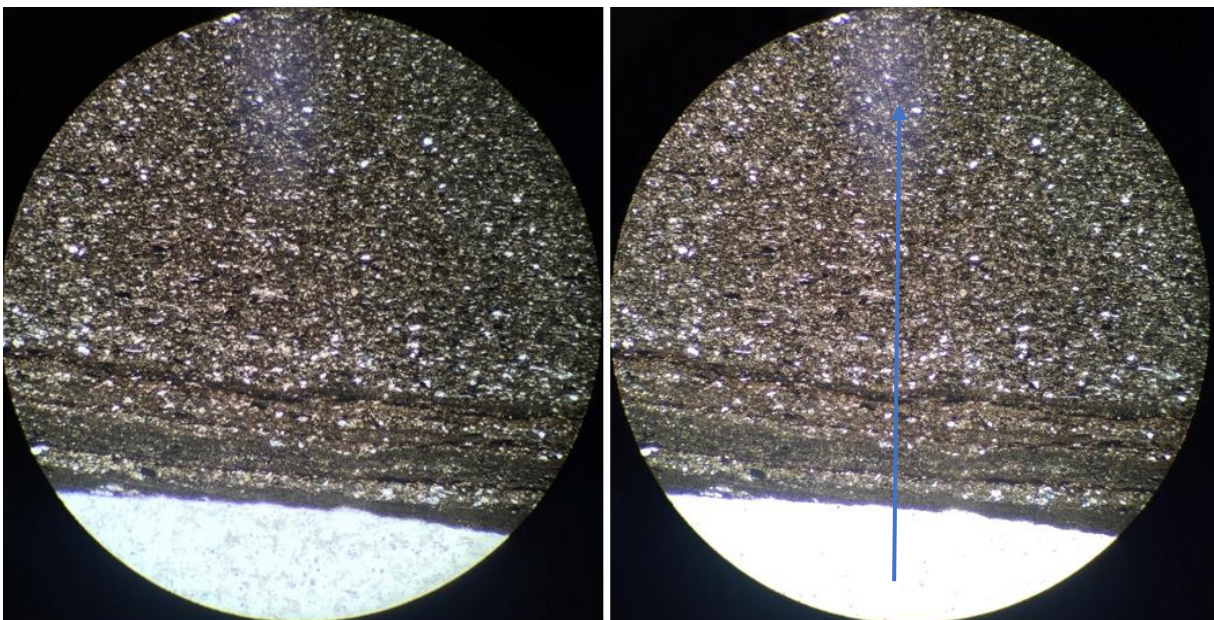
One of the thin sections was taken from a gypsum interval composed of two clean gypsum beds. The gypsum crystals occurs in the thin section as elongated to tabular crystals with size from 5mm to 20mm. The gypsum crystals are observed colourless in plane polarized light and black to grey in cross-polarized light. The crystals are observed recrystallized due to small grained and individual extinction under crossed polarized light. Figure 3.5 shows gypsum composed of two pure gypsum beds. Boundary is observed where the orange arrow is pointing.



*Figure 3.1: Thin section from a coarse sandstone dominated by quartz with some feldspar showing secondary porosity. Thin section taken from Core 6611/09-U-01 at depth 195.83m. The blue arrow show the upright way. Left: Microscope photo in cross-polarized light. Right: Microscope photo in plane-polarized light.*

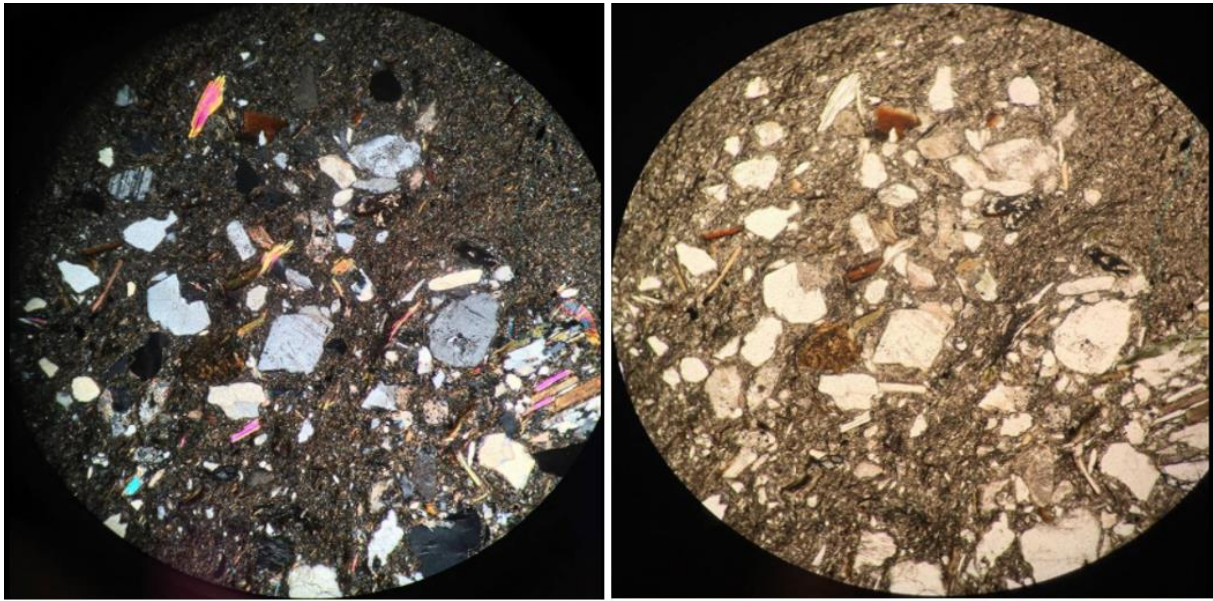


*Figure 3.2: Thin section from an interpreted heterolith facies association taken from Core 6611/09-U-01 at depth 128.79m. The heterolith facies association shown here is composed of fined grained sand on top and silt at base. The blue arrow show the upright way. Left: Microscope photo in cross-polarized light. Right: Microscope photo in plane-polarized light.*

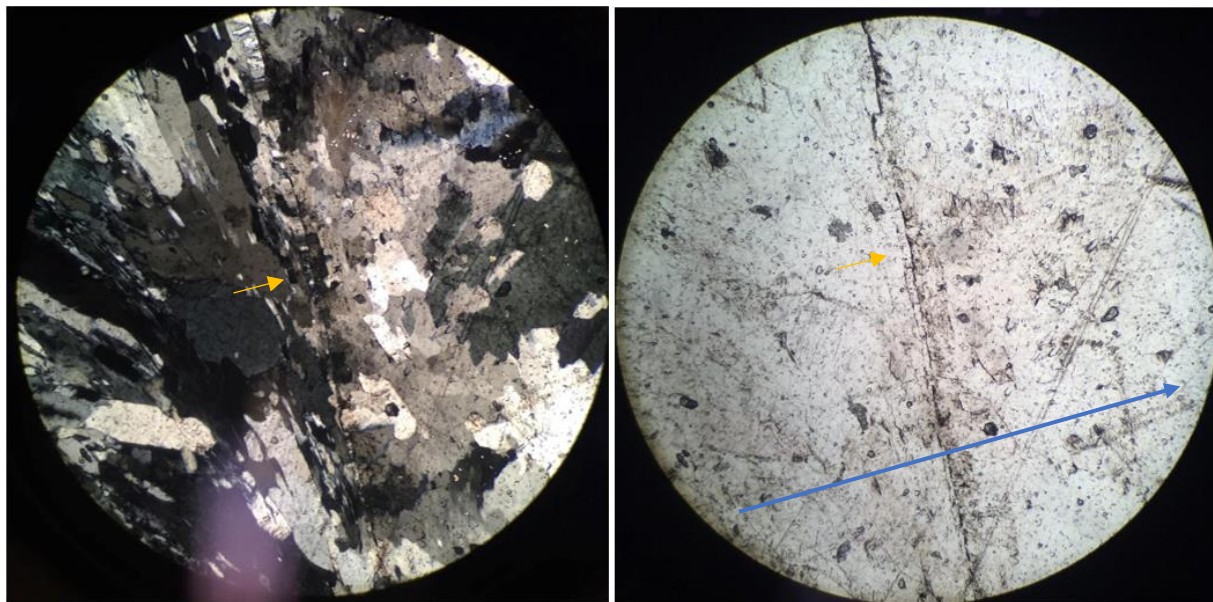


*Figure 3.3: Thin section from a transitional facies association with a laminated sole pointing up, interpreted as Facies association 3a. The blue arrow show the upright way. The thin section is taken from core 6611/09-U-01, at depth 50.7m. Left: Microscope photo in cross-polarized light. Right: Microscope photo in plane-polarized light.*





*Figure 3.4: Thin section from a mixed sandstone/matrix interpreted as Facies association 1. The thin section is taken from core 6611/09-U-02, at depth 42.42m. The blue arrow show the upright way. Left: Microscope photo in cross-polarized light. Right: Microscope photo in plane-polarized light.*



*Figure 3.5: Thin section from a gypsum bed interpreted as Facies association 4b. the layer is composed of two beds shown by the orange arrow. The blue arrow show the upright way. The thin section is taken from core 6611/09-U-01, at depth 64.45m. Left: Microscope photo in cross-polarized light. Right: Microscope photo in plane-polarized light.*

## 4 Facies description and interpretation

### 4.1 Lithofacies

The different lithofacies were classified based on sand-mud ratio, bed thickness, grain size and sedimentary structures. In this chapter the lithofacies are given descriptive names, but on the drawn log and in Figure 4.1 to Figure 4.6 the names are shortened to codes. Lithofacies codes are used on the sedimentological logs and in the spreadsheets applied for statistical analysis.

#### 4.1.1 Clean fining up sandstone (Sst1)

##### Description

Lithofacies Sst1 consists of very coarse to medium coarse fining up into a fine clean sandstone (Figure 4.1) with frequently coal laminae interbedded (this is not seen in Figure 4.1 but observed and marked on the logs). The sandstone is composed of angular to sub-rounded grains of mainly quartz, feldspar and mica (fig XX, Ch: 3.1.1). Other observed minerals include muscovite flakes, carbonate grains, garnet and pyrite. The sandstone is mostly well sorted with no visible structures, and no signs of any marine trace fossils observed either in the core or in the thin sections. Bed thicknesses vary from 0.02-1.5m with a greyish beige to more yellow grey colour. Generally, the thin beds (0.02-0.2m) vary from medium to fine sand and the thicker beds from coarse to fine sandstone, all grading upwards into silt (Figure 4.1). The upper boundary is gradational while the lower boundary of the bed is in most cases sharp, occasionally with load structures or alternatively appear erosive. Some sandstone units exceeding 1m in thickness may consist of two or more individual beds, called amalgamated beds. The amalgamation surfaces are identified as surfaces with abrupt textural changes between sandstone lithologies. Because of difficulty identifying some composite beds they have been interpreted and logged as one bed.

##### Interpretation of depositional processes

The lack of structures for lithofacies Sst1 suggests rapid suspension fallout from a dense flow (Southern et al., 2017). The absence of bioturbation indicates a stressed environment or absence of animals in the environment. The thick structureless coarse sandstone together with the absence of bioturbation can be interpreted as a lobe or channel deposit (Botterill et al, 2014; Spychala et al., 2015).

#### 4.1.2 Fining up sandstone with mud clasts (Sst2)

##### Description

Lithofacies Sst2 is dominated by a well sorted fining up sandstone with one to several horizontal aligned rip-up clasts of silt and mud towards the top (Figure 4.2). The rip-up clasts vary in size from 1-4cm. The shape of the rip-up clasts varies from rounded to square, and the clasts have a dark grey-black to brown colour. The sandstone is composed of angular to sub-rounded grains with a grainsize of the framework grains from very coarse to medium coarse sand, fining up into medium and fine sandstone. The sandstone is composed of mainly quartz, feldspar and mica, with some clay matrix, muscovite flakes, carbonate grains, garnet and pyrite in addition (section 3.1.1). No signs of marine trace fossils have been observed in the core. The thickness of the sand bed varies from 0.02m-1m, and the colour of the sandstone alternates from grey to beige. In most cases the boundary of the bed is sharp, but it can show load structures or be erosive in nature.

##### Interpretation of depositional processes

The lack of structures suggests the presence of rapid suspension fallout from a dense flow (Southern et al., 2017). The rip up mud clasts indicate sufficient flow strength to erode and transport a muddy and semi-consolidated substrate (Ichaso and Dalrymple, 2009) by passing water flows. The absence of bioturbation suggests a stressed environment (Botterill et al., 2014).

#### 4.1.3 Fining up sandstone with current ripples (Sst3)

##### Description

Lithofacies Sst3 is characterized by fine grained sandstone with parallel lamination and current ripples (Figure 4.3). The grain size of the sandstone varies from medium coarse to medium, fining up into clay. The sandstone is mostly well sorted with angular to rounded grains of mainly quartz, feldspar and mica. Also observed are thin muscovite flakes, carbonate grains, garnet, pyrite and clay minerals between the framework grains. The sandstone has a light grey colour, fining up grainsize with no sign of marine trace fossils. The thickness of the beds varies from 0.02-0.3m with gradational boundaries going from fine sand at the lower boundary and grading into mud at top.

### Interpretation of depositional processes

The grain size profile suggests a waning flow with sand dropping out from suspension in a unidirectional current with no or little internal shear, which results from decreasing energy within the flow as the mass moves and loses energy (Southern et al., 2017).

#### 4.1.4 Unsorted sandstone (Ds1)

##### Description

Lithofacies Ds1 is dominated by unsorted sandstone in a mud-matrix with varying grain-sizes and sphericity (Figure 4.4). The matrix consists of fractions of broken mica grains and carbonate mix, supported by clay minerals. Sandstone grains in the matrix are dominated by quartz, feldspar and mica (Figure 3.4). The facies shows no sign of grading and internal structures but can show significant shearing of mud and mud clasts. The thickness of the bed varies from 0.03 to 1.5m with an average of 0.25m. The facies often has a scoured base and a light grey to dark grey colour.

##### Interpretation of depositional processes

Lithofacies Ds1 can be interpreted as a gravity-induced mass movement. The unsorted sandstone mass is mobilization as a result of collapse of an unstable slope (Costa, 1984).

#### 4.1.5 Patchy sandstone (Ds2)

##### Description

Lithofacies Ds2 consist of a very coarse to medium coarse sandstone with a weak trend of fining up with light-white sand patches (Figure 4.5). The sandstone is composed of quartz, feldspar and mica with observations of muscovite, carbonate, garnet and pyrite in addition (Figure 3.1). Thicknesses of the bed for the patchy sandstone varies from 0.02m to 1m. The sand patches are observed as fined grained sandstone composed of mainly quartz, felspar and mica. Dimensions of the light-white patches of mixed material are visible in the grey/light grey sandstone. The boundary of the bed is sharp in most cases, but it can also have load structures or be erosive.

##### Interpretation of depositional processes

Lithofacies Ds2 is interpreted as a mass movement of sand clasts and matrix in a dilute suspension. The flow is almost a turbulent flow because of the high-water content in the flow,

but still has traces of unsorted and mixed sediment like a debris flow (Felix and Peakall., 2006).

#### 4.1.6 Laminated mudstone (Mm/Fa5)

##### Description

Facies Mm/Fa5 is characterized by black to dark grey mudstone with occurrence of pyrite and no signs of bioturbation (Figure 4.6). The thickness of the mud laminations varies from some few mm to few cm. The upper boundary of the bed is in most cases sharp, while the lower boundary is either transitional from silt and sand or sharp.

##### Interpretation of depositional processes

The hemipelagic mud is interpreted to have been deposited in a low-energy environment like a deep-sea plain below the reach of waves or currents due to the lack of sedimentary structures (Garrison, 1990). Because of the quiet conditions the fine material could settle quietly from the water column (Stow, 1985; Einsele, 2013).



Figure 4.1: Lithofacies clean fining up sandstone (Sst1). The red lines indicates base and top of the lithofacies. A) Clean medium coarse sandstone fining up into fine sand from core 6611/09-U-01. B) Coarse sandstone fining up into medium sandstone from core 6611/09-U-02.



Figure 4.2: Fining up sandstone with clasts (Sst2). The red lines indicates base and top of the lithofacies. A) Clean medium coarse sandstone fining up into fine sand with mud clast at top, from core 6611/09-U-01. B) Coarse sandstone fining up into medium sandstone from core 6611/09-U-02. Horizontally aligned mud clasts in middle and on top.



Figure 4.3: Fining up sandstone with current ripples (Sst3). The red lines indicates base and top of the lithofacies. A) Fine sandstone in horizontal lamination at base and current ripples at top from core 6611/09-U-02. B) Very fine sandstone with lamination at base and current ripples at top from core 6611/09-U-01.





Figure 4.4: Unsorted sandstone (Ds1). The red lines indicates base and top of the lithofacies. A) Mixed sandstone and mud with significant shearing, from core 6611/09-U-01. B) Coarse sandstone and mud in chaotic mix with shearing and sand patches from core 6611/09-U-02.



Figure 4.5: Patchy sandstone (Ds2). The red lines indicates base and top of the lithofacies. A) Medium coarse sandstone fining up into fine sand with sand patches at top, from core 6611/09-U-01. B) Coarse sandstone fining up into medium sandstone with sand patches through the bed, from core 6611/09-U-02.

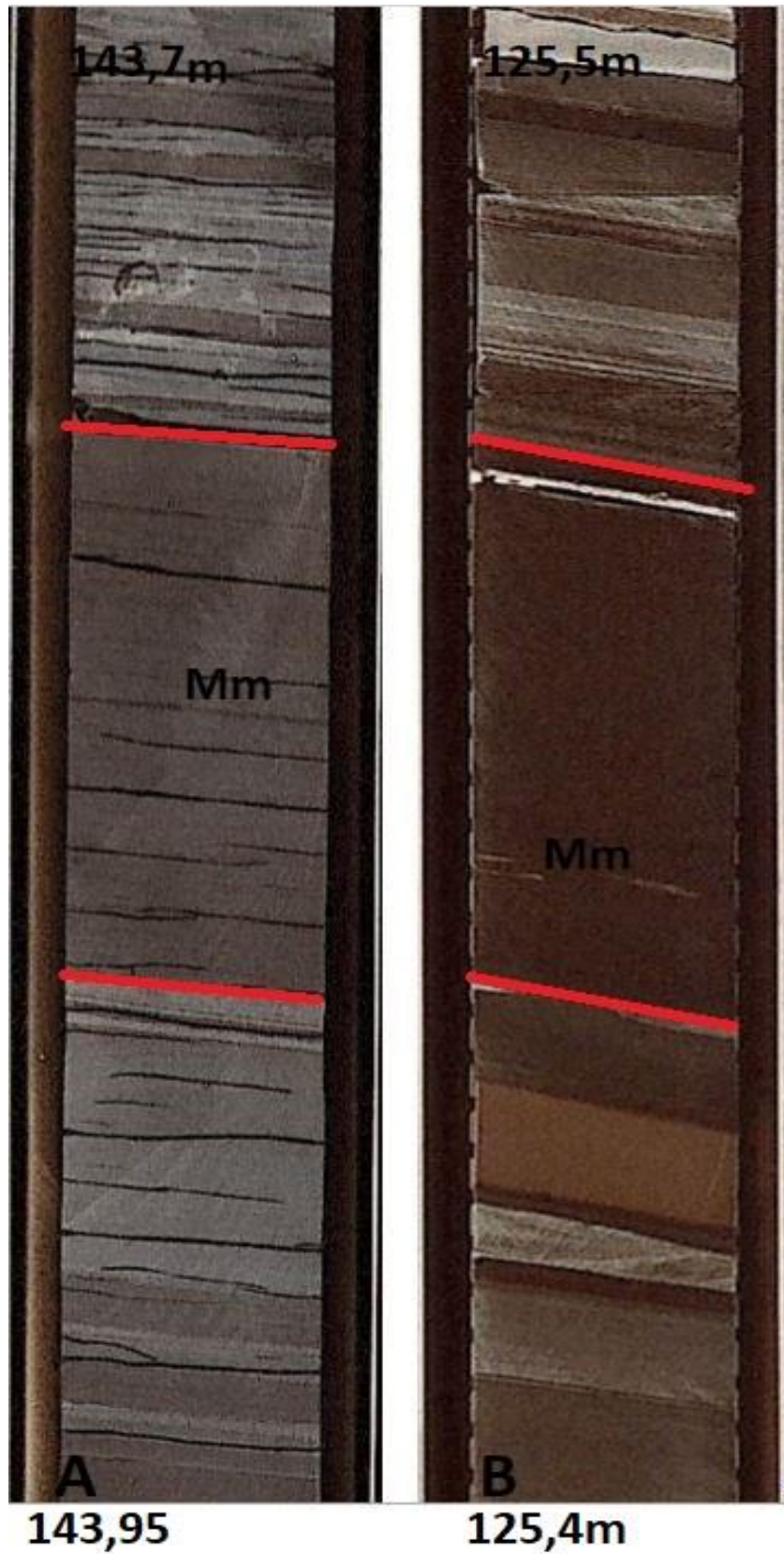


Figure 4.6: Laminated mudstone (Mm). The red lines indicates base and top of the lithofacies. A) Dark black mudstone in cm thick layers from core 6611/09-U-02. B) Grey cm thick layers of mudstone from core 6611/09-U-01.

## 4.2 Facies associations

The facies association in this thesis were built based on the characteristics of lithofacies definition presented in section 1.3.1. In this chapter, facies associations are given interpretative names linked to the depositional processes assumed to form the facies association. In the sedimentological log sheet (Appendix 8.3-8.8), the code for the facies is used to make it easier to compare and perform calculations for statistical/ quantitative analysis. Six lithofacies were identified and combined here into 4 facies associations based on the stacking patterns and interpreted flow behaviour. The histograms are made by measuring the thickness of the facies association down to 1cm. Layers with several very thin beds were counted as one events were the number of beds were marked as an observation. The information were plotted in excel and used to make histogram by plotting the thicknesses for each facies association to look at the thickness distribution. Due to few observations of facies association Fa3a and Fa3b, Fa4a and Fa4b they are counted as one alternatively as Fa3 and Fa4.

### 4.2.1 Debrite facies association (Fa1)

#### Description

The debrite facies association consists of thin to thick-bedded (0.02-0.7m), non-stratified poorly sorted sandstone or deformed heterolithic strata (interbedded deposit of sand and mud). Significant sub-angular to rounded mud clasts and some sand clasts are present in varying sizes. Bed bases are sharp or scoured. The facies association is a combination of Ds1 and Ds2. It is frequently followed by thin bedded sandstone (sst3). Figure 4.9 show two types of a debrite bed with mud clasts, shearing and mud streaks.

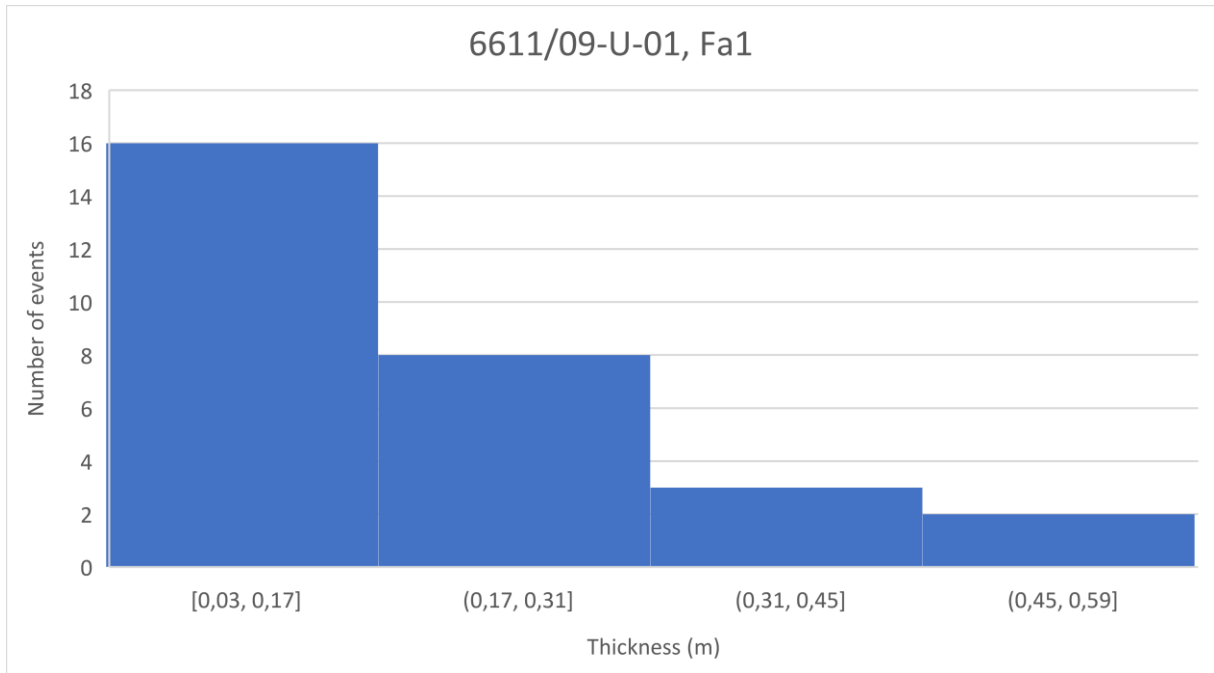


Figure 4.7: Histogram showing thickness distribution of Fa1, core 6611/09-U-01.

In the histogram of thicknesses of facies association 1 for core 6611/09-U-01 (Figure 4.7), it is possible to observe a range in thicknesses from 0.03m to 0.59m for each deposited debrite bed. The debrite facies association can be observed as having most common thickness from 0.03-0.31m with an average of 0.19m. The histogram in Figure 4.7 shows there is a decrease in number of beds with increasing thickness.

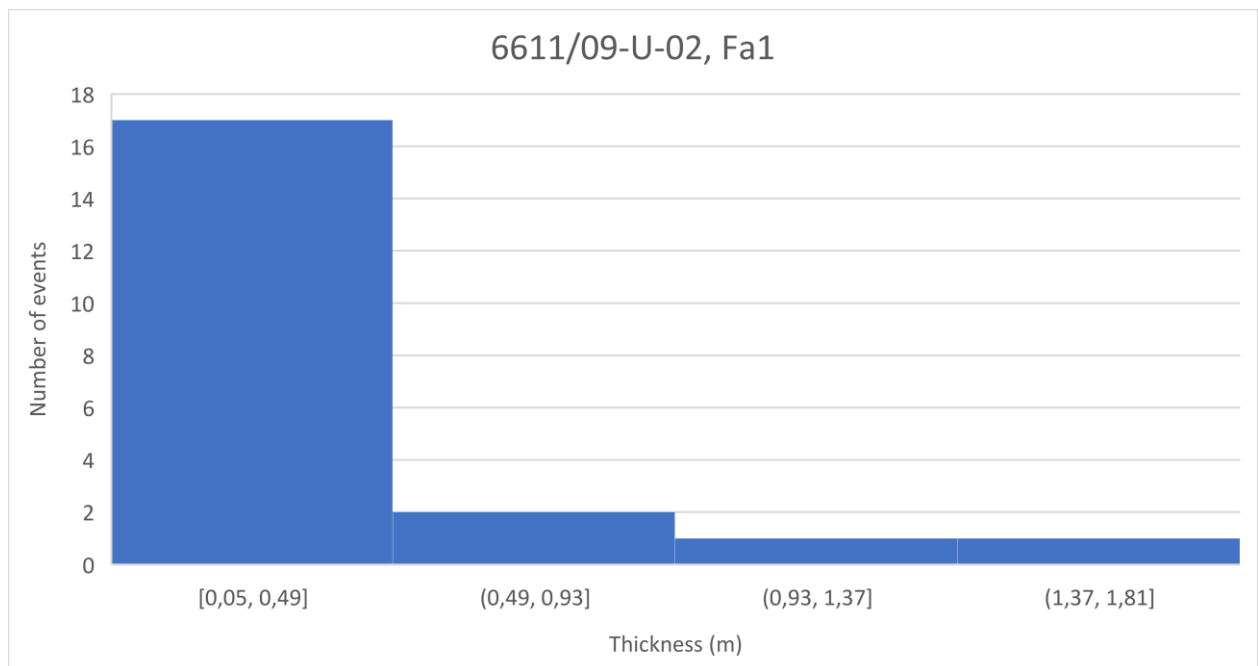


Figure 4.8: Histogram showing thickness distribution of Fa1, core 6611/09-U-02.

Thicknesses of Fa1 for core 6611/09-U-02 varies from 0.05- 1.81m with an average thickness of 0.28m. The histogram in Figure 4.8 shows there is a decrease in number of events with increasing thickness so the debrite facies association can be observed as having most common thicknesses from 0.05-0.49m. For the general debrite facies association the most common thicknesses are in the range of 0.03m to 0.49m with an average thickness of 0.235m.

#### Interpretation of depositional processes

The debrite facies association is the result of a cohesive, laminar debris flow which was able to carry large clasts within or on top of the mud matrix within the flow (Allen, 1985; Southern et al., 2017). The debris flow is mobilization as a result of collapse of an unstable steep slope (Costa, 1984). Facies association Fa1 is often described in association with turbidite channel fill (channel margin collapse) or with submarine slopes (Costa, 1984).



Figure 4.9: Debrite facies association. The red lines indicates base and top (if observed) of lithofacies. A) Debrite with significant mud shearing and clasts (Core 6611/09-U-01) B) Debrite with unsorted matrix and mud streaks (Core 6611/09-U-01).

### 3.2.2 Turbidite facies association (Fa2)

#### Description

The turbidite facies association is a medium to thick bedded sandstone (0.1-2m). The beds are dominated by structureless beds of fine to coarse sandstone with poor grading. Commonly contains parallel lamination with some lenticular rip up mudstone chips (mm to cm). In the upper part of a turbidite facies association bed fine- grained sand with ripples can be observed. The base of the bed are in most cases observed sharp but are also seen loaded or erosive in nature. In most cases the bed base is sharp, but it can also be loaded or erosive. This facies association is commonly composed of a combination of lithofacies Sst1, Sst2 and Sst3. The most common sequence is Sst1 followed by Sst3: a fining up sandstone with ripples at the top. Figure 4.12 show three types of a turbidite facies association with the lithofacies codes marked on the core.

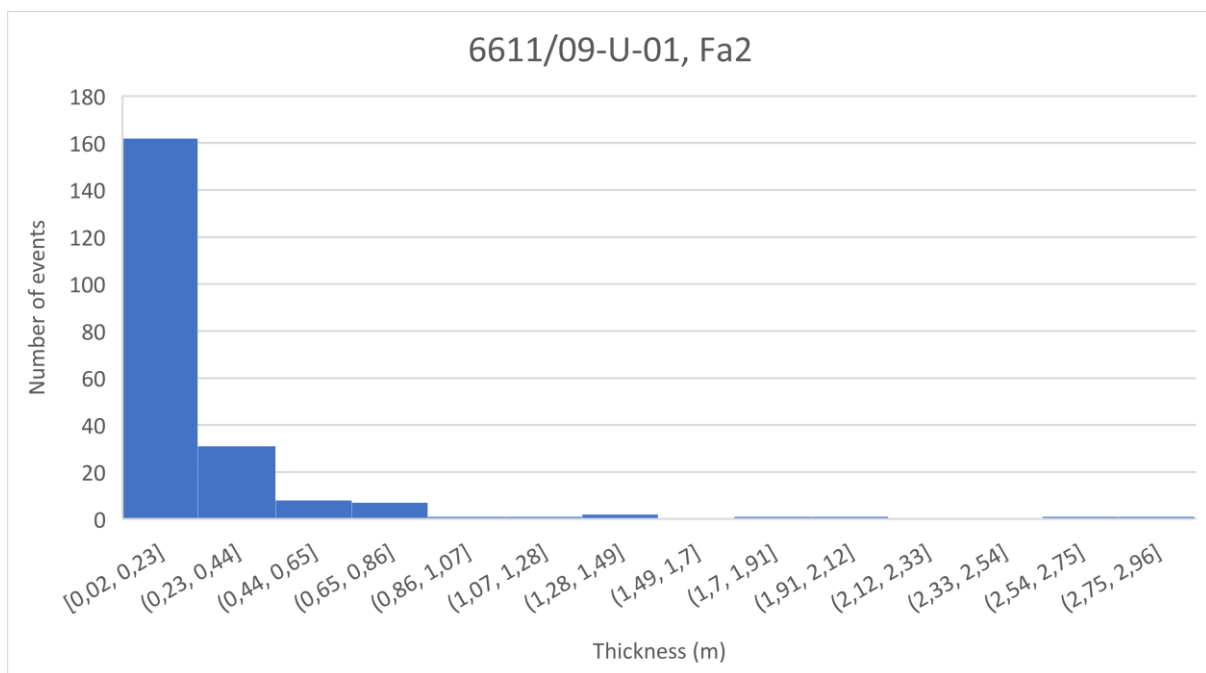


Figure 4.10: Histogram showing thickness distribution of Fa2, core 6611/09-U-01.

In the histogram of thicknesses of facies association 2 in core 6611/09-U-01 (Figure 4.10), there is a clear trend in decrease of number of depositional events with increasing thicknesses. The thicknesses range from 0.02 to 0.23 showing a distinct high number of events. The average thickness for Fa2 is 0.23 m.



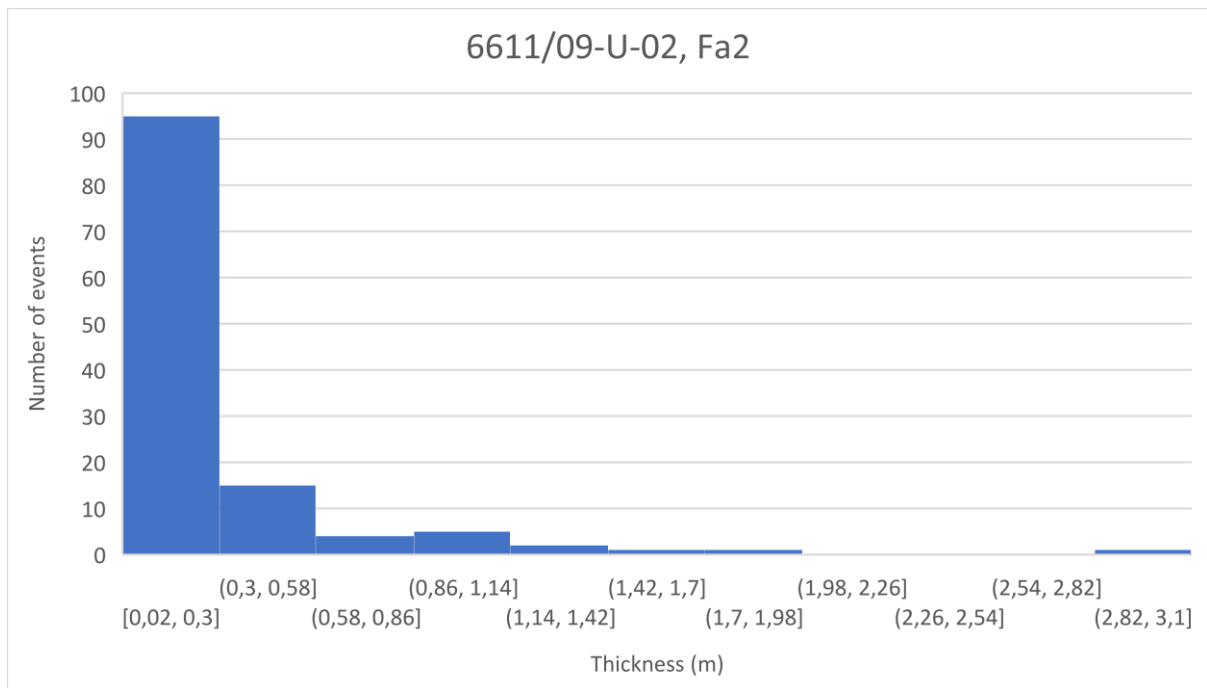


Figure 4.11: Histogram showing thickness distribution of Fa2, core 6611/09-U-02.

Core 6611/09-U-02 shows a thickness interval from 0.02- 0.3m as the most common with an average thickness of 0.27m (Figure 4.11). The histogram in Figure 4.11 shows a similarity with the high number of beds are the thinnest. For both core 6611/09-U-01 and 6611/09-U-02 the most common thickness interval for the turbidite facies association is observed from 0.02- 0.3m with an average thickness of 0.25m.

#### Interpretation of depositional processes

The structureless and amalgamated sandstone can be interpreted as a high-density turbidity current deposit while the sandstone with planar lamination and ripples can be linked to low-density turbidity currents, produced beneath dilute turbulent flows (Hofstra et al., 2015; Southern et al., 2017). The low density turbidite flows can be interpreted as part of the Bouma sequence. The high-density turbidites are characterized by coarser grain sizes than the low-density turbidites (Southern et al., 2017).

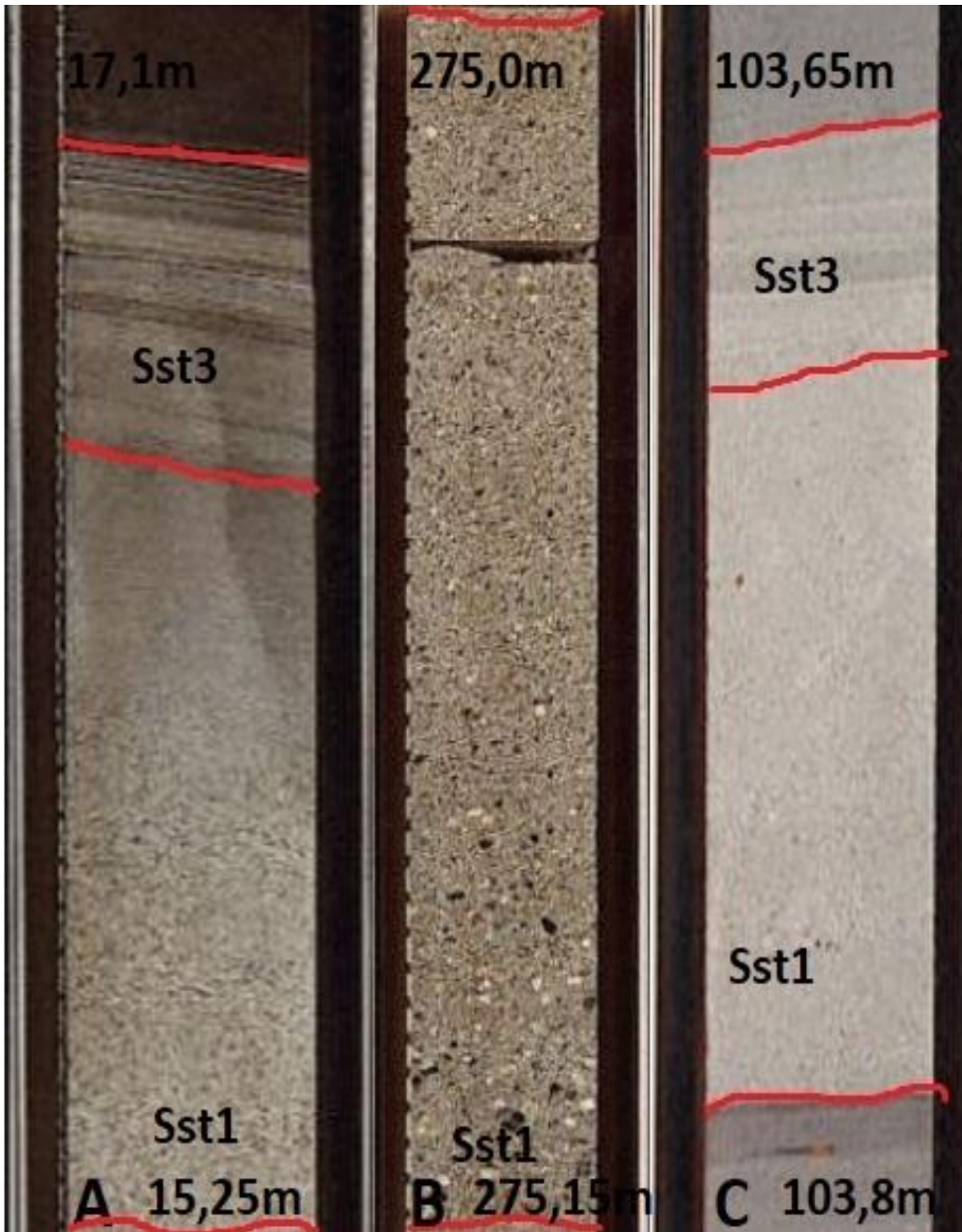


Figure 4.12: Turbidite facies association. The red lines indicates base and top (if observed) of lithofacies. A) Fining up turbidite from medium to very fine sand (Core 6611/09-U-02, depth 17.1m). B) Fining up turbidite from conglomerate to medium coarse sand (Core 6611/09-U-02, depth 275.0m). C) Fining up turbidite from fine sand to very-fine sand (Core 6611/09-U-01, depth 103.65m).

### 3.2.3 Transitional facies association (Fa3)

#### Description

- A) Facies association Fa3a is characterized by a debrite facies on top of a fining up sandstone. The debrite facies has thin silt and clay seams interbedded and is often overlain by lithofacies Mm. Facies association Fa3a is a medium bedded to thick bedded (0.25-2m) deposit with a sharp base and a gradational top. This facies association is commonly composed of three parts: a base of lithofacies Sst1, Sst2 or Sst3, a mid-section of lithofacies Ds1 or Ds2 and a top of lithofacies Mm. Figure 4.15 B and C show two types of a debrite facies association with the lithofacies codes marked on the core.
- B) Facies association Fa3b is observed as a patchy sandstone on top of a fining up sandstone. The base sandstone is a fining up coarse to fine sandstone overlain by a weak fining up sandstone with white patches of mixed material in it. The facies association is a medium bedded to thick bedded (0.25-2m) deposit which consists of a combination of several lithofacies. The base of the facies association consists of lithofacies Sst1, Sst2 or Sst3 with a mid-section of lithofacies Ds1. Figure 4.15A show a patchy sandstone interpreted as a Fa3b facies association with the lithofacies codes marked on the core.

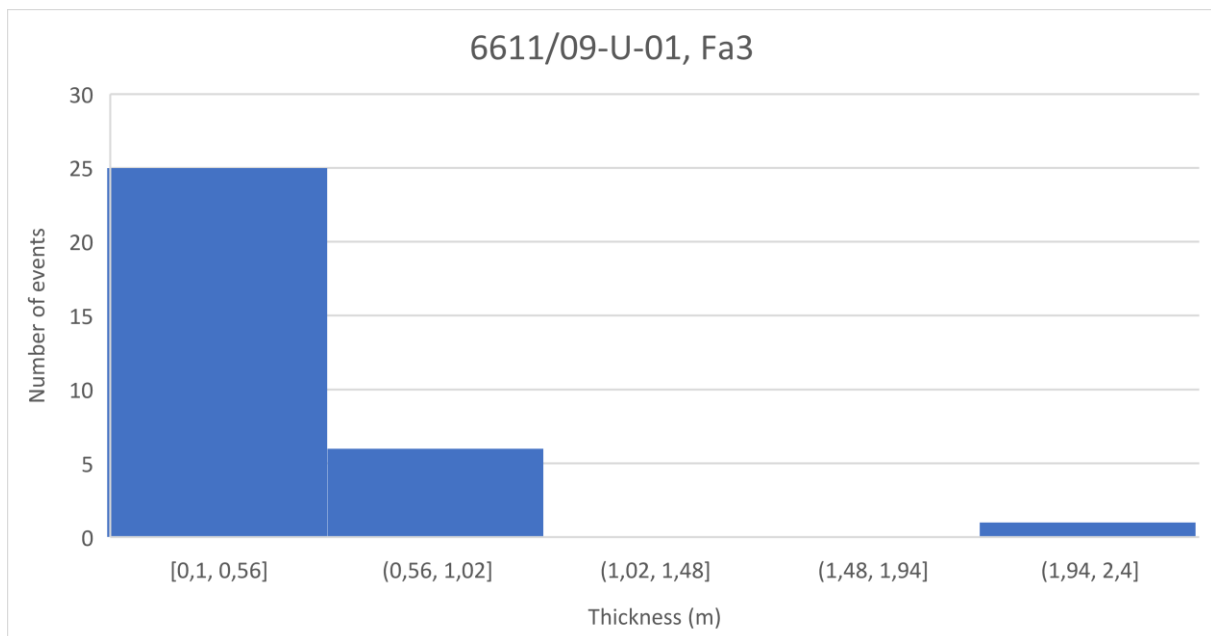


Figure 4.13: Histogram showing thickness distribution of Fa3, core 6611/09-U-01.

The histogram of thicknesses for Fa3 in core 6611/09-U-01 (Figure 4.13) shows a decrease in number of events for increasing bed thickness. The most common thickness is between 0.1 and 0.56m, but there are also some beds with thickness up to 2.4 metres which gives an average bed thickness of 0.42m.

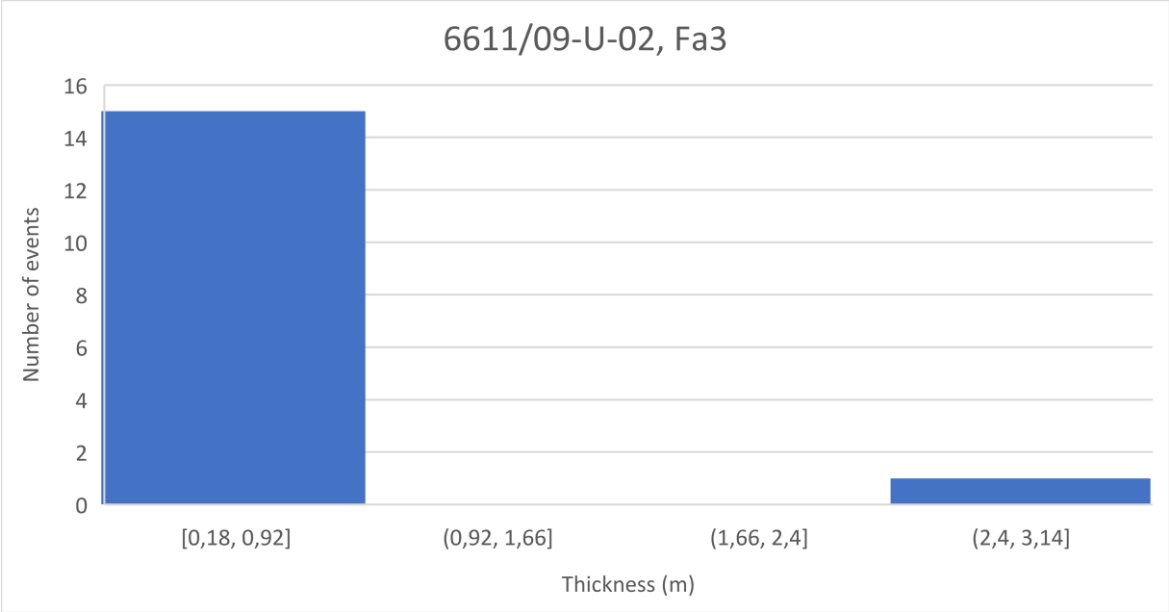


Figure 4.14: Histogram showing thickness distribution of Fa3, core 6611/09-U-02.

The histogram of thicknesses of facies association 3 for core 6611/09-U-02 (Figure 4.14) shows an uneven distribution of thicknesses through the core with a large number of bed thicknesses of 0.18- to 0.92m. In Figure 4.13 there is a similar distribution of the bed thicknesses with no event of 1-2 metres bed thickness. The average bed thickness for facies association 2 for core 6611/09-U-02 is 0.52m so the average bed thickness for both cores for facies association 3 is 0.47m.

Interpretation of depositional processes

Facies association 3 can be interpreted as a frozen ore-debrite where a laminar debris flow is transformed into a more turbulent flow. The flow begins with a laminar flow of mixed material. When the flow moves down the slope the water content increases and the flow loses strength and gradually transforms into a more turbulent flow. The bed are transformed into a transitional bed where the sub-layer is fully mixed, while the rest is still a debrite plug. The bed is overlain by a mudstone which can be interpreted as a turbidite mud generated by the turbidity current tail. Transitional flows typically occur at the base of sandy lobe packages, they are particularly common in long-runout, mud-rich systems on passive margins (Kane and Pontèn, 2012).

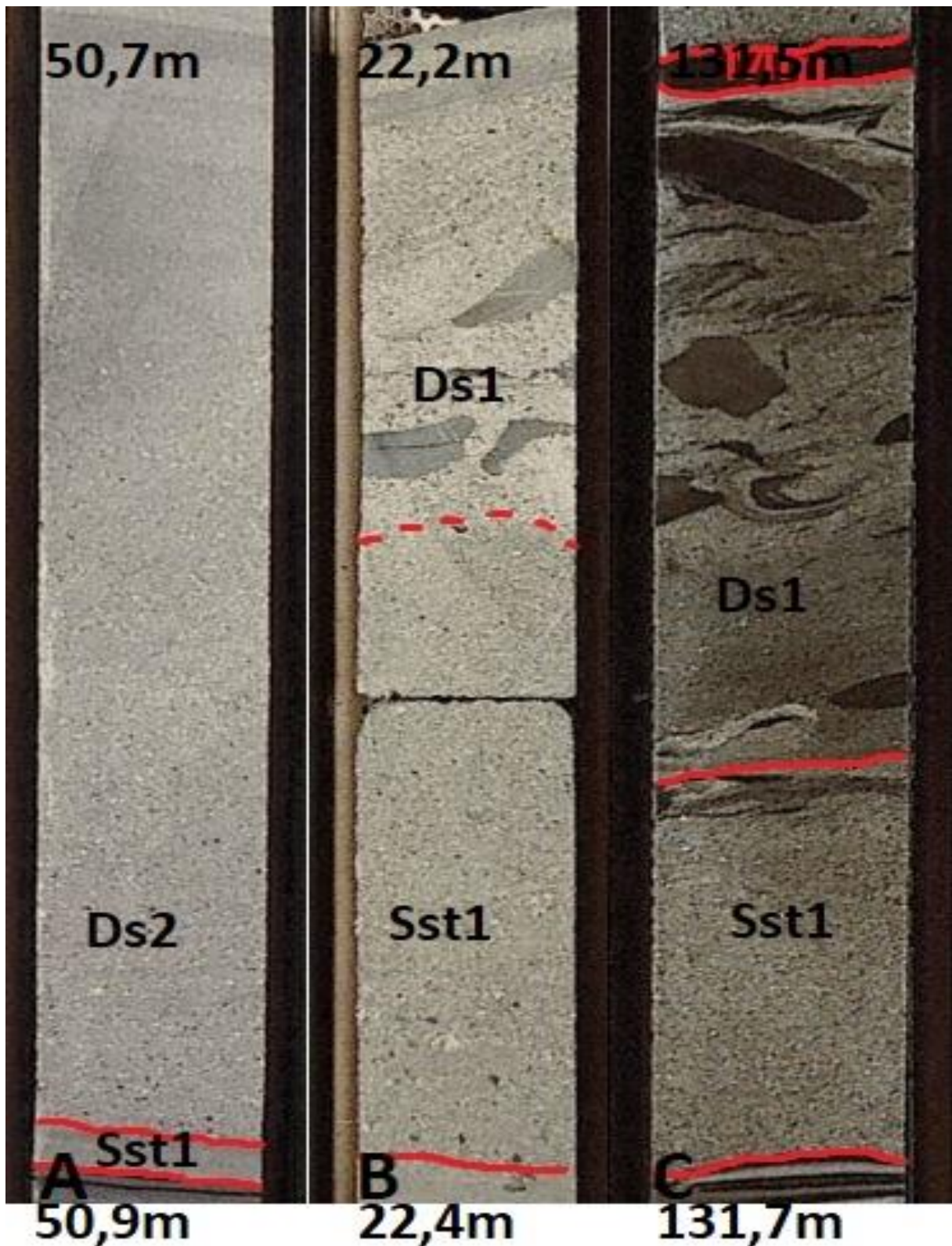


Figure 4.15: Transitional facies association. The red lines indicates base and top (if observed) of lithofacies. A) transitional facies association with a thin turbidite base, overlain by a patchy sandstone (Core 6611/09-U-01, depth 50-7m). B) Fining up turbidite overlain by debrite without mud on top (Core 6611/09-U-01, depth 22.2m). C) Fining up turbidite overlain by debrite and mud (Core 6611/09-U-02, depth 131.5m).

### 3.2.4 Heterolithic facies association (Fa4)

#### Description

- A) Facies association Fa4a is characterized by a thin to thick bedded (5cm-2m) heterolithic facies consisting of fine to very fine-grained sandstone interbedded with sandy siltstone and coarse to fine siltstone and clay. Sandstone beds show current ripples or wavy lamination while siltstone shows planar lamination. The mudstone shows significant numbers of small pyrite nodules. Base contacts are mostly sharp with significant loading into the clay but can also see gradational bases and tops. The facies association consists of beds up to several metres, with usually no significant trend or changes in grain sizes or thickness, although a weak trend of fining up in the sand layers can be present. Facies association Fa4a consists of an alternation of lithofacies Mm and Sst3. Figure 4.18B and 4.18C show a heterolithic facies association composed of mudstone and fined grained sand.
- B) Facies association Fa4b is a thick bedded (1m-5m), very fine-grained sandstone interbedded with sandy siltstone, coarse to fine siltstone, clay and gypsum. Sandstone beds show current ripples while siltstone shows planar lamination. The mudstone shows significant small pyrite nodules. A few double mudstone drapes with clear, sharp, thin sand layers are observed in the gypsum interval. This facies association is commonly composed of a combination of lithofacies Mm, Sst3 and gypsum. Figure 4.18A show a Fa4b facies association composed of Mm, Sst3 and gypsum.

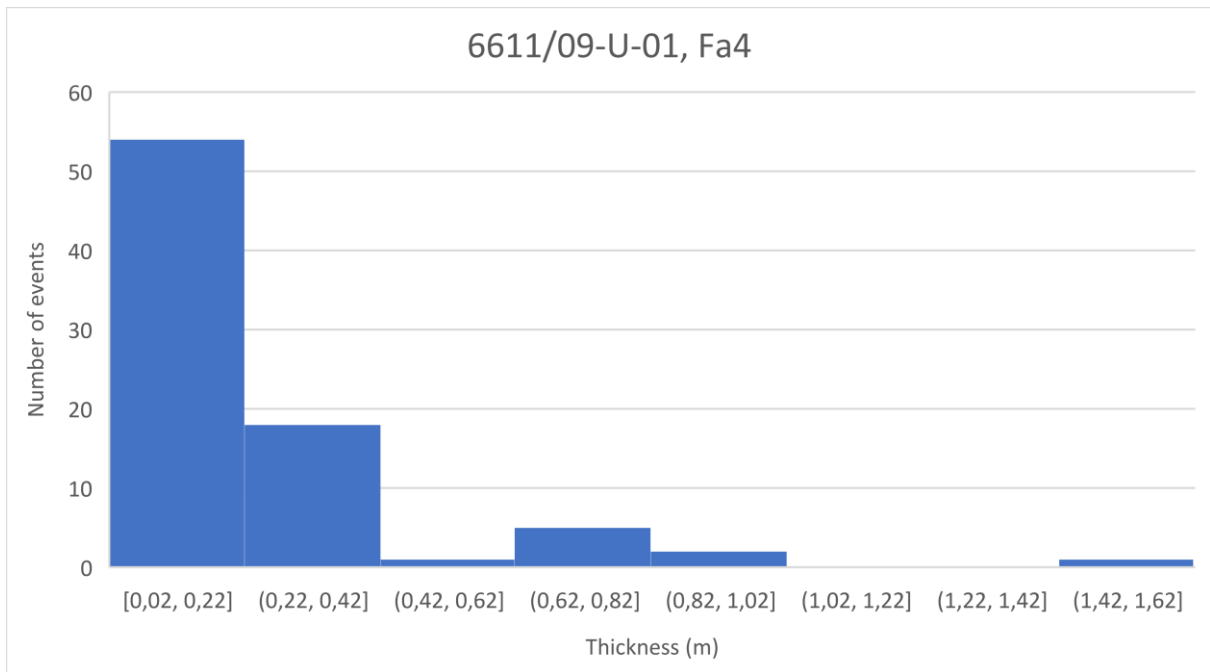


Figure 4.16: Histogram showing thickness distribution of Fa4, core 6611/09-U-01.

In the histogram of thicknesses of facies association 4 core 6611/09-U-01 (Figure 4.16), it is possible to see a range of thicknesses from 0.02m to 1.62m for each deposited facies association. There is a decreasing number of events with increasing thickness so the heterolithic facies association for core 6611/09-U-01 can be interpreted as having most common thicknesses from 0.02-0.42m with an average of 0.22m.

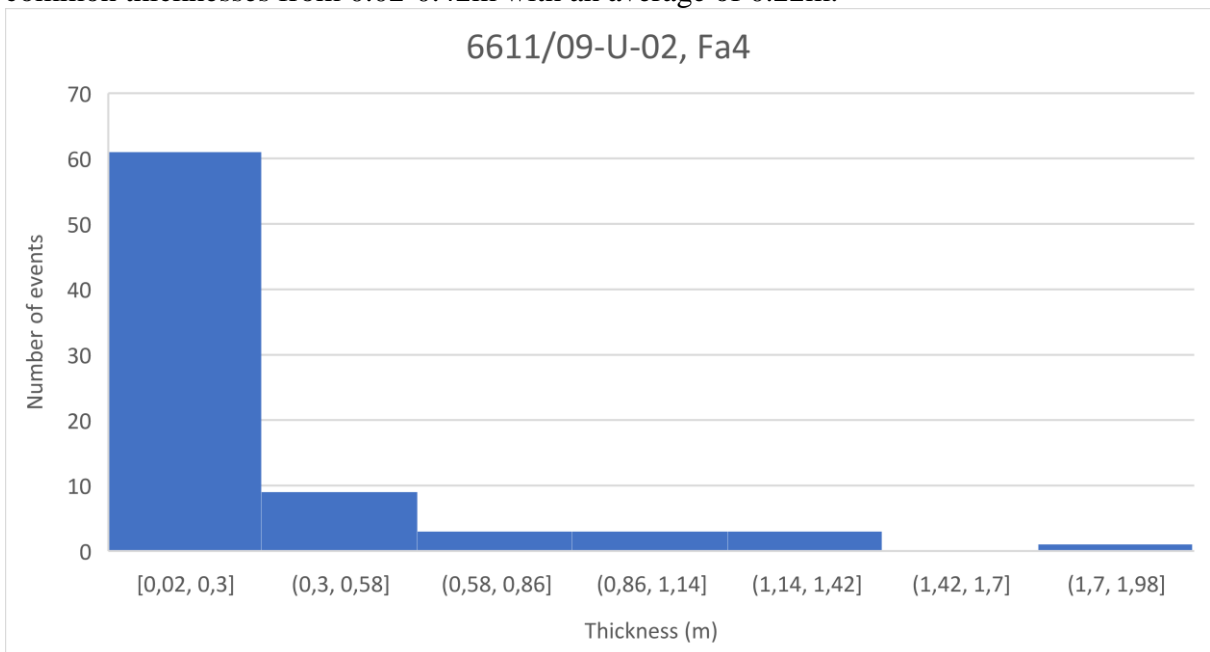


Figure 4.17: Histogram showing thickness distribution of Fa4, core 6611/09-U-02.

In the histogram of thicknesses of facies association 4 core 6611/09-U-02 (Figure 4.17), it is possible to see a similar trend as for core 6611/09-U-01 (Figure 4.16) with a range in thicknesses from 0.02m to around 2 metres for each deposited bed. There is again a decrease in number of events with increasing thickness so the heterolithic facies association can be observed as having most common thicknesses from 0.02-0.58m with an average of 0.26m. For the heterolithic facies association for both cores the average bed thickness is 0.24m.

#### Interpretation of depositional processes

The dark grey and grey mudstone are interpreted on basis of Lien et al. (2006) as hemipelagic mud, deposited in a quiet environment below storm wave base while the graded sandstone beds represent the distal deposits of dilute turbidity currents. The thin laminated clay and sand can also be evidence of background sedimentation in a storm-based system which generates the thin sand intervals.

For the thin bedded laminated sand, mud and gypsum there are several alternative depositional models that might be applied.

The first is a change in the environment from deep marine to shallow marine with a closed basin. Gypsum is generated by a sequence of evaporation of saltwater from the sediment into the atmosphere. This can happen in a closed basin where the water input is below the net rate of evaporation or by uplift above the water table (Bugge et al., 2002; Ramberg, 2008). The clear, sharp, thin sand layers and the double mud drapes can be interpreted as tidal environment with shallow water level. The second theory is that the heterolithic is deposited in the deep marine basial plain and the gypsum is transported from nearby source due to changes in sea level or tectonic activity. The third theory is that the gypsum is a result of diagenetic recrystallization after burial. Gypsum might originally be transported into the system by dilute turbidity currents after changed conditions in the sediment source are due to base level fall or tectonic activity. The changes in the source area result in evaporation events which subsequently is transported into the system (A. Næss 2018, pers.comm). During burial the gypsum/silt layers becomes recrystallized.



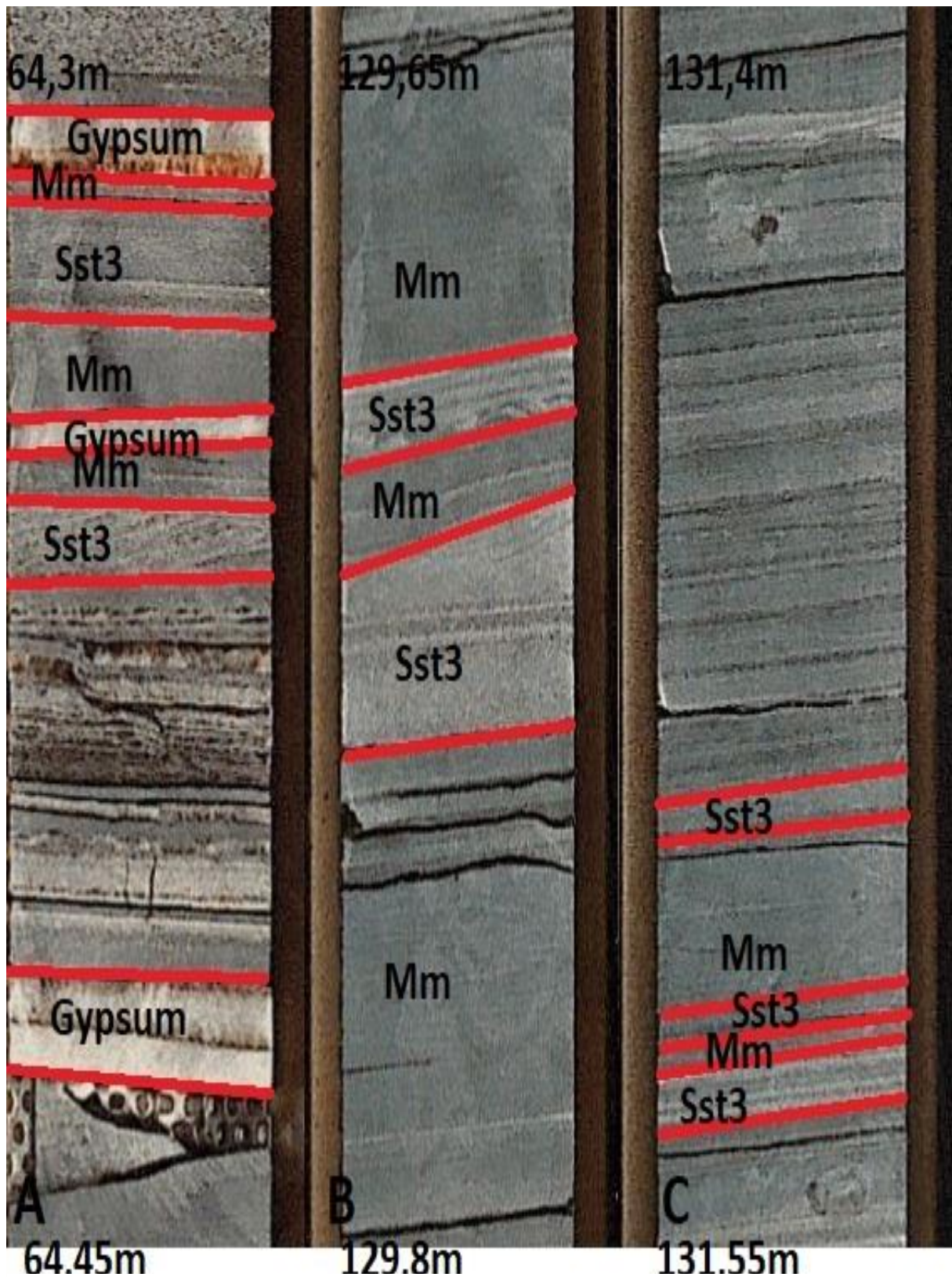


Figure 4.18: Heterolithic facies association. The red lines indicates base and top (if observed) of lithofacies. A) Thin bedded sand, silt, clay and gypsum (Core 6611/09-U-02, depth 64.3m). B) Thick bedded sand, silt and clay (Core 6611/09-U-02, depth 129.65m). C) Thin bedded sand, silt and clay (Core 6611/09-U-02, depth 131.4m).

## 5 Depositional model

### 5.1 Introduction

The interpreted facies and facies associations of well 6611/09-U-01 and 6611/09-U-02 show a variety of different depositional processes and environments. A motivation for introducing a refined depositional model is the application of sand body geometry and the lateral extent of the sediment beds in reservoir characterisation. In this chapter geometries and lateral extents of sand bodies and facies association is discussed and a depositional model is proposed. A correlation of well 6611/09-U-02 and 6611/09-U-01 is also performed based on similarities in the sedimentological logs, core photos and statistical analysis.

### 5.2 Thickness variations

Thickness trends of a facies association through a core are interpreted to be an expression of depositional events, development of basins, proximity to the source area and prograding vs retrograding system (A. Næss, 2018, pers. comm.). By looking at the thickness trends in core 6611/09-U-01 and 6611/09-U-02 it is therefore possible to describe a depositional model for the Helgeland Basin.

The thicknesses were measured in the interval 11m-111m for core 6611/09-U-01 and interval 195m-280.5m for core 6611/09-U-02. This interval is chosen to cover the 60m stratigraphic overlap in addition to approximately 40 metres of sediment to investigate trends in thicknesses. The same method as presented in section 4.2 is used for counting the thicknesses for each facies association. To look at the thickness variation through the core a statistical analysis of both a scatter plot and a histogram were performed. The plots were made by plotting the core depth towards the thickness of individual observations for each facies association. The histogram show observed number of events in the core for each depth interval, while the scatter plots show thickness variations through the core at certain depth. Both the histogram and the scatter plot are made for each main facies association. Due to few observations of facies association Fa3a and Fa3b, Fa4a and Fa4b they are counted as one alternatively as Fa3 and Fa4. In Section 5.2.1 and 5.2.2 thickness trends and frequency of depositional events for the different facies in core 6611/09-U-01 and 6611/09-U-02 will be discussed.

### 5.2.1 6611/09-U-01

*Fa1- debrite:* The debrite facies association is not observed in the first 30 metre of core 6611/09-U-01 so the first occurrence of the debrite facies is at 40.15m as seen on the histogram in Figure 5.1. From Figure 5.1 there can be seen that the greatest amount of events is from 86-109m with thicknesses ranging from 0.01-0.5m. The histogram and the scatter plot can be interpreted to have an increasing trend of events with increasing thicknesses as it gets deeper.

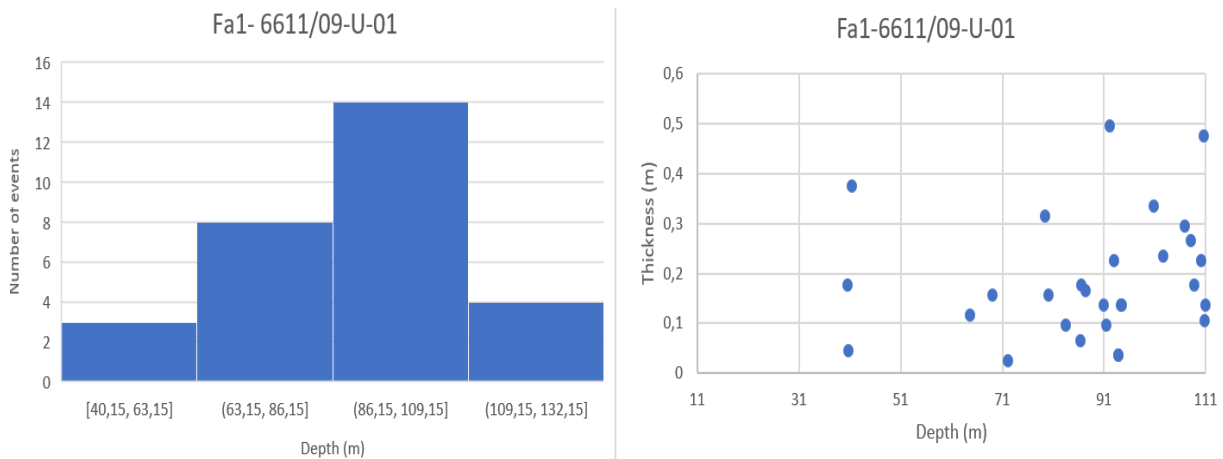


Figure 5.1: Left: Histogram showing number of observations for depth intervals of 13m for Fa1- Core 6611/09-U-01. Right: Scatter plot showing thickness variation vs depth for Fa1- Core 6611/09-U-01.

*Fa2- Turbidite:* From Figure 5.2 there can be see the thickness variations and distributions in the turbidite facies association (Fa2). From the histogram in Figure 5.2 there can observed that we have a normal distribution of facies in core 6611/09-U-01 with the highest number of events in the upper-middle interval (56-101.98m). At the upper part of the cored interval we can see from Figure 5.2 that the histogram show a low number of events, but the scatter plot show bed thicknesses up to 3m. With increasing depth, the number of interval increase, and the thickness of the Fa2 show a weak trend of thinning with a low average thickness (0.5m).

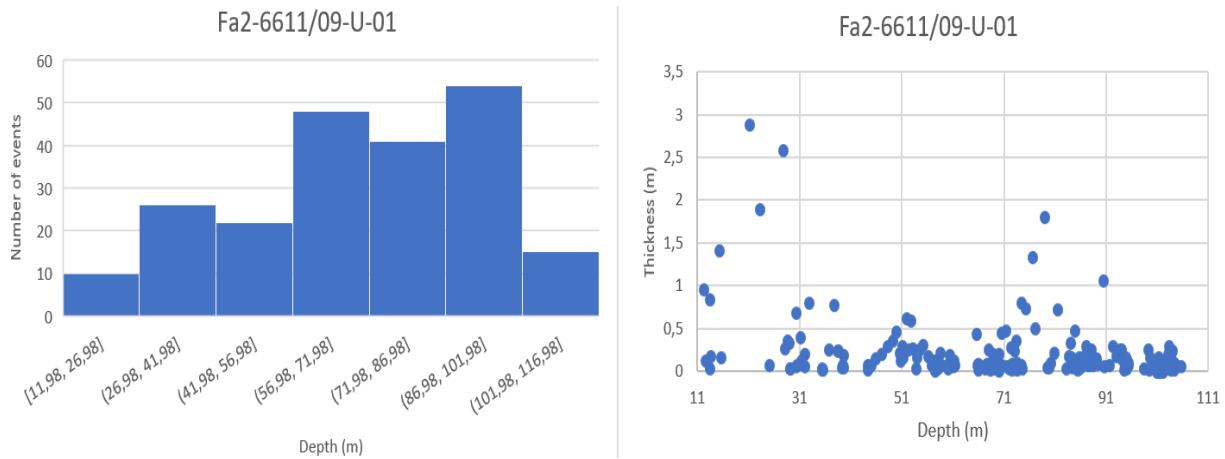


Figure 5.2: Left: Histogram showing number of observations for depth intervals of 13m for Fa2- Core 6611/09-U-01. Right: Scatter plot showing thickness variation vs depth for Fa2- Core 6611/09-U-0.

**Fa3- Transitional:** The histogram in Figure 5.3 show a clear trend of decreasing amounts of events with increased depth. From the scatter plot in Figure 5.3 there is possible to observe a weak trend of thinning with increased depth. The last occurrence of a transitional flow is at 17.59m with a thickness of 2.35m. The shallowest interval from 17.50 to 46.59m has an observed average thickness of 0.5m from Figure 5.3, while the average thickness for the whole core interval decreases through the core to approximately 0.25m as observed in Figure 5.3.

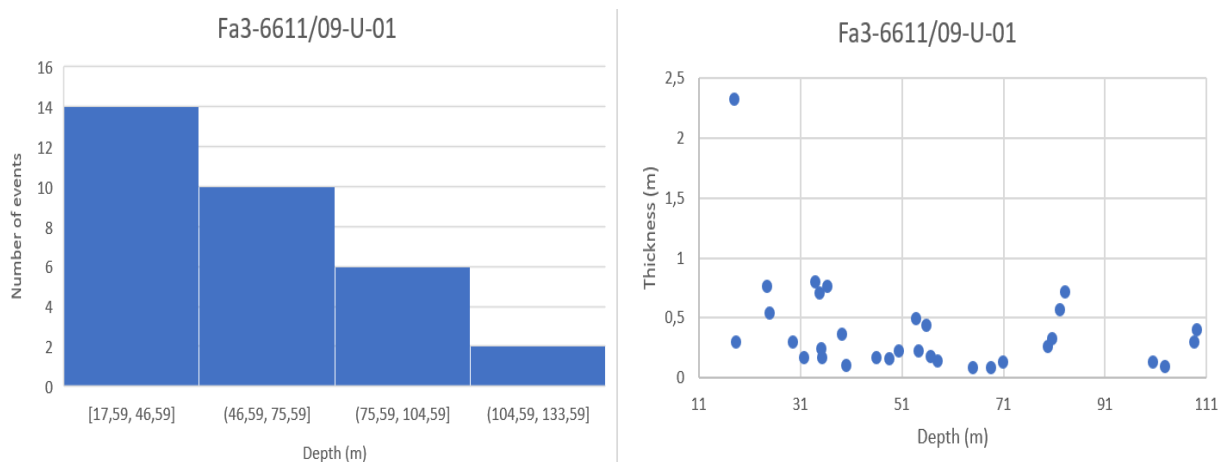


Figure 5.3: Left: Histogram showing number of observations for depth intervals of 13m for Fa3- Core 6611/09-U-01. Right: Scatter plot showing thickness variation vs depth for Fa3- Core 6611/09-U-01.

*Fa4- heterolithic*: From the histogram and scatter plot in Figure 5.4, Fa4 show a peak in thicknesses from 51-71, with the thickness ranging from 0.1-0.8 metre with average of 0.4m. The trend of the histogram and scatter (Figure 5.4) can be interpreted as when the bed is thick, the number of events is small. Alternatively, when the thickness is small the number of events are high.

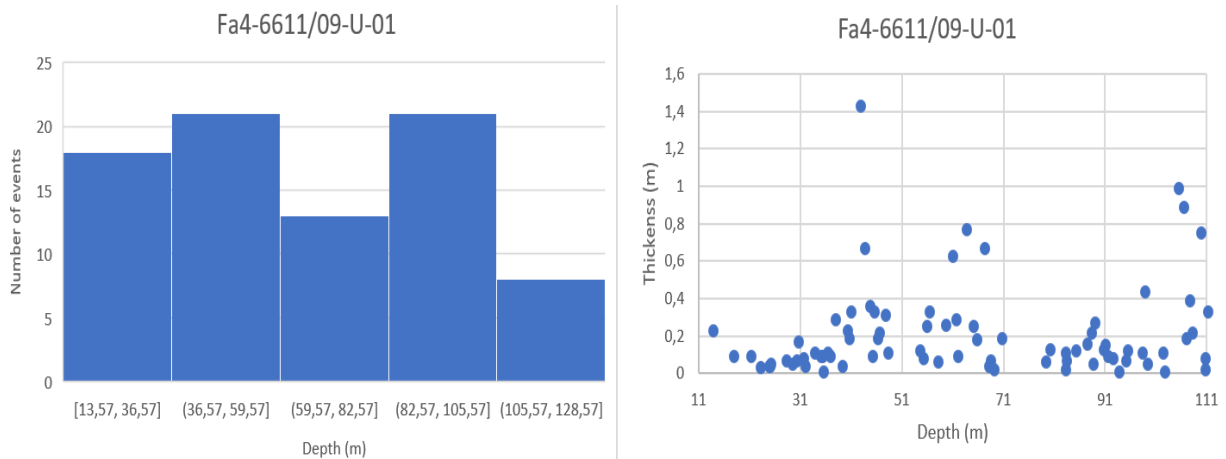


Figure 5.4: Left: Histogram showing number of observations for depth intervals of 13m for Fa4- Core 6611/09-U-01. Right: Scatter plot showing thickness variation vs depth for Fa4- Core 6611/09-U-01.

*Fa5- Hemipelagic*: Lithofacies Mm show from the histogram (Figure 5.5) a decrease in number of events with increasing depth. The scatter plot in Figure 5.5 shows a distribution of thicknesses with peak at 60m and thickness of maximum 0.8m. The average thickness for Mm is observed as 0.1m

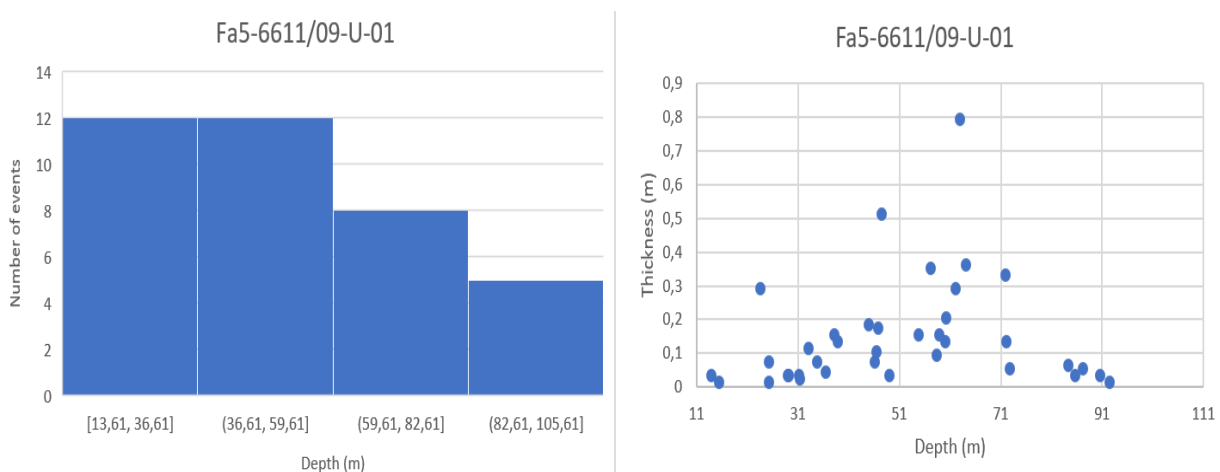


Figure 5.5: Left: Histogram showing number of observations for depth intervals of 13m for lithofacies Mm- Core 6611/09-U-01. Right: Scatter plot showing thickness variation vs depth for lithofacies Mm- Core 6611/09-U-01

### *Thickness variations for core 6611/09-U-01*

Figure 5.6 show a plot with calculated percentages of each facies in core 6611/09-U-01. The plot is made in the stratigraphic overlap interval which is between 11m and 70m for core 6611/09-U-01. The plot is made by calculating the percentage of each facies in a 1-metre window. All the percentages are plotted based on depth, so it is possible to see changes in the occurrence of the facies associations through the core.

By Figure 5.6, the histograms and the scatterplots it is possible to observe that the deepest part of the core interval is dominated by thicknesses of the heterolithics facies association. There are an alternation of turbidites and heterolithic facies associations until approximately 67.5 metres where the heterolithic gypsum layer is observed for some few metres. Above the gypsum interval there is observed thick packages (2-7metres) of alternatively heterolytic, turbidite and transitional facies association. The debrite and the hemipelagic facies association is never very dominant through the core.

# 6611/09-U-01

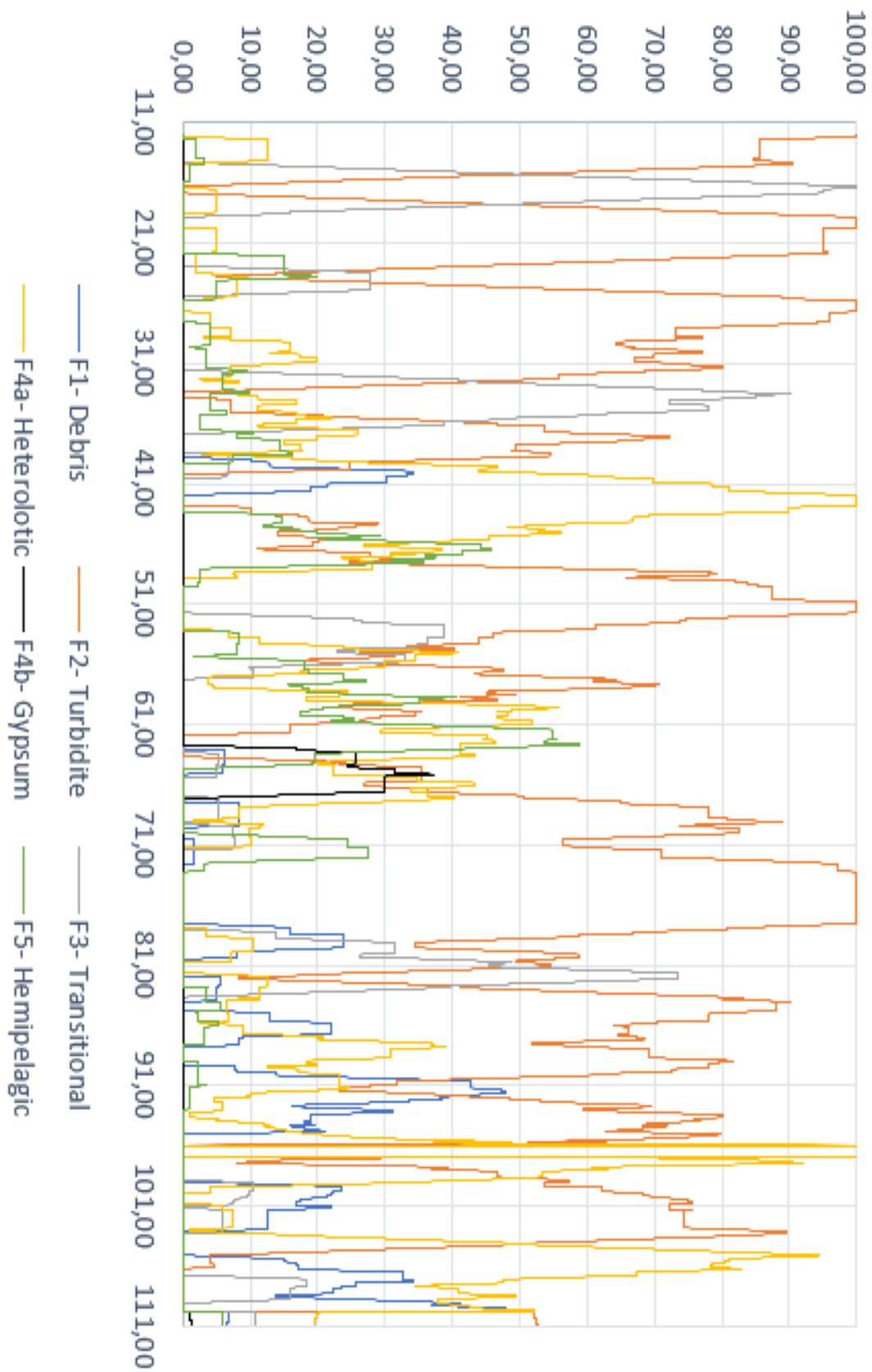


Figure 5.6: Distributions of facies associations through core 6611/09-U-01 calculated as percentages of each facies association.

### 5.2.2 6611/09-U-02

*Facies association 1- debrite:* Facies association 1 shows (Figure 5.7) that the observations of the debrite facies association is found in the 20cm upper part of the 6611/09-U-02 interval and the lower 30m part of the interval. From 225m to 255m deep there are no debrite facies associations observed. The histogram shows a maximum number of events from 258m deep with 15 observed events. The thicknesses range from 0.05 to 1.4 metre with an average thickness of 0.28 metre.

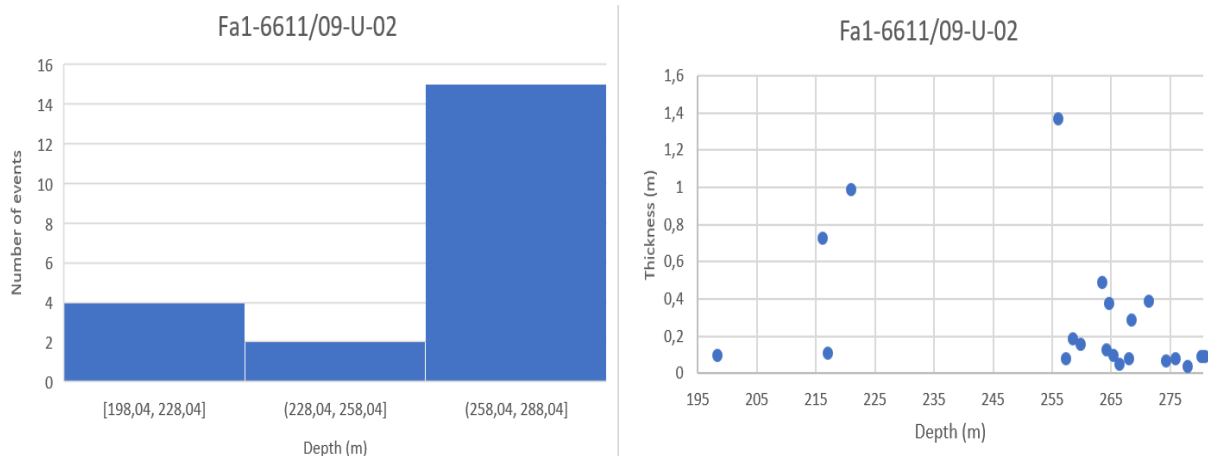


Figure 5.7: Left: Histogram showing number of observations for depth intervals of 13m for Fa1- Core 6611/09-U-02. Right: Scatter plot showing thickness variation vs depth for Fa1- Core 6611/09-U-02.

*Facies association 2- Turbidite:* The histogram in Figure 5.8 shows a distribution in core 6611/09-U-01 with the maximum number of events in the upper-middle interval (259.69-275.69m). The thicknesses of the facies association range between 0.01m- 2.75 metre with a maximum at a depth of 234m. The average thickness is around 0.05m with a weak trend of thinning with increasing depth.

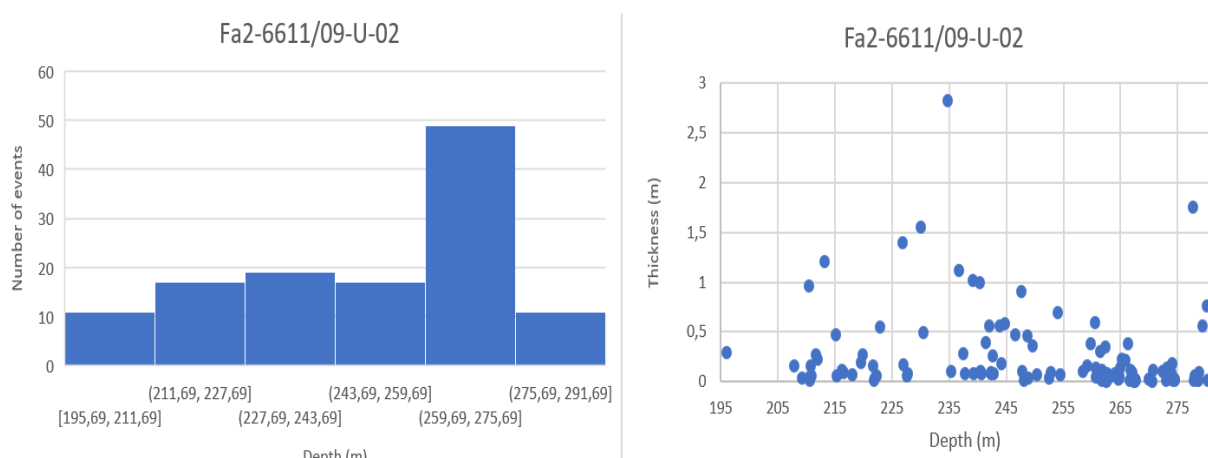


Figure 5.8: Left: Histogram showing number of observations for depth intervals of 13m for Fa2- Core 6611/09-U-02. Right: Scatter plot showing thickness variation vs depth for Fa2- Core 6611/09-U-02.



*Facies association 3- Transitional flow deposit:* The histogram in Figure 5.9 shows that the last occurrence of a transitional facies association is at 213.54m. From the scatter plot in Figure 5.9 it is possible to interpret a weak trend of thickening with decreasing depth. The first occurrence of transitional flow is observed in the interval 213.54-243.54m with 6 events. By the scatterplot in Figure 5.9 it is possible to calculate an average thickness for Fa3 in core 6611/09-U-02 to 0.3 metre.

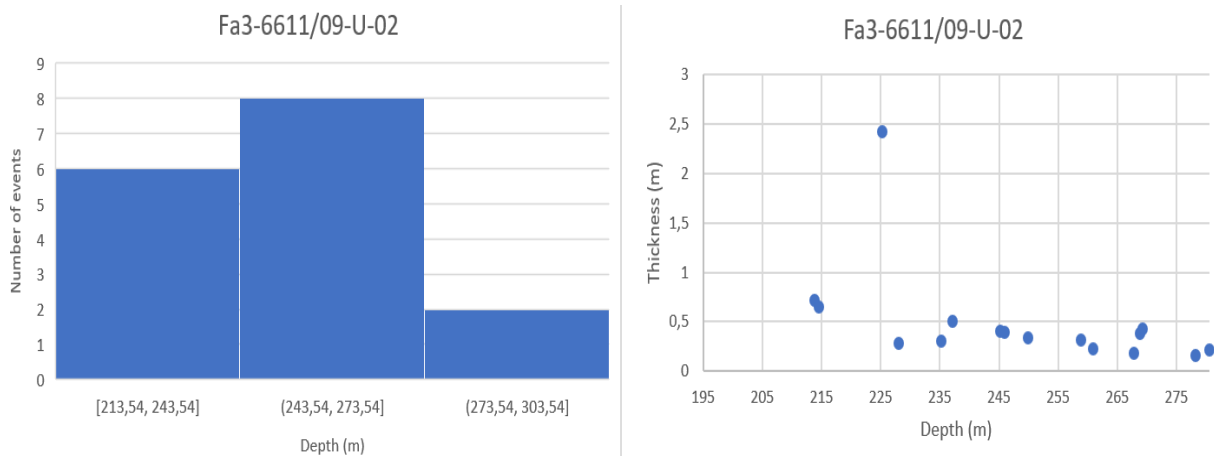


Figure 5.9: Left: Histogram showing number of observations for depth intervals of 13m for Fa3- Core 6611/09-U-02. Right: Scatter plot showing thickness variation vs depth for Fa3- Core 6611/09-U-02.

*Facies association 4- heterolithic:* From the histogram and scatter plot in Figure 5.10, facies association 4 shows a normal distribution of events through depth. The average thickness of facies association 4 determined from the scatter plot (Figure 5.10) is 0.03m. The distribution of the facies association thickness shows some peaks through the core but is overall quite uniform.

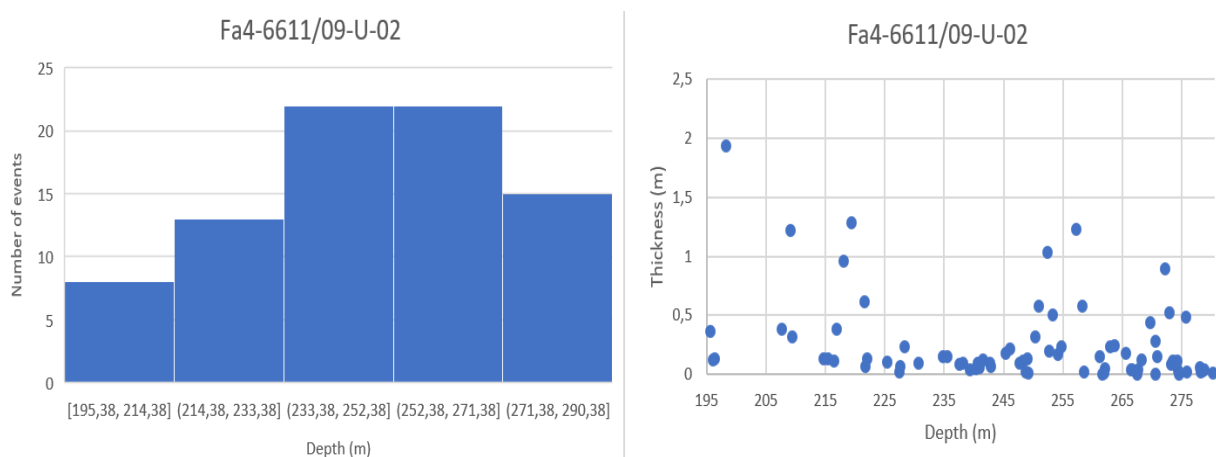


Figure 5.10: Left: Histogram showing number of observations for depth intervals of 13m for Fa4- Core 6611/09-U-02. Right: Scatter plot showing thickness variation vs depth for Fa4- Core 6611/09-U-02.

*Facies 5- Hemipelagic:* Facies 5 shows from the histogram (Figure 5.11) a maximum number of events between 232.03m and 253.03m with 15 events while the other depths have evenly distributed events through the core with 3 events per 13m. The scatter plot in Figure 5.11 shows a range of thicknesses from 0.02 to 0.25m with the thickest beds in the deepest part of the core. The average thickness for Facies 5 for core 6611/09-U-02 is 0.05m.

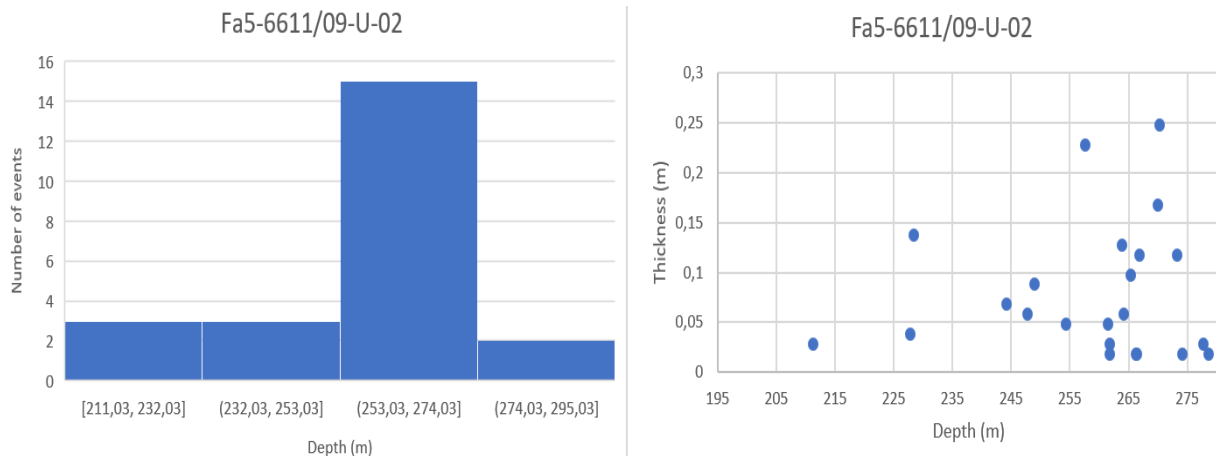


Figure 5.11: Left: Histogram showing number of observations for depth intervals of 13m for Fa5- Core 6611/09-U-02. Right: Scatter plot showing thickness variation vs depth for Fa5- Core 6611/09-U-02.

#### *Thickness variations for core 6611/09-U-02*

Figure 5.12 show a plot with calculated percentages of each facies association in core 6611/09-U-02. The plot is made by the same method described in section 5.2.1: Thickness variations for core 6611/09-U-01.

Based on Figure 5.12, the histograms and the scatterplots it is possible to observe a turbidite facies association in the deepest part of the investigated core interval. On top of the turbidite facies association the heterolytic facies association with gypsum interbedded is observed. On top of the gypsum interval there are a series of intermediate thick (1-3metre) heterolithic and turbidite facies association sequences. There are also observed some thin debrite facies in the interval. From 245 to 225 there are a 20-metre thick interval dominated by turbidite facies association. The upper part of the core interval are again alternatively dominated by heterolithic and turbidite facies association.

# 6611/09-U-02

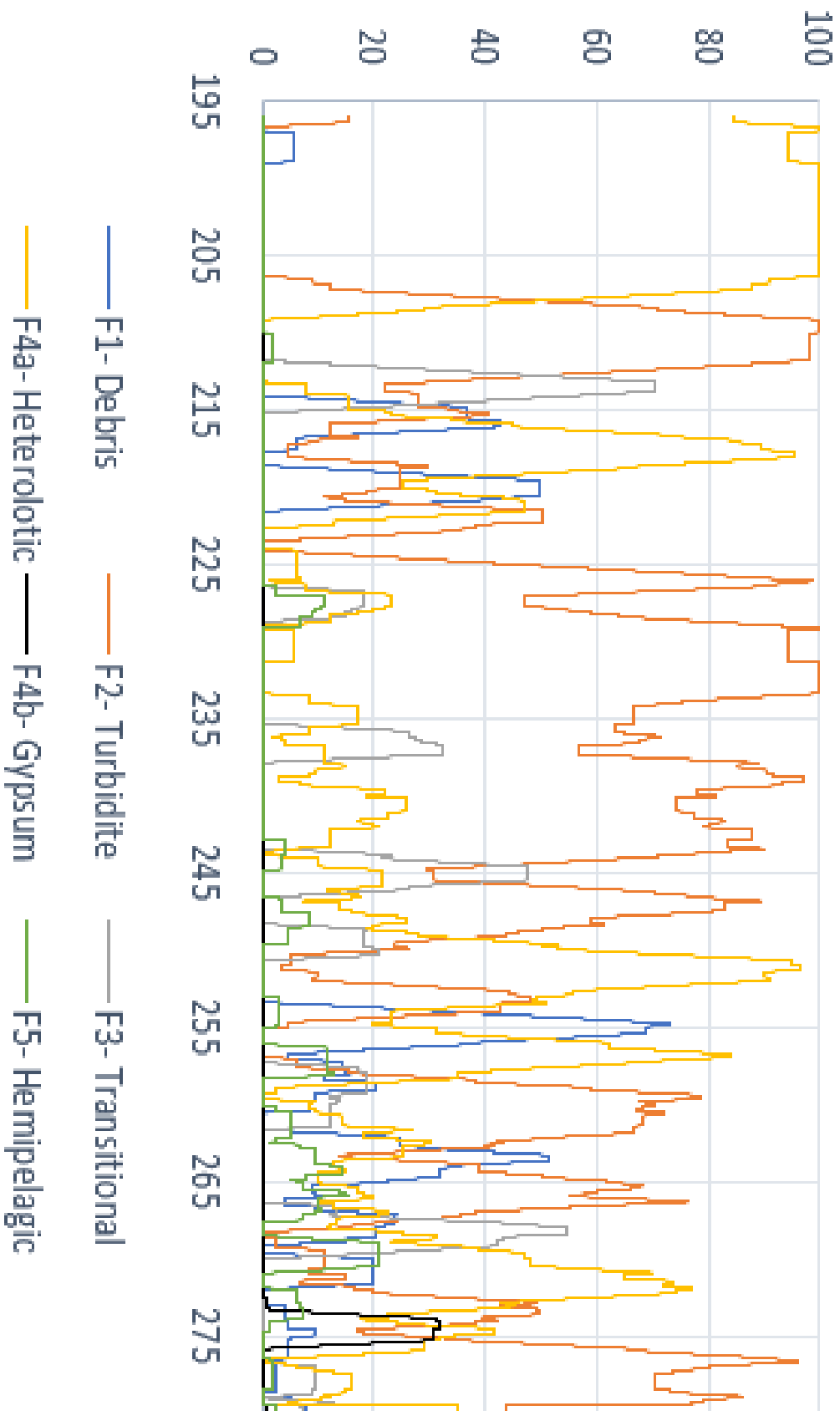


Figure 5.12: Distributions of facies associations through core 6611/09-U-02 calculated as percentages of each facies association.

### 5.3 Correlation

Cores 6611/09-U-01 and 6611/09-U-02 were drilled with a distance of 1200 metres from each other with a 60 metre stratigraphic overlap. In core 6611/09-U-01 and 6611/09-U-02 a layer with gypsum is observed between 270 and 275 metres below drilled seabed. Figures 3.5 and 4.18 show the core photos showing the gypsum layer and the sediment above and below. Based on the observations described in chapter 5.2 and the interpreted sedimentological logs, a conceptual correlation of wells 6611/09-U-01 and 6611/0 -U-02 will be presented in this section.

#### 5.3.1 Interpretation of gypsum

In general, the formation of gypsum is thought to be by evaporation processes in hypersaline basins, sabkha and playas, but in nature there are several ways to generate gypsum. In this thesis three possible models for the generation of gypsum are considered. The models were presented in brief introduction in section 3.2.4: Heterolithic facies association but will now be presented in further detail.

The first model predicts that the gypsum is an evaporitic gypsum deposited in a shallow marine environment with a closed basin. The gypsum is generated by evaporation of saltwater from the water and the sediment into the atmosphere. This can happen in a closed basin where the water input is below the net rate of evaporation or by uplift above the water table (Bugge et al., 2002; Ramberg, 2008).

The second model present the gypsum as transported. The gypsum is deposited one place and transported into the deep marine environment. The gypsum is formed in a shallow environment by evaporation of saltwater from the sediment into the atmosphere, but after deposition it is transported from the original deposition area into the deep marine environment (A. Næss 2018, pers.comm.).

The third model is based on a combination of diagenesis and transportation. Changes in the sediment source can be a result of base level fall or tectonic activity. If the changes in the source area result in evaporation events, dilute turbidity currents can subsequently transport the mixed silt and evaporite material into the deep marine system. When the gypsum/silt layers are deposited and buried the recrystallization takes place.

In this thesis gypsum is found in a mid-lower Triassic interval with heterolithic sand, silt and clay above and below. From Figure 5.13 and Figure 5.14 there is not observed any changes in

the depositional environment either on the cores or on the statistical analysis. The gypsum layers are observed in the cores as a horizontal bed with a clear lower boundary. There are not observed a clear boundary top of the gypsum interval. By looking at the three theories presented earlier, it is possible to interpret that the gypsum is not generated by evaporation of saltwater into the atmosphere. It is difficult to imagine that the depositional environment will shift that abruptly from a deep marine environment depositing turbidites and heterolithic deposits to a very shallow marine/closed basin. The sediments below and above the observed gypsum package are also interpreted to be have been deposited in a deep marine environment so since there are no observed changes in the depositional environment in the core the gypsum is interpreted to have been generated by a different process.

The gypsum could have been deposited in a sabkha environment where there are possibilities for evaporation of saltwater to the atmosphere and then after deposition it could have been transported by a tectonic influence or changes in the sea level. Gypsum is a soluble mineral which dissolves over time in water so if the gypsum in core 6611/09-U-01 and 6611/09-U-02 is re-transported it must have been buried fast to not be dissolved.

Since the gypsum is observed in so horizontal beds it is interpreted it as a part of the original sediment packages which in turn were affected by a diagenetic process. When the evaporitic dilute turbidity currents are transported from the source area into the deep marine environment the turbidity currents loose strength and deposit sediment. the deposited sediment are buried, and a recrystallization occur during burial or after. The recrystallization of the evaporitic sediments are resulting in a horizontal gypsum bed. This theory is supported by observation from thin sections showing recrystallized gypsum grains (Figure 3.5).

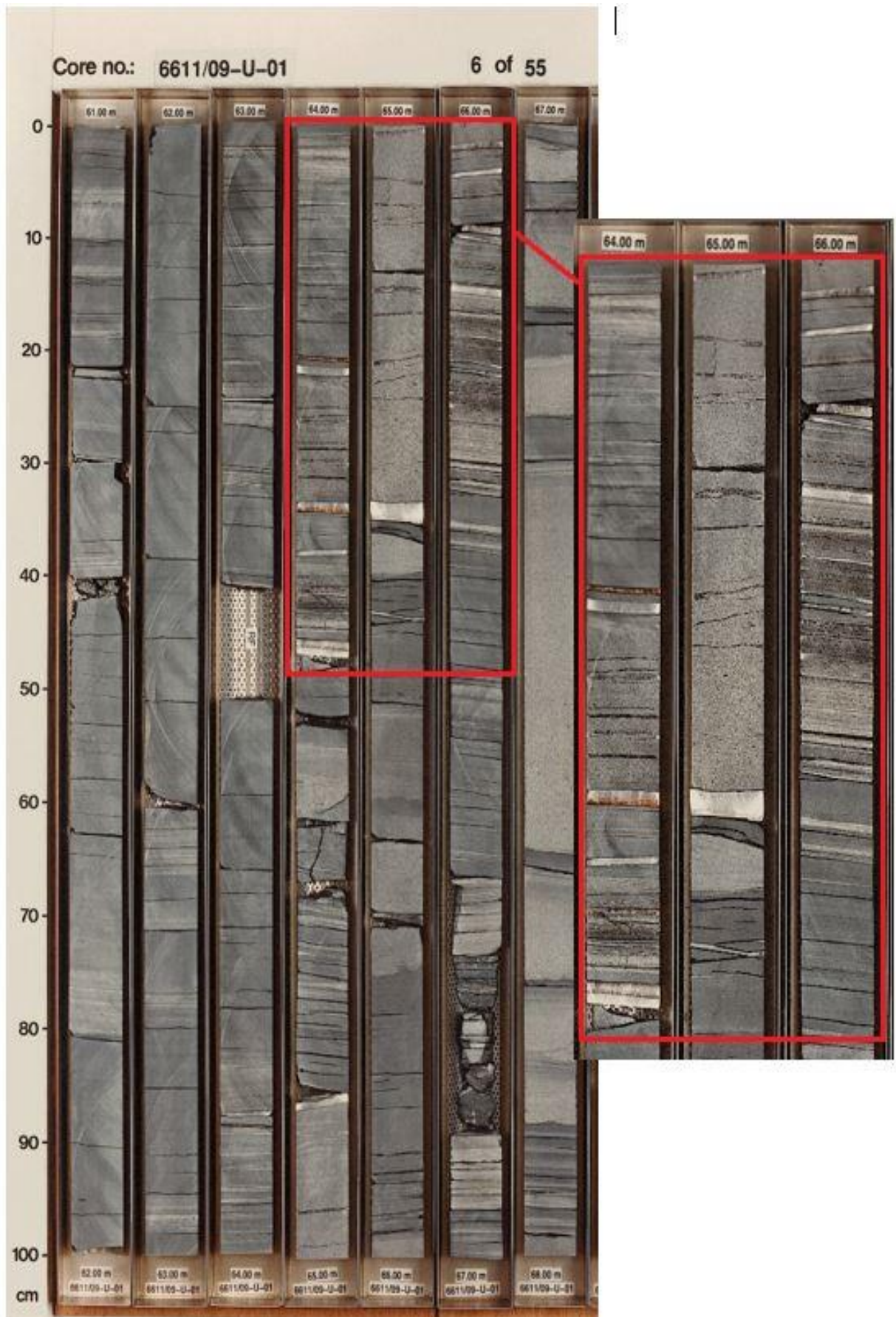


Figure 5.13: Core photos of core 6611/09-U-01 with gypsum intervals in red.

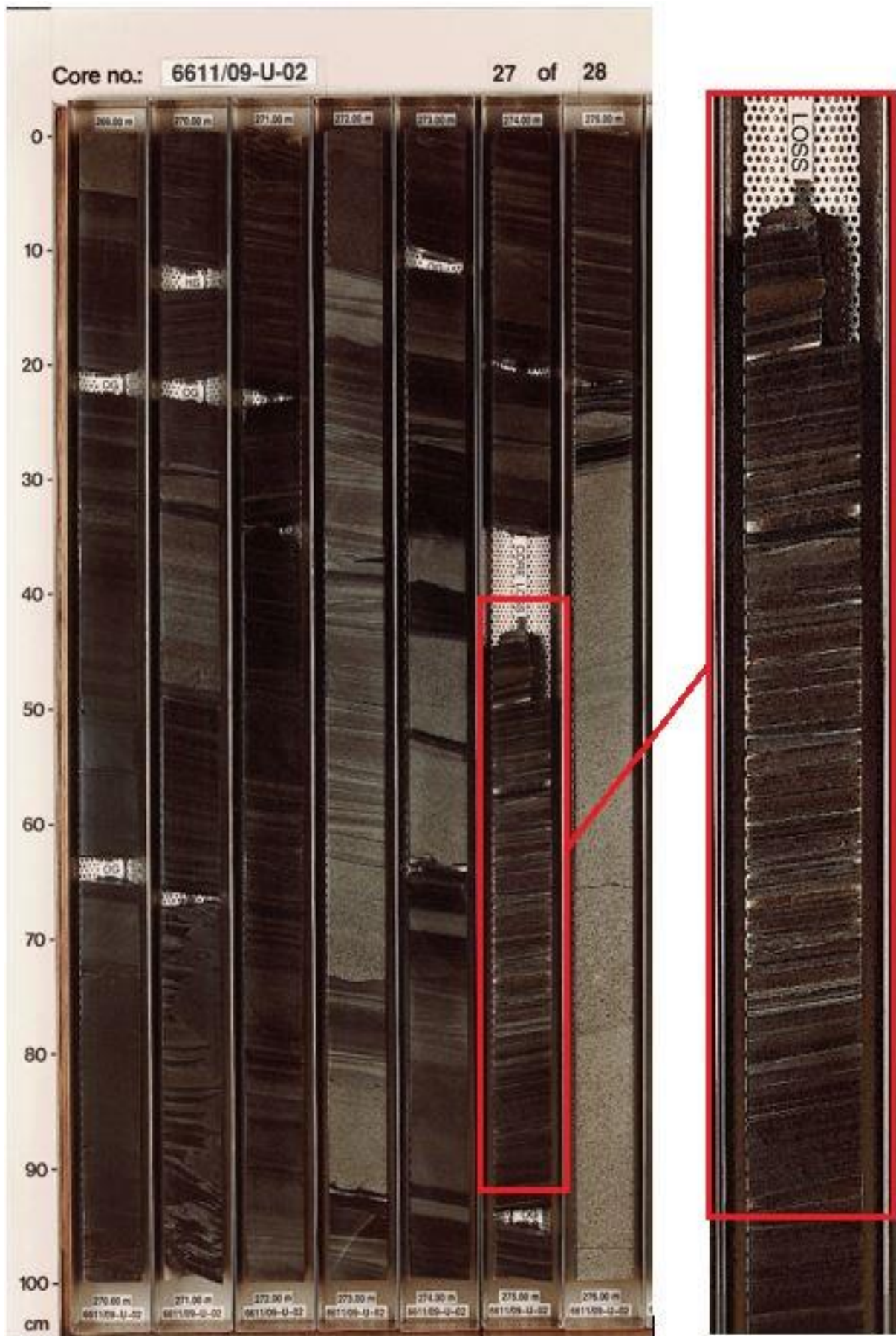


Figure 5.14: Core photo of core 6611/09-U-02 with gypsum interval marked in red.

Based on the interpreted process forming gypsum it is believed in this thesis that the gypsum is a recrystallized layer in the sedimentological package transported from a shallow marine environment by dilute turbidity currents. It is therefore possible to correlate based on the first occurrence and the last occurrence of gypsum. In this thesis the correlation will be based on the first occurrence of gypsum where it is possible to observe a clear boundary.

### 5.3.2 Correlation based on facies associations

Figure 5.15 show a plot with calculated percentages of each facies. The plot is made by the same method presented in section 5.2.1: Thickness variations core 6611/09-U-01. In this plot the interval is limited to the stratigraphic overlap of core 6611/09-U-01 and 6611/09-U-02 in the interval: 11-70 metre for core 6611/09-U-01 and 225-2805. metre for core 6611/09-U-02. Based on the dominant facies association on the plot it is possible to correlate the cores. In the correlation the lithofacies associations Fa3a and Fa3b are grouped together as there are only a few observations of each and interpreted as similar depositional process.



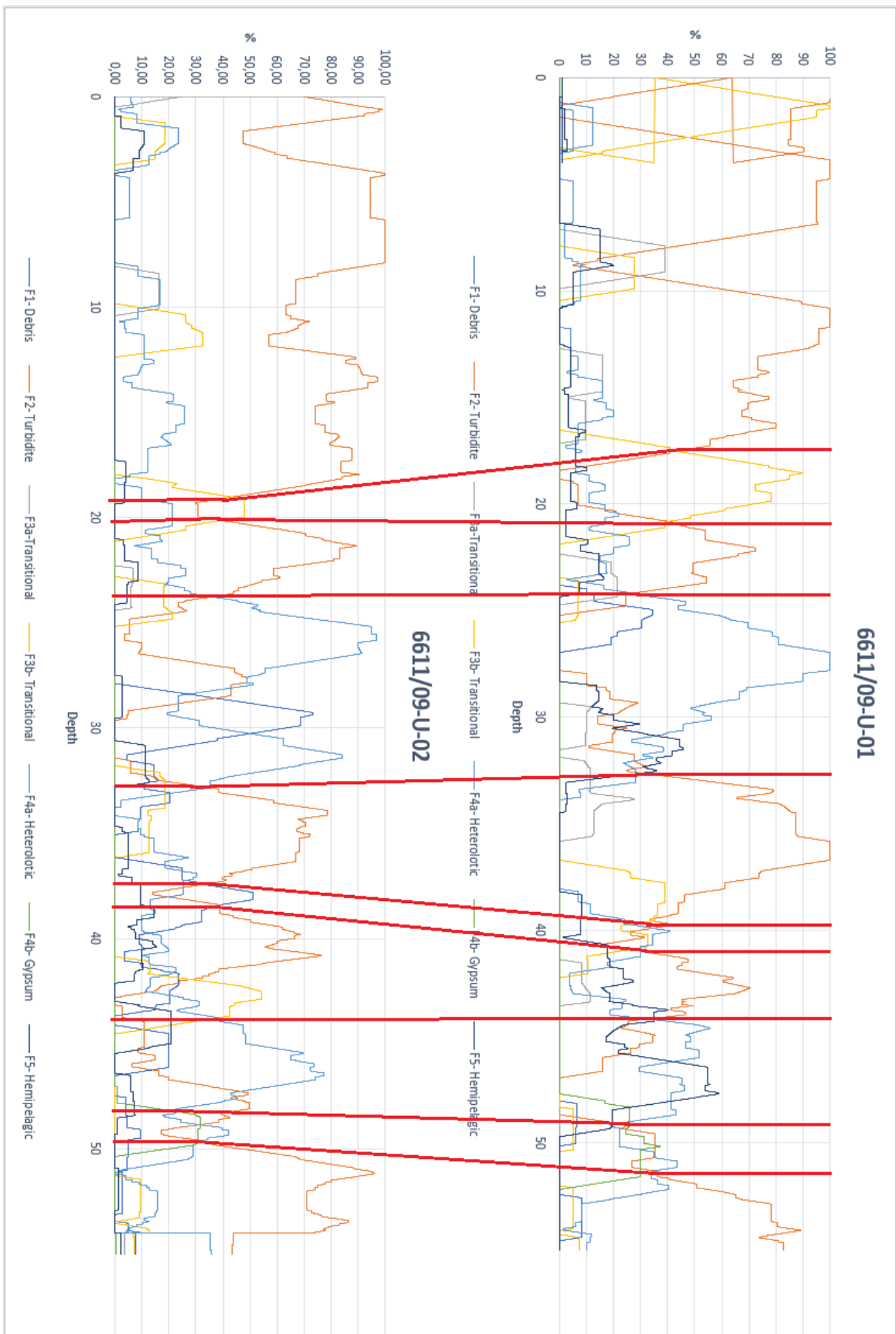


Figure 5.15: Correlation of core 6611/09-U-01 and 6611/09-U-02 based on the percentage of each facies association observed.

From the correlation of core 6611/09-U-01 and 6611/09-U-02 from Fig 5.15 it is observed that the base of the overlap succession is observed as a thick turbidite sequence. Because of the great thickness of the bed is interpreted to be a thick fining-up turbidite sequence deposited in a channel. The heterolithic silt, clay and gypsum sequence (Fa4b) is deposited on top of the turbidite sequence. This is interpreted to have been deposited on a basin plain with dilute turbulent flows transporting silt and evaporitic minerals to the system. The 1-5m thick heterolithic gypsum layer is overlain by a series of intermediate thick (1-5m) turbidites in alternation with heterolithic intervals. This sequence is interpreted to have been deposited as thin turbidites on a lobe deposit while the thinner, more clay rich heterolithic intervals are deposited more distally from the source on a basin plain. Between 32-37 metres there are some thick packages of thick fining up turbidites interpreted to be deposited in a channel. Between 20-30 metres there is again a heterolithic interval with thin layers of silt, fine sand and clay in alternation interpreted to be deposited as a background process. In the upper part of the overlap interval there are thick intervals of fining up turbidites. Here there is a larger amount of coarser grained material which can be interpreted as channel deposition, close to the source. The distinct peaks for core 6611/09-U-01 plotted at depth 2m and 10 metres are interpreted as a result of wrong interpretations of the sedimentological cores due to similarities in many transitional and turbidite facies associations.

### 5.3.3 Correlation based on the sedimentary logs

Another way to correlate the two wells is by using the drawn sedimentological logs. The logs are drawn on a 1:500 scale where the average grainsize, and lithology are used to combine facies associations. Facies association Fa2 (turbidite) and Fa3 (transitional) are grouped together as one based on the high sand ratio and similar flow processes, while Fa4 (heterolithic) and Fa5 (Laminated mudstone) are grouped based on the high mud ratio and similar depositional processes. Fa4b are marked on the log and used for the base of the correlation since it is assumed in this thesis that the first occurrence of the gypsum is the same layer in both core 6611/09-U-01 and 6611/09-02.

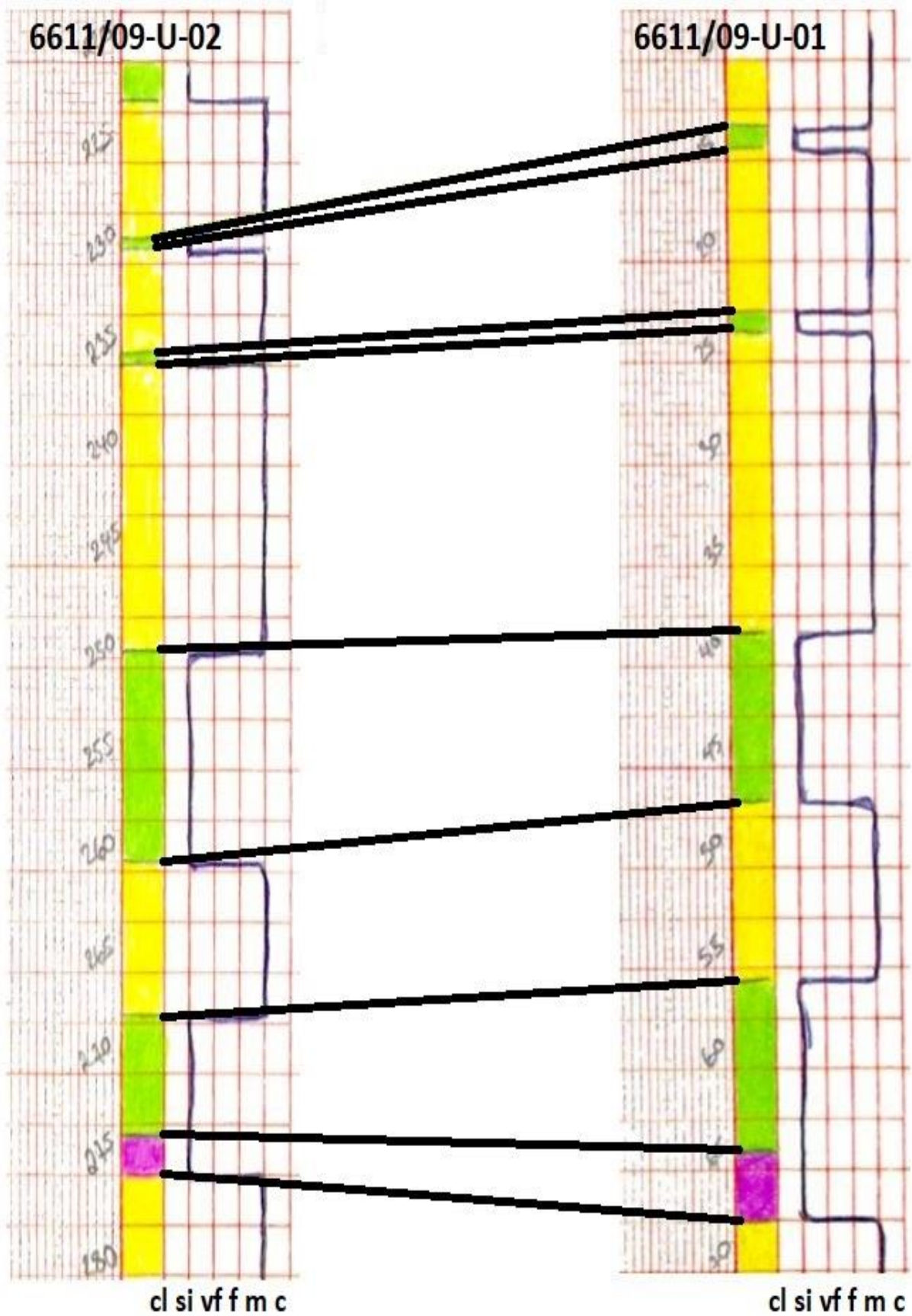


Figure 5.16: Correlation of core 6611/09-U-01 and 6611/09-U-02 based on interpreted facies associations. Scale 1:500. Black lines show correlation lines.

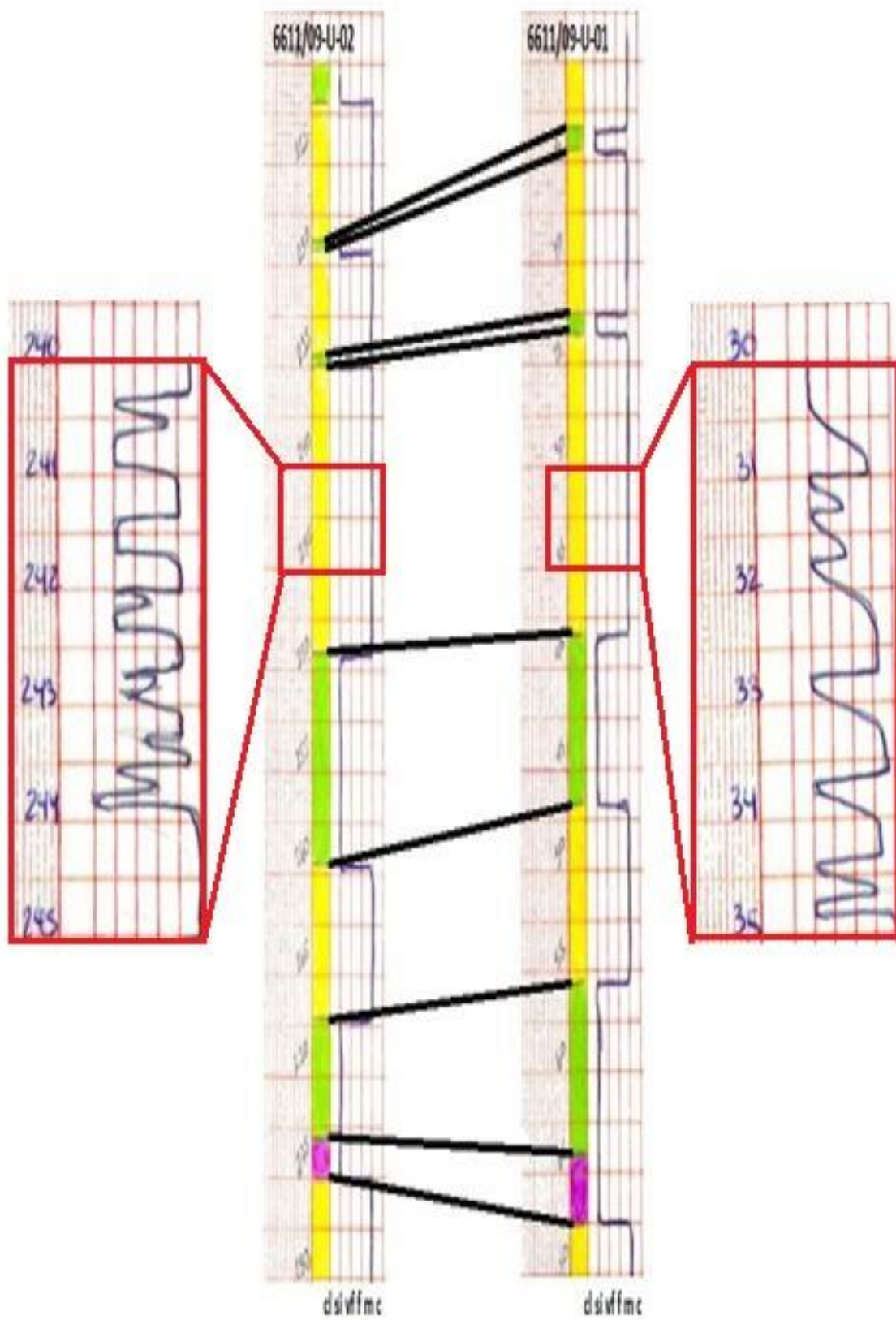


Figure 5.17: Correlation based on sedimentological log. Area in red show sedimentological log in scale 1:100.

As seen on Figure 5.16 there is a change in sand dominated and mud dominated sediment throughout the overlap interval for core 6611/09-U-01 and 6611/09-U-02. The translation from a sand dominated to a mud dominated and back to a sand dominated again can be interpreted as a translation from a setting with high energy, to a setting with lower energy and then back again. Within a turbidite system there are a lot of local variations in a deposit due to different energy setting. The transportation energy can be a result of change in sea level, lobe shifting, tectonic activity or sediment input from land.

What is evident from the observations above for core 6611/09-U-01 and 6611/09-U-02 is that sand bodies are largely correlatable along this transect. However, if the correlation were performed in a larger scale than 1:500 more local variations are observed as shown in Figure 5.17. This can be due to local tectonics activity, sediment input from land or lobe shifting.

The correlation in Figure 5.16 is based on the first appearance of gypsum, but it is also possible to correlate based in the last occurrence of gypsum or any other bed in the sedimentological package.

#### 5.4 Conceptual model

Core 6611/09-U-01 and 6611/09-U-02 are located offshore Mid-Norway in the Helgeland Basin. In the Early Triassic, the Helgeland basin was affected by subsidence due to the break-up of Pangaea which generated a deep marine basin with extension from W to E. The continent was located to the east of the basin with the sediment influx from east (Figure 2.5).

In this thesis 4 facies associations and hemipelagic mud were identified which were interpreted in terms of depositional processes. These processes can be interpreted to have deposited sediment in various parts of a deep marine system. As can be seen from the interpreted log (Appendix 8.3-8.8) there is a stacking pattern with thin fining up turbidite sequences, alternating with thick fining up turbidite sequences. In between the thick turbidite sequences there are thin layers of silt, clay and thin turbidite sand in alternation. The following sections will discuss the facies association and interpret them in a deep-marine environment.

### 5.4.1 Deep-marine system

Figure 5.18 shows a deep-marine system building out of the continent and shelf by a slope leading into the basin floor.

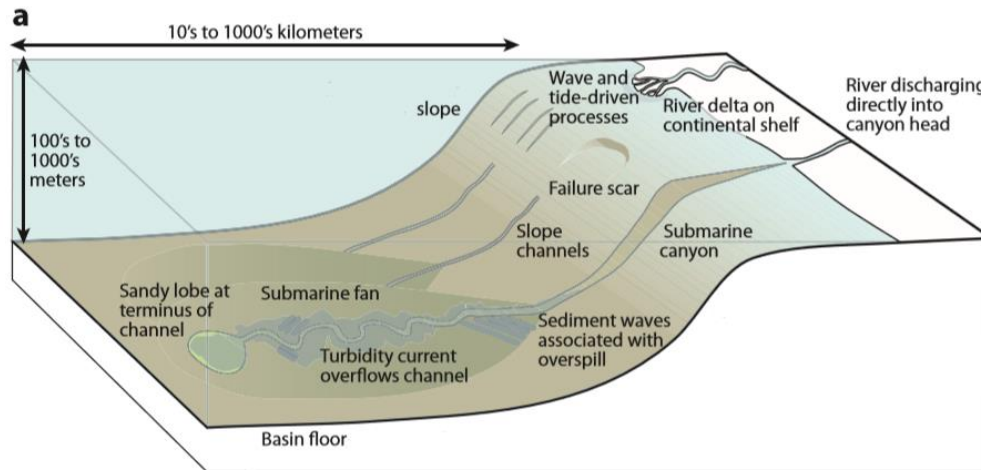


Figure 5.18: Schematic model of a deep-marine system, Modified from Meiburg and Kneller (2010).

The slope leading from the shelf into the deep marine system is a place for generation of debris flows. When a mass is mobilized as a consequence of slope collapse or channel margin collapse, a debris flow can be generated. Fa 1 is interpreted as a debrite facies association described in association with submarine slopes.

A submarine fan consists of canyons, channels and lobes as presented in chapter 2.4: Submarine fan. The turbidite facies association is interpreted as high-density turbidites that were deposited in the proximal part of the submarine fan close to the source area while the low-density turbidites are deposited in the more distal part of the lower submarine fan complex. The structureless coarse sandstone (facies Sst1) observed in this thesis is interpreted as a proximal lobe or channel deposit, while the finer grained sandstone with ripples and lamination (Sst3) is interpreted as a low-density turbidite deposited more distally by a decrease in energy. Thin fining up turbidite sequences interpreted as facies Sst3 can be interpreted as a low-energy turbidite deposited in a lobe environment (Figure 5.19). The coarser grained amalgamated turbidites interpreted as facies Sst1 are observed thick bedded which can be interpreted as deposited in a proximal channelized environment.

The transitional facies association (Fa3) is interpreted as a laminar debris flow in transformation into a more turbulent flow with increased water content. Fa3 is interpreted deposited in an environment from a transition between slope/channel/lobe.

In a submarine fan environment with channels and lobes fine grained sediments will be deposited from suspension between the active channels and lobes and on the basin plain in the outer fan. Facies associations 4 and 5 are characterized by combinations of mud, silt and very fine sand generated from hemipelagic settling and/or dilute turbidite currents or storm-based sedimentation. Even though the facies are interpreted in a similar way, the hemipelagic mud without any sandstone sheets suggests a more distal environment than the one described for Facies association 4 (heterolithic facies). The hemipelagic sedimentation reflects extended periods of abandonment of the fan system with low energy. Extended periods of hemipelagic sediment deposition in a submarine fan environment can be related to sea level rise as one example.

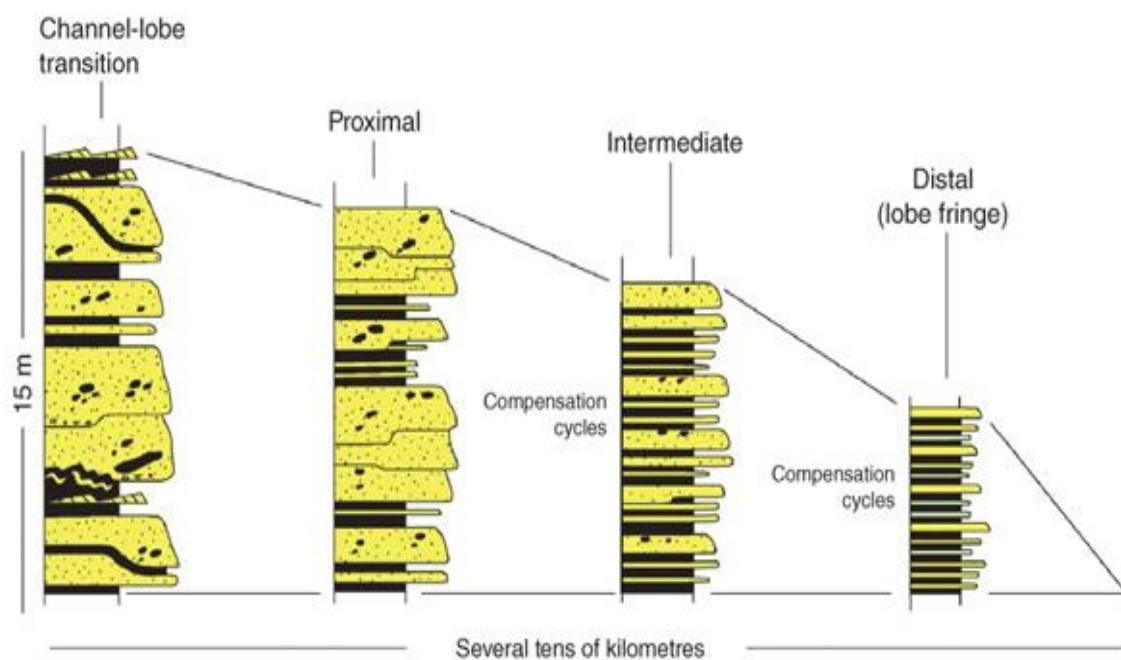


Figure 5.19: Different turbidite deposits with interpreted depositional environment. From Pickering et al. (2016).

#### 5.4.2 Conceptual model for the Helgeland basin

Interpretation of the geological history, sedimentary logs, the statistical analysis and the facies suggest a deep-marine system with source area located east leading out to a submarine fan. The submarine fan is characterized by fining up turbidites and intervals of silt and mud.

From the scatter plots in section 5.2.1 and 5.2.2 a weak trend in thickness variation is observed for some of the interpreted facies associations. In both core 6611/09-U-01 and 6611/09-U-02 it is possible to observe a weak thickening with decreasing depth for facies associations Fa2 and Fa3. It is assumed that if the Helgeland basin is a prograding system (outbuilding of strata in sea-ward direction) it is possible to observe a thickening of the facies beds with decreasing depth in core.

In the studied cores changes are observed in frequency of the interpreted facies associations, and specifically there is an increase in observed turbidites towards the top of the cores. The increased number of turbidite sequences can be a result of changes in source area from the coastline with a lateral outbuilding of the source area and a new feeder channel or as a consequence of increased sea level.

Figure 5.20 and 5.21 show a vertical stacking pattern of turbidite sand and heterolithic mud with interpreted correlation and lateral extent of the layers. Figure 5.20 shows the vertical section in a 1:500 scale where it is possible to see the continuation of the layers in both the cores. Figure 5.21 shows in more detail the middle part of Figure 5.20 at a 1:100 scale where it is not possible to correlate all layers since many of the small layers are pinching out.

It is reasonable to say that there are too few quantitative data to be certain about the orientation of the system, but some weak trends are observed. The thickening of turbidite sand packages, increased frequency of turbidites and difficulty in correlating on a small scale can be interpreted as a prograding or an aggradational system with proximal fans for the investigated interval.

The combination of facies and the vertical trend in facies proportions suggest the system to be a proximal part of a larger fan system or a set of smaller aggradational fans. A small-scale fan system stacked in an aggradation pattern is favoured here as the conceptual depositional model for the Helgeland basin. The discussion for choosing a fan system is due to the large-scale sand packages interpreted as turbidite sand in alternation with the heterolithic background sedimentation. The interpretation of a small-scale system is due to significant difficulty in correlating layers on a 1:1 scale. The observation that individual gravitational



flows deposits cannot be correlated confirms this theory. Figure 5.22 shows a proposed conceptual model for the Helgeland basin.

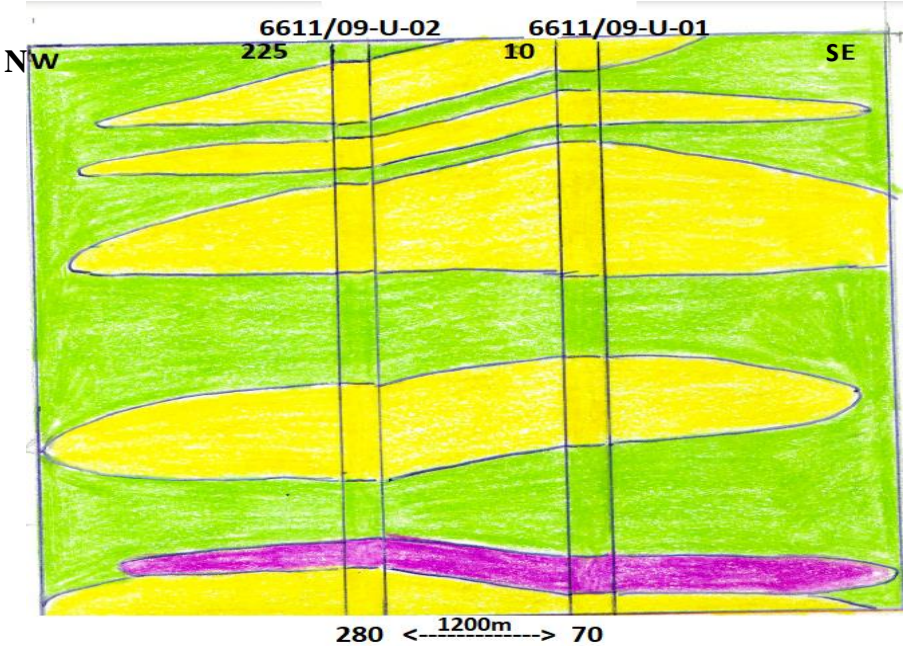


Figure 5.21: Vertical section of interpreted stacking pattern from core 6611/09-U-01 and 6611/09-U-01 on a 1:500 scale.

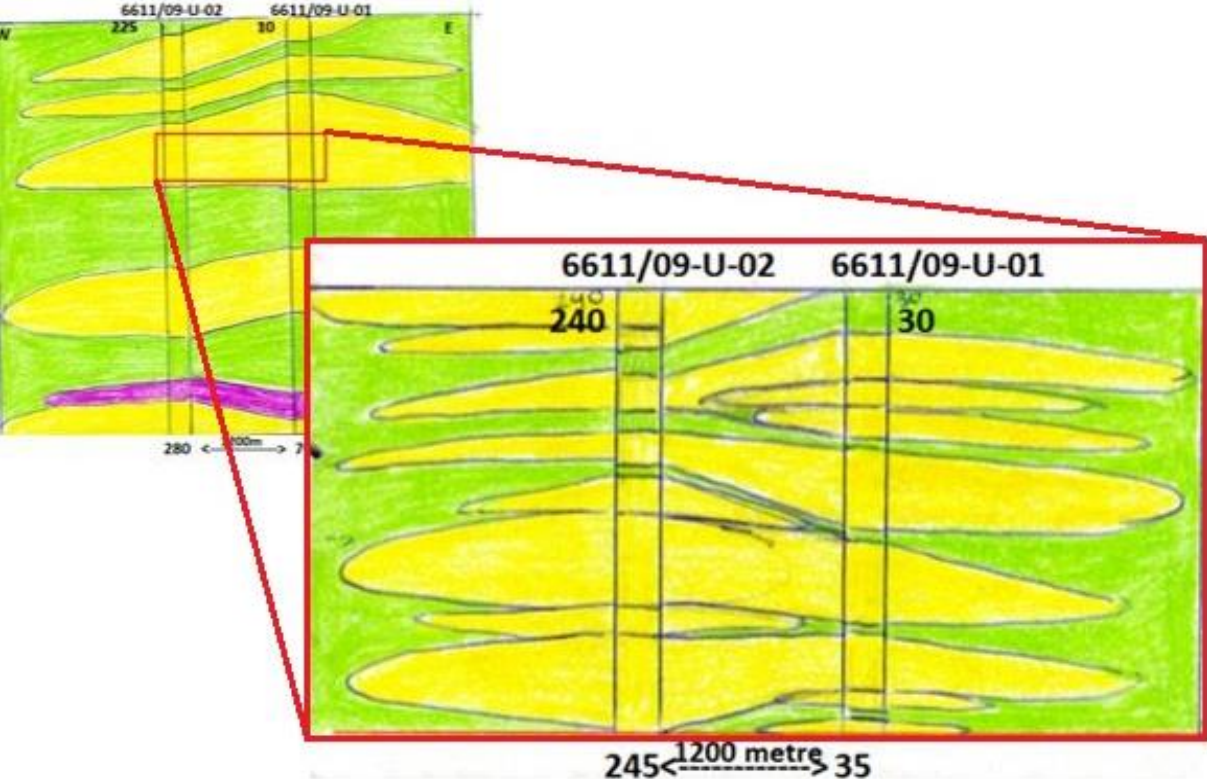
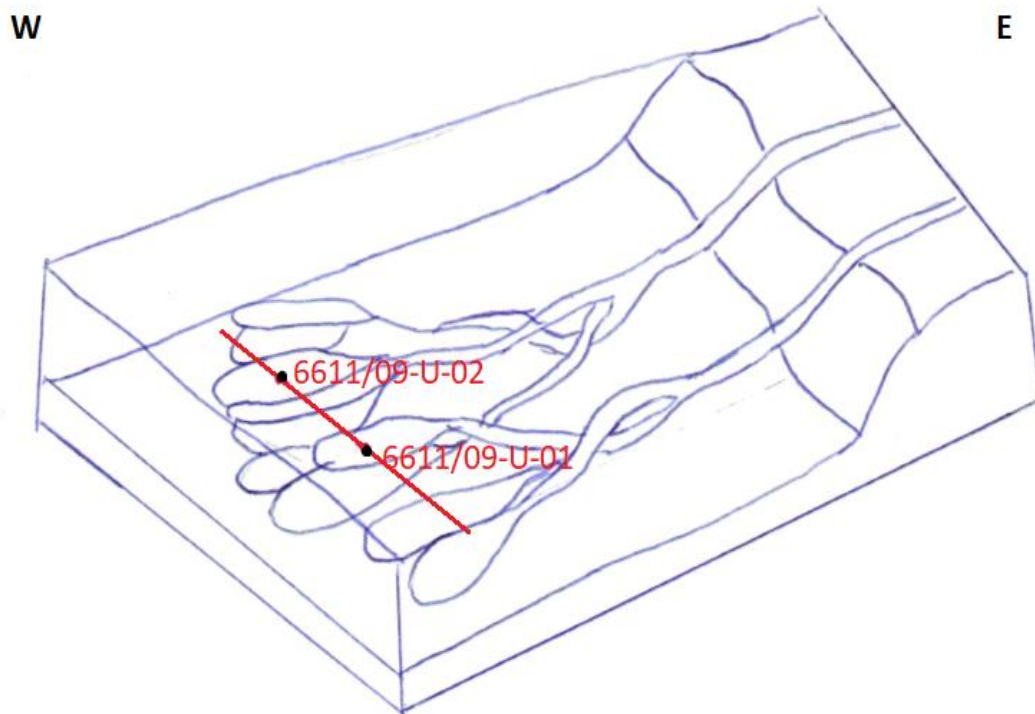


Figure 5.20: Vertical section of interpreted stacking pattern from core 6611/09-U-01 and 6611/09-U-01 on a 1:100 scale. Red box shows outlined area.



*Figure 5.22: Illustration of a proposed conceptual depositional model for the Helgeland basin. Well 6611/09-U-01 and 6611/09-U-02 indicated with black. Red line indicates vertical section.*

## 6 Conclusions

The core description of core 6611/09-U-01 and 6611/09-U-02 in the Helgeland basin with subsequently facies interpretations and statistical analysis has resulted in a proposed sedimentological description and a conceptual depositional model of the study area.

The main conclusions in this thesis are:

- 1) Four facies associations were interpreted from detailed facies analysis of core 6611/09-U-01 and core 6611/09-U-02 in the Helgeland basin (Debrite facies association (Fa1), Transitional facies association (Fa3), Turbidite facies association (Fa2) and Heterolithic facies association (Fa4). In addition to a sedimentological description a statistical analysis of thickness trends for each facies association was developed. The statistical analysis showed a thinning in beds for Fa1, Fa4 and Fa5 subsequently with a thickening in bed for Fa2 and Fa3 with decreasing depth for core 6611/09-U-01. For core 6611/09-U-02 a thinning in bed for Fa4 is observed with a thickening in bed for Fa1, Fa2, Fa3 and Fa4 with increasing depth.
- 2) Characteristic evaporitic intervals were observed in both core 6611/09-U-01 and 6611/09-U-02. Three models were proposed for interpreting the depositional process for the gypsum interval: generation in a sabkha environment, transportation of gypsum from a sabkha environment to a deep marine environment or transportation of evaporitic material from a shallow marine environment and recrystallization of the material to gypsum. Based on thin sections and core observations the diagenetic model with transportation and recrystallization was favoured.
- 3) Two methods for correlation of well 6611/09-U-01 and 6611/09-U-02 was carried out based on the thicknesses of each facies association and the lithology. Correlation of the two cores were performed based on the theory that the first occurrence of gypsum is the same. They correlation in 1:500 scale confirmed the continuance of the gypsum layer in addition to other continued layers. However, significantly differences in the two cores were observed in the correlation of 1:100 scale.

- 4) Due to limited quantitative data it is difficult to conclude with an orientation of the system, but weak trends in thickening of turbidite sand packages towards the top, increased frequency of turbidites with decreasing depth and difficult in correlation on a small scale can be interpreted as a prograding or an aggradational system with proximal fans for the investigated interval. Based on facies description, statistical analysis and geological history a conceptual depositional model for a deep-marine environment was proposed by a small-scale submarine fan system stacked in an aggradation pattern with sediment input by several feeder channels from east to west.

## 7 References

- Allen, J. R. L. (1985).** Principles of Physical Sedimentology. London: Chapman & Hall.  
doi:DOI 10.1007/978-94-010-9683-6
- Blystad, P., Brekke, H., Færseth, R.B., Larsen, B.T., Skogseid, J. & Tørudbakken, B. (1995).** Structural elements of the Norwegian continental shelf, Part II: The Norwegian Sea region. *Norwegian Petroleum Directorate Bulletin no 8*, 44p.
- Botterill, S., Campbell, S., Gingras, M. (2014).** Bioturbation Intensity: A Proxy for Evaluating Environmental Stresses in the Bluesky Formation, Northeastern Alberta., *GeoConvention 2014: Focus*.
- Brekke, H. & Riis, F. (1987).** Tectonics and basin evolution of the Norwegian shelf between 62°N and 72°N. *Norsk Geologisk Tidsskrift*, vol.67, pp. 295-322.
- Brekke, H., Sjulstad, H.I., Magnus, C., Williams, R. (2001).** Sedimentary environments offshore Norway – an overview. *Norwegian Petroleum Society Special Publication*, vol.10, pp. 7-37
- Bugge, T., Ringås, D., Leigh, A., Mangerud, G., Weiss, H.M., Leith, T.L. (2002).** Upper Permian as a new play model on the mid-Norwegian continental shelf: Investigated by shallow stratigraphic drilling. *AAPG Bulletin*, v. 86, no. 1, pp. 107–127
- Bukovics, C. & Ziegler, P.A. (1985).** Tectonic development of the Mid-Norway continental margin. *Marine and Petroleum Geology*, vol.2, pp. 2-22.
- Compton, R.R. (1962).** Manual of Field Geology. In *Soil Science*. New York: Wiley. 295 p
- Costa. (1984).** Physical Geomorphology of Debris Flows. In *Development and Application of Geomorphology*. Berlin: Springer. Ch:9
- Felix, M., Peakall, J. (2006).** Transformation of debris flows into turbidity currents: mechanisms inferred from laboratory experiments. *Sedimentology*, vol 53. pp. 107-123
- Garrison, R.E (1990).** Pelagic and Hemipelagic sedimentary rocks as source and reservoir rock. *SEPM (Society for Sedimentary Geology)*, 123.

**Gowers, M., & Lunde, G. (1984).** The geological history of Trænabanken. In A. M. Spencer (Ed.), *Petroleum Geology of the North European Margin*. pp. 237-251. Springer Netherlands.

**Hochuli, P. A., Vigran, J. O., Hermann, E., & Bucher, H. (2010).** Multiple climatic changes around the Permian-Triassic boundary event revealed by an expanded palynological record from mid-Norway. *Geological Society of America Bulletin*, 122(5-6), 884-896.

**Hofstra, M., Hodgson, D.M., Peakall, J., Flint, S.S. (2015).** Giant scour-fills in ancient channel-lobe transition zones: Formative processes and deposition architecture. *Sedimentary Geology*. Vol 329. Pp. 98-114.

**Kane, I. A., & Pontén, A. S. (2012).** Submarine transitional flow deposits in the Paleogene Gulf of Mexico. *Geology*, vol. 40(12), pp. 1119-1122.

**Lien, T., Midtbø, R.E., Martinsen, O.J. (2006).** Depositional facies and reservoir quality of deep-marine sandstones in the Norwegian Sea. *Norwegian Journal of Geology*, Vol.86, pp.71-92.

**Meiburg, E. & Kneller, B. (2010).** Turbidity Currents and Their Deposits, *Annual Review of Fluid Mechanics*, Vol.42, pp.135-156.

**Mosar, J., Eide, E.A., Osmundsen, P.T., Sommaruga, A. & Torsvik, T.H. (2002).** Greenland-Norway separation: A geodynamic model for the North Atlantic. *Norwegian Journal of Geology*, Vol. 82, pp. 281-298.

**Mulder, T., Hüneke H. (2014).** Bouma Sequence. In: Harff J., Meschede M., Petersen S., Thiede J. (eds) *Encyclopedia of Marine Geosciences*. Springer, Dordrecht

**Müller, R., Nystuen, J. P., Eide, F., & Lie, H. (2005).** Late Permian to Triassic basin infill history and palaeogeography of the Mid-Norwegian shelf—East Greenland region. *Norwegian Petroleum Society Special Publications Onshore-Offshore Relationships on the North Atlantic Margin, Proceedings of the Norwegian Petroleum Society Conference*, 165-189.

**Mutti, E., & Lucchi, F. R. (1978).** Turbidites of the northern Apennines: Introduction to facies analysis. *International Geology Review*, 20(2), 125-166.

**Nøttvedt, A., Johannessen, E.P and Surlyk, F. (2008).** The Mesozoic of western Scandinavia and eastern Greenland. *Episodes*, 31, 59-65.

**NPD (2014).** CO<sub>2</sub> atlas for the Norwegian Continental Shelf, NPD.

**Pickering, K. T., Hiscott, R. N., & Heard, T. (2016).** *Deep marine systems: Processes, deposits, environments, tectonics and sedimentation*. Washington DC: American Geophysical Union.

**Powers, M.C. (1953).** A New Roundness Scale for Sedimentary Particles. *Journal of Sedimentary Petrology*, Vol.23, pp. 117-119.

**Ramberg, I. B., Bryhni, I., Nøttvedt, A. and Ranges, K. (2008).** The making of a land: Geology of Norway. Trondheim: Norwegian Geological Survey

**Riis, F., & Halland, E. (2014).** CO<sub>2</sub> Storage Atlas of the Norwegian Continental Shelf: Methods Used to Evaluate Capacity and Maturity of the CO<sub>2</sub> Storage Potential. *Energy Procedia*,63, 5258-5265.

**Shanmugam, G. (2016).** Submarine fans: A critical retrospective (1950–2015). *Journal of Palaeogeography*,5(2), 110-184.

**Shanmugam, G., & Moiola, R. (1988).** Submarine fans: Characteristics, models, classification, and reservoir potential. *Earth-Science Reviews*,24(6), 383-428.

**Southern, S. J., Kane, I. A., Warchol, M. J., Porten, K. W., & McCaffrey, W. D. (2017).** Hybrid event beds dominated by transitional-flow facies: character, distribution and significance in the Maastrichtian Springar Formation, north-west Vøring Basin, Norwegian Sea. *Sedimentology*,64(3), 747-776.

**Spychala, Y.T, Hodgson, D.M, Flint, S.S, Mountney, S.P. (2015).** Constraining the sedimentology and stratigraphy of submarine intraslope lobe deposits using exhumed examples from the Karoo Basin, South Africa. *Sedimentary Geology* 322, 67-81.

**Stow, D. A. (1985).** Fine-grained sediments in deep water: An overview of processes and facies models. *Geo-Marine Letters*,5(1), 17-23.

**Walker, R. G. (2006).** Facies Models Revisited: Introduction. In H. W. Posamentier & R. G. Walker (Eds.), *Facies Models Revisited*. Tulsa, Oklahoma, USA: Society for Sedimentary Geology.

## 8 Appendix

Content in Appendix:

8.1: Thin section analysis

8.2: Legend for sedimentological log description

8.3: Sedimentological log for core 6611/09-U-02 in scale 1:20

8.4: Sedimentological log for core 6611/09-U-01 in scale 1:20

8.5: Sedimentological log for core 6611/09-U-01 in scale 1:200


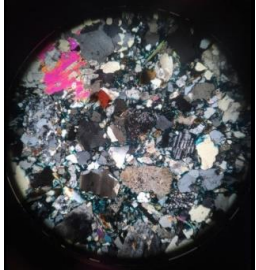
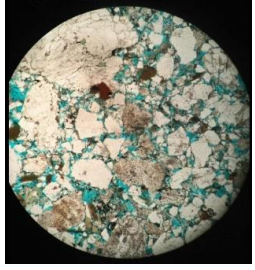

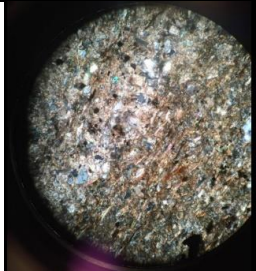
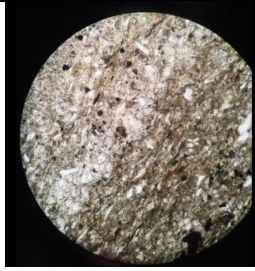
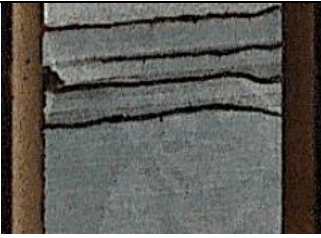
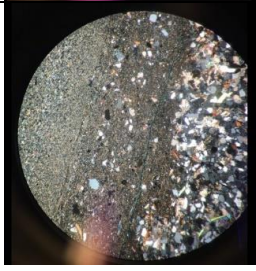
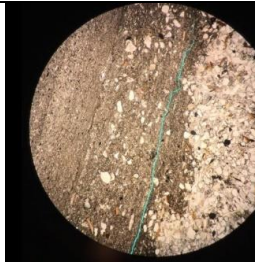

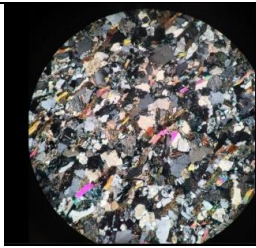
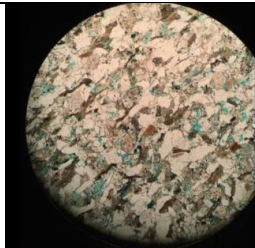
8.6: Sedimentological log for core 6611/09-U-02 in scale 1:200



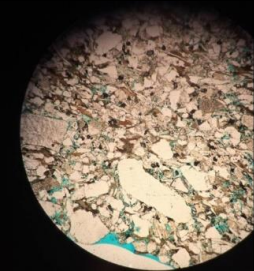


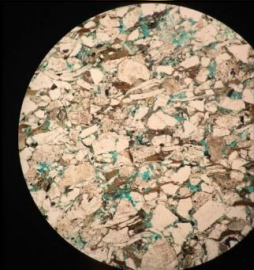

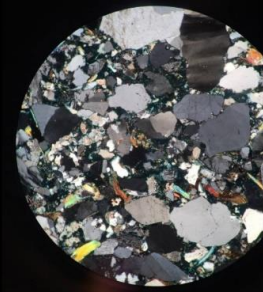
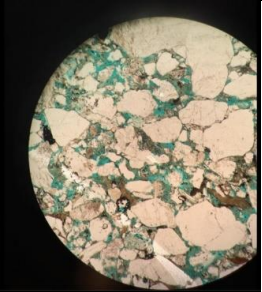

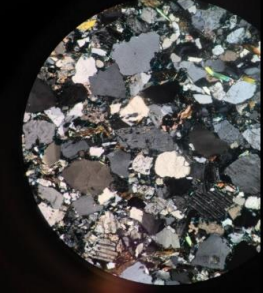
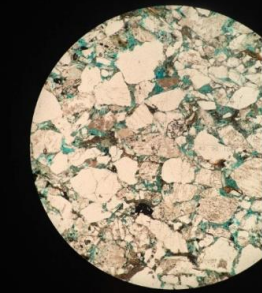

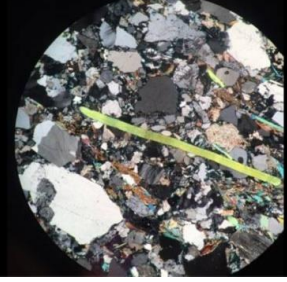
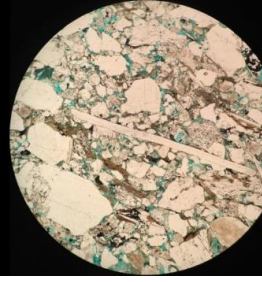
8.7: Sedimentological log for core 6611/09-U-01 in scale 1:500


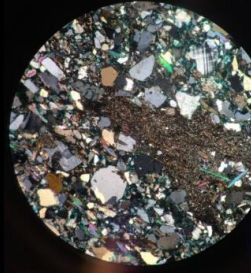
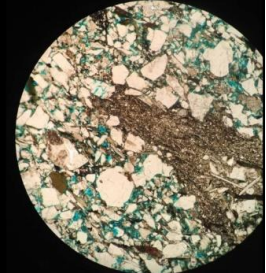

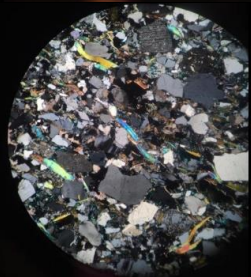
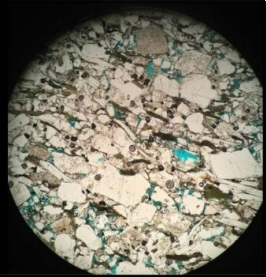

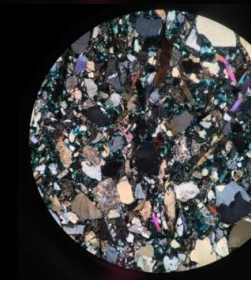
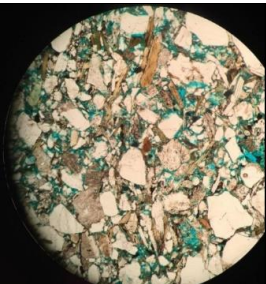


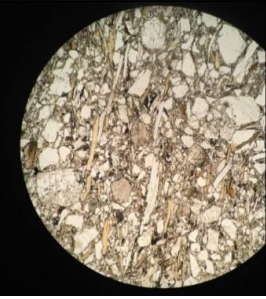

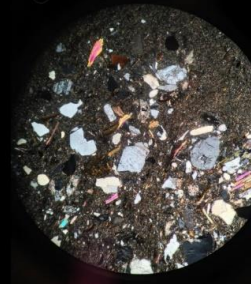
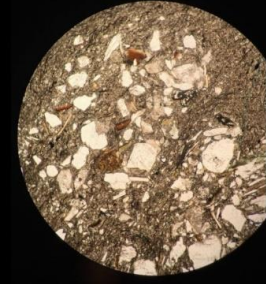
8.8: Sedimentological log for core 6611/09-U-02 in scale 1:500


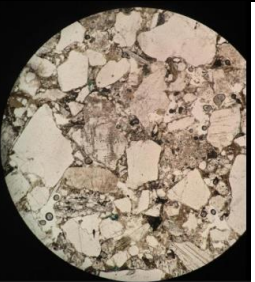
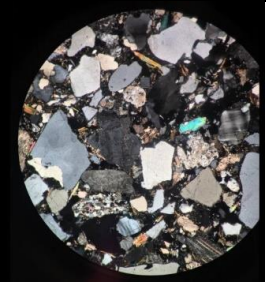

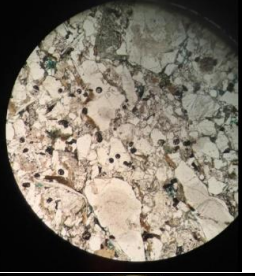
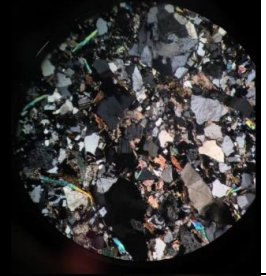

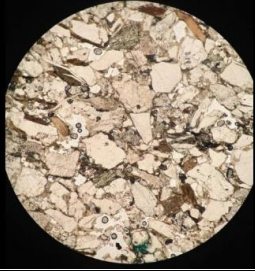
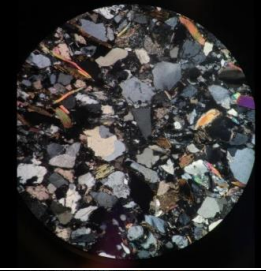

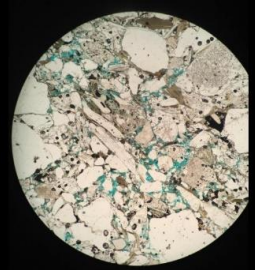
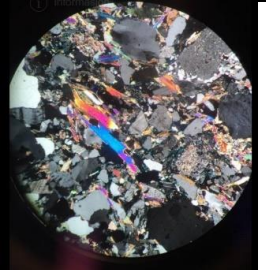

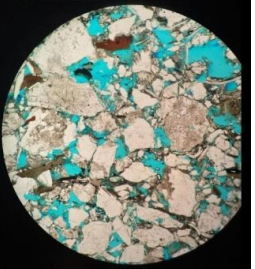
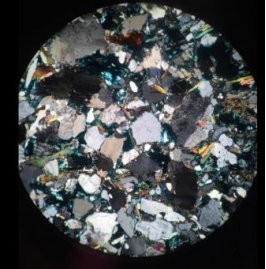

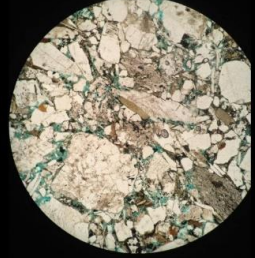
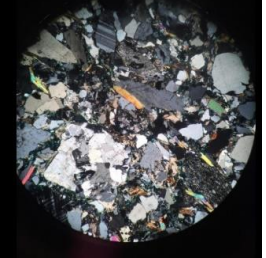



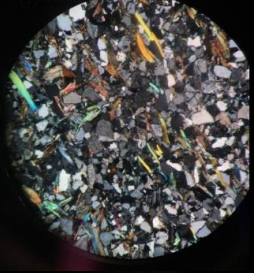
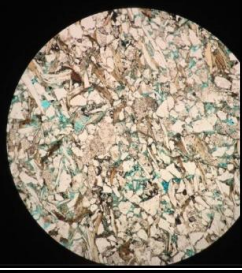

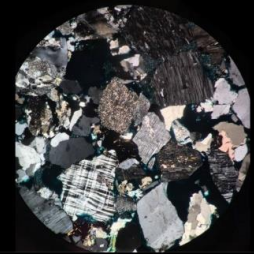
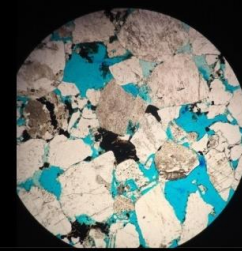

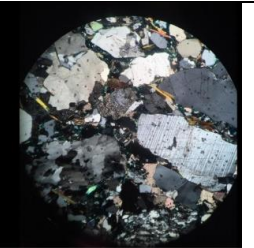
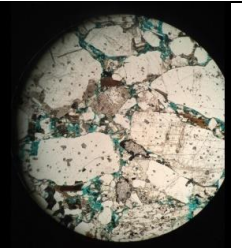

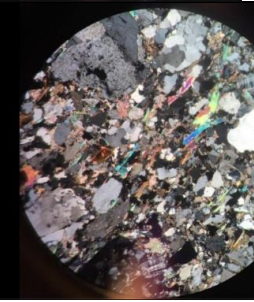
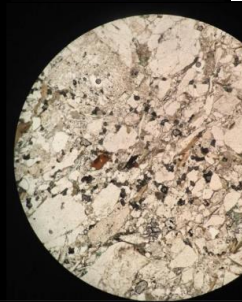
8.1 Appendix: Thin sections

6611/09-U-01				
Depth	Mineralogy	Picture	Microscope, xpl	Microscope ppl
15.14	Transition from sandstone turbidite to conglomerate. Grains up to 50mm. quartz, mikroklin, biotite. Dårlig sortert. Carbonat fragment. Mange Bergartsfragmenter av ulike slag. Duktile fragmenter			
115.67	Grey mud with turbidite. Little porosity and very fine-grained sst with flat horizontally aligned grains.			
128.79	Grey mud. Boundary of mud and sandstone. Mixed layer at boundary with quartz, placioclase and biotite grains interbedded in mud.			
190.19	Grey sst. Some grains up to 60mm in diameter. Little porosity			

190.68	Grey sst			
192.67	Grey sst			
193.42	Grey conglomerate. Grains of quartz, biotite, plagioclase, orthoclase, microclin, olivine. Grainz up to 100mm. some porosity			
195.83	Grey vc sst. Kompaksjon av duktile korn. Noe sekundær porøsitet i feltspat. Dårlig sortering. Granater. Umoden sammensetning. →granat			
200.95	Grey conglomerate, broken core			
6611/09-U-02				
Depth	Mineralogy	Picture	Microscope, xpl	Microscope, ppl

12.1	Coarse sst, turbidite. Little porosity. Mud clast interbedded in the sand.			
13.69	Sst. Little porosity			
21.95	Coarse sst, turbidite. Some porosity			
37.94	Fine sst. Fine grained minerals. grain sized up to 30mm. little porosity. Umodent.			
42.42	Slump/injectite: sst & mud. Chaotic mix of sand and mud. Varying grain sizes. Mye glimmer, og karbonat. Noe leireminerale og omdannede kort.			

76.64	Conglomerate			
77.54	Grey conglomerate			
80.35	Vc sst			
93.75	Vc sst			
95.21	Vc sst with mud clasts			
117.22	Vc sst			


224.07	Grey sst			
230.42	Grey vc sst/ congl			
236.52	Grey congl			
279.71	Vc grey sst			

## 8.2 Appendix: Legend

### Legend

 Sandstone

 shale/clay streaks

 siltstone

 Horizontal laminae

 soft sediment deformation

 Mudflake

 sand laminae


 load cast

 slumping

 Flame structure

 erosional surface

 sharp boundary

 Gradual boundary

 ripples

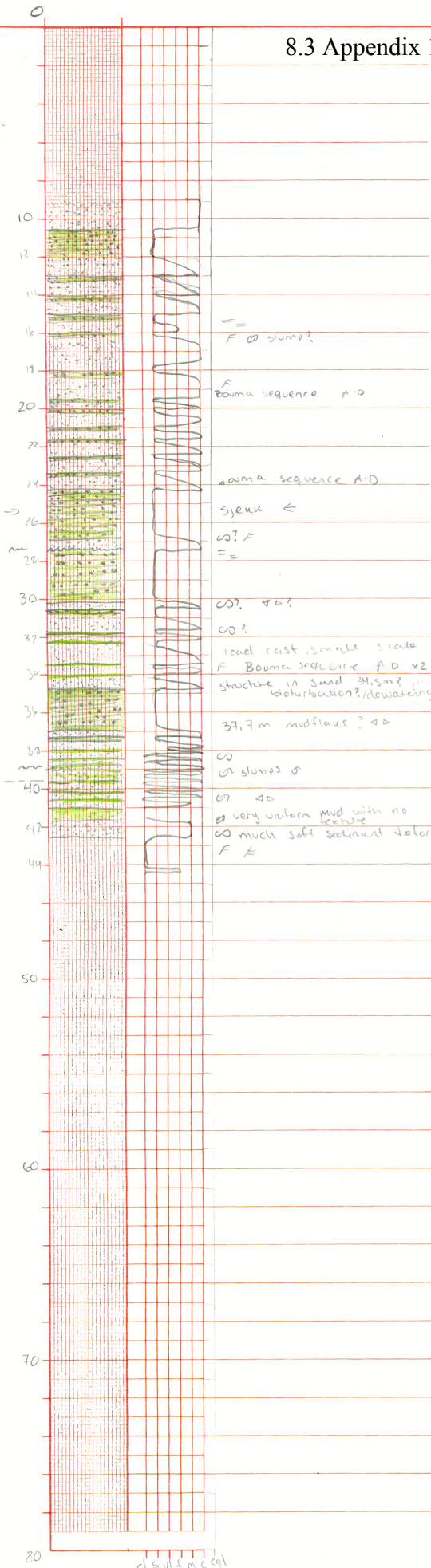
 conglomerate

 Sandstone

 Mudstone

 Gypsum

8.3 Appendix 1:20 Core 6611/09-U-02



Legend

- sandstone
- siltstone
- horizontal lamination
- shale/clay streaks
- soft sediment deformation
- mudflats
- sand laminae
- load cast
- slumping
- flame structure
- erosion surface
- sharp boundary
- gradational boundary
- bioturbation
- conglomerate
- scattered pebbles/gravel clasts
- low angle lamination

F slump?

Booma sequence A-D

Booma sequence A-D

slump ←

CO? \*

CO? \*

CO?

load cast, small scale flame structure, small structure in sand, some bioturbation/dewatering?

37.7m mudflats? \*

CO

slumps \*

CO \*

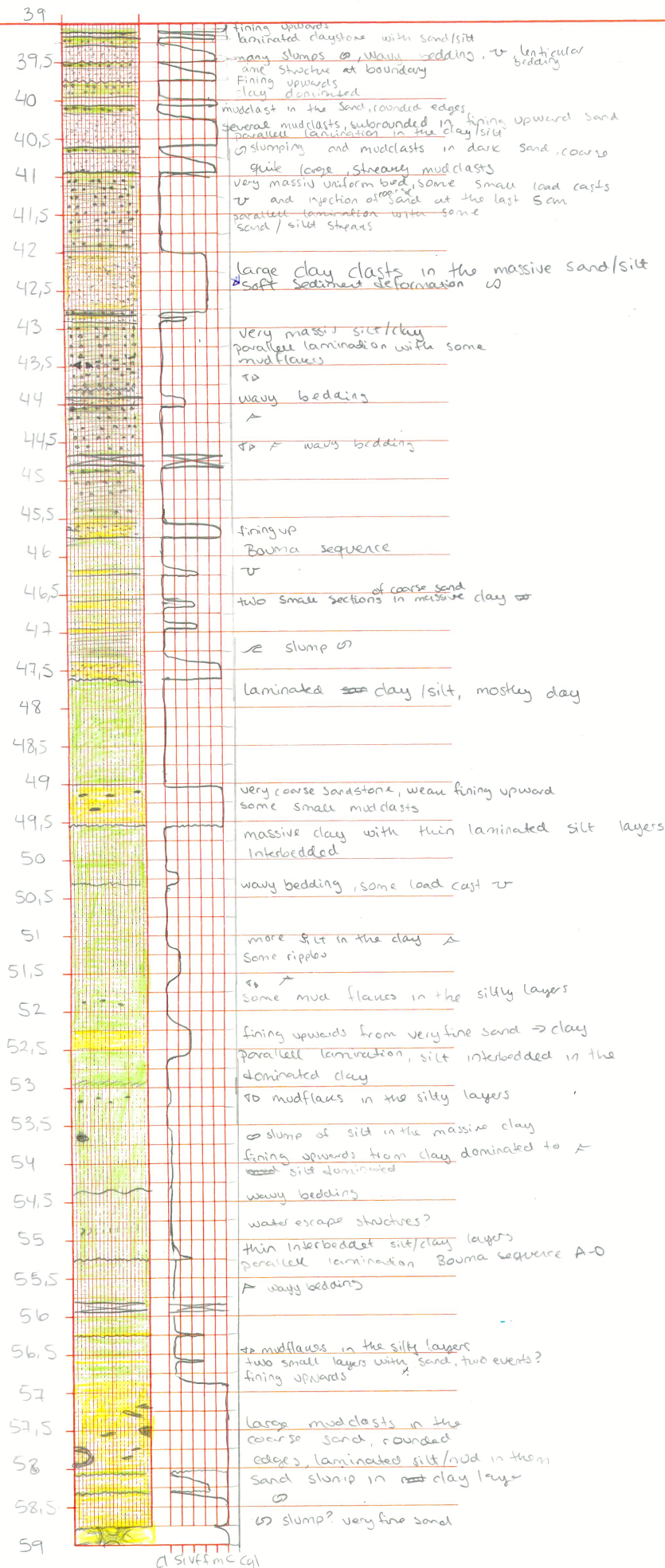
Very uniform mud with no texture

CO much soft sediment deformation

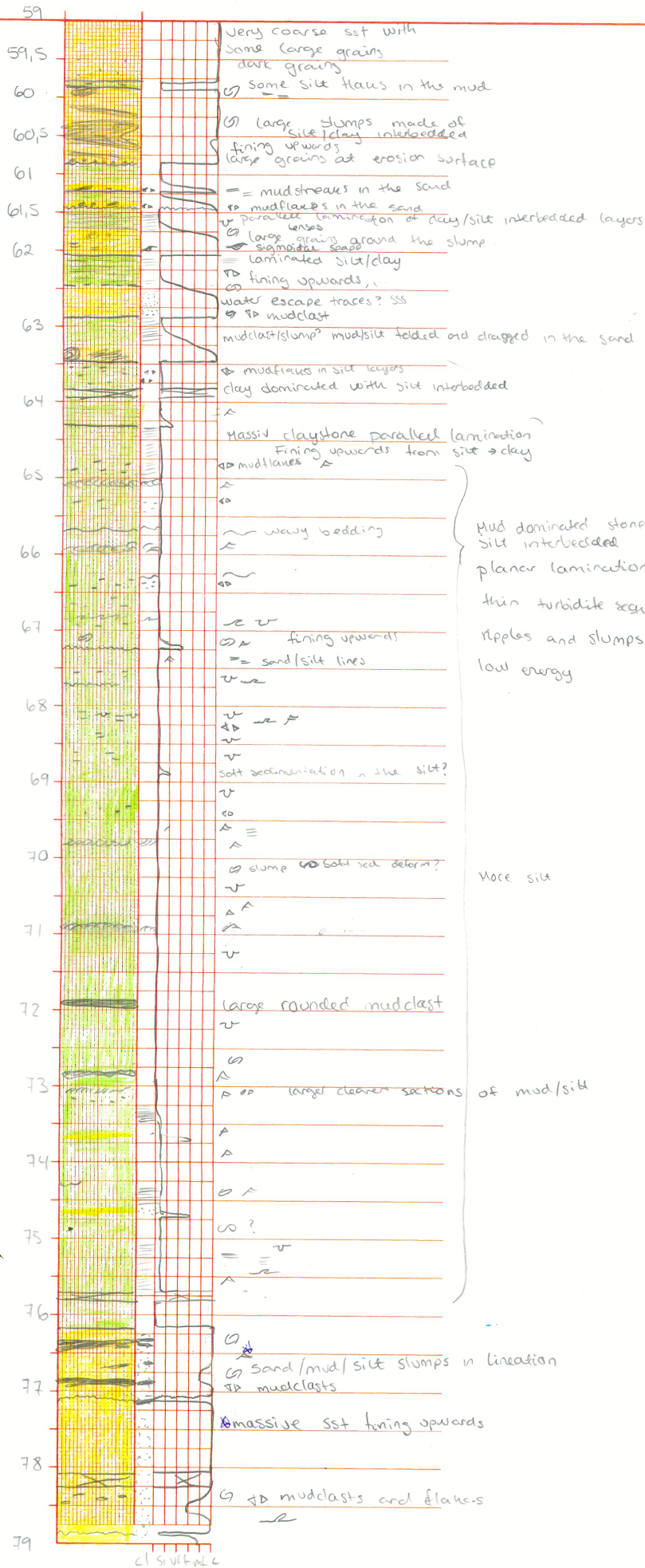
F \*

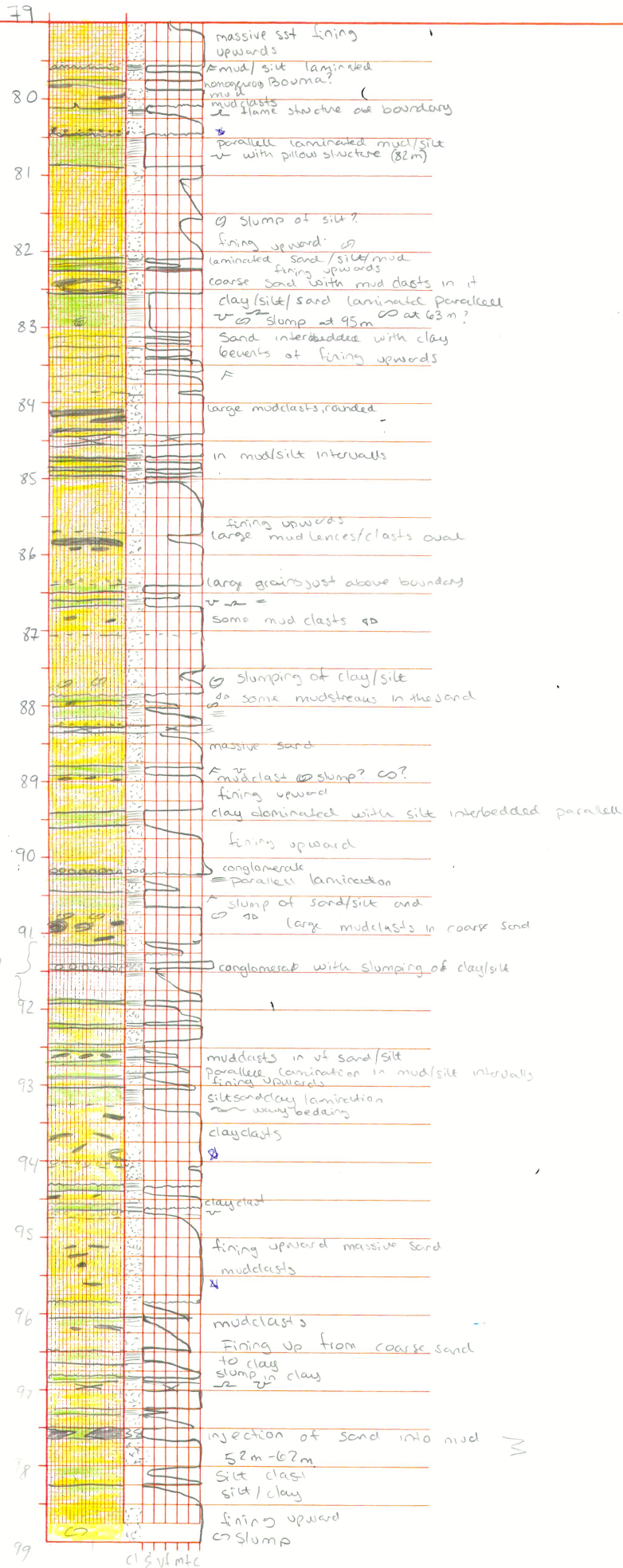


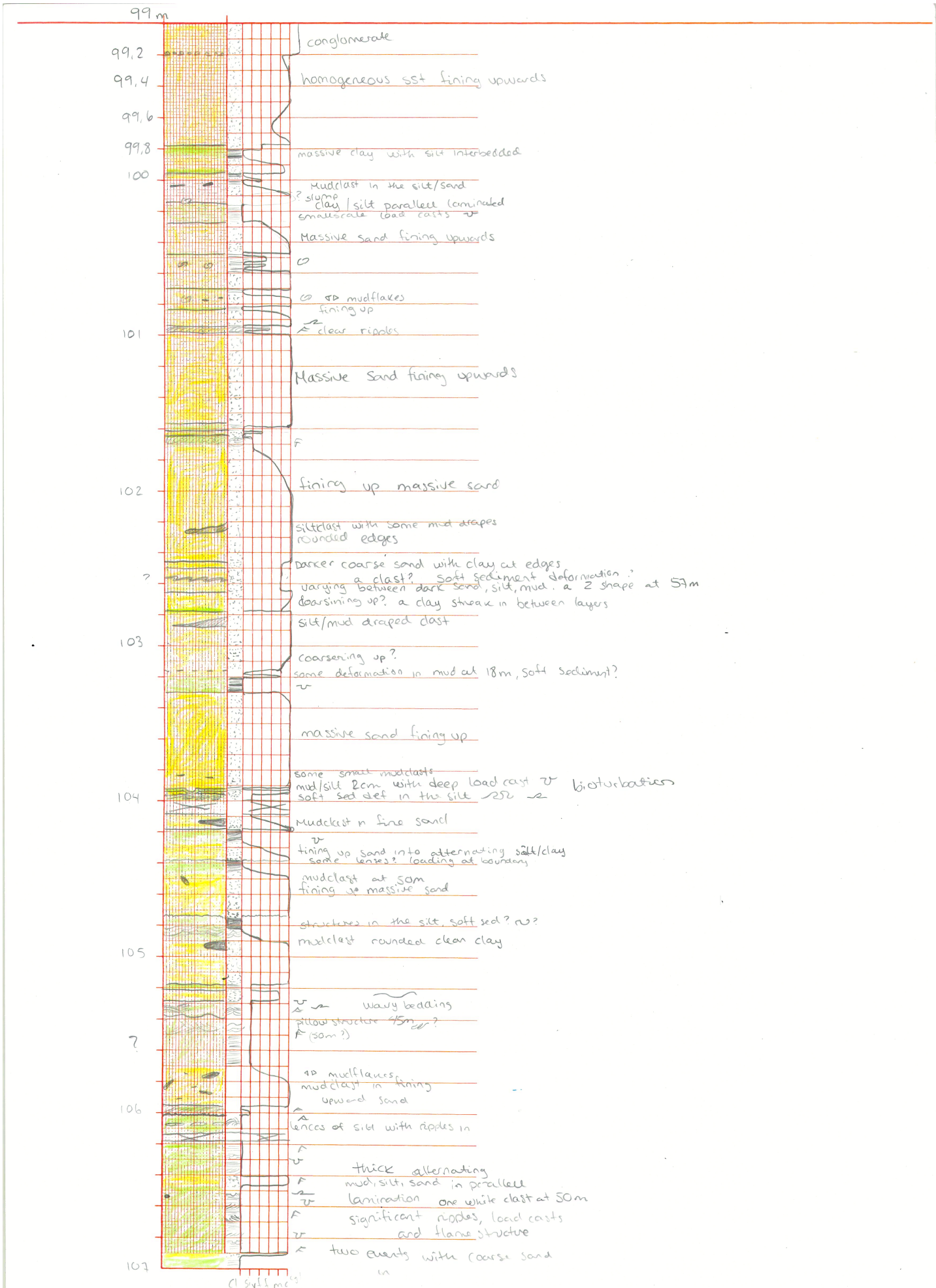


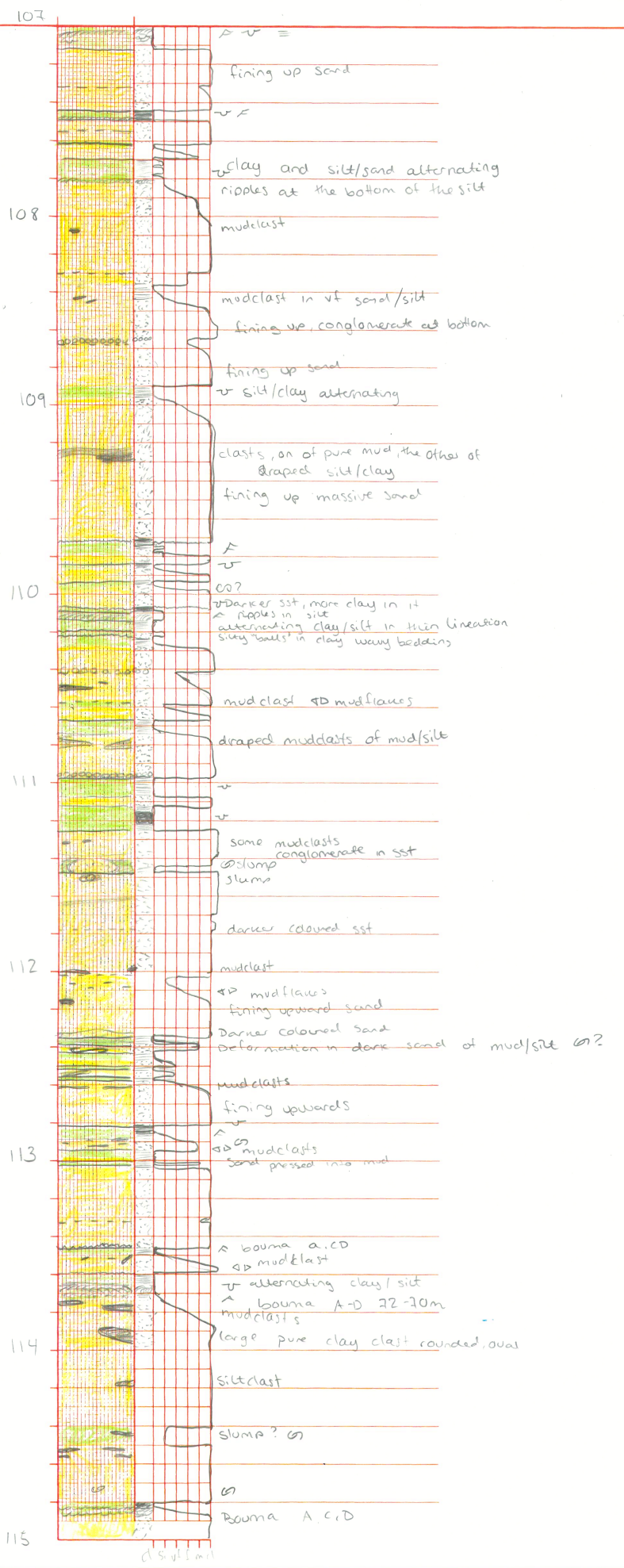


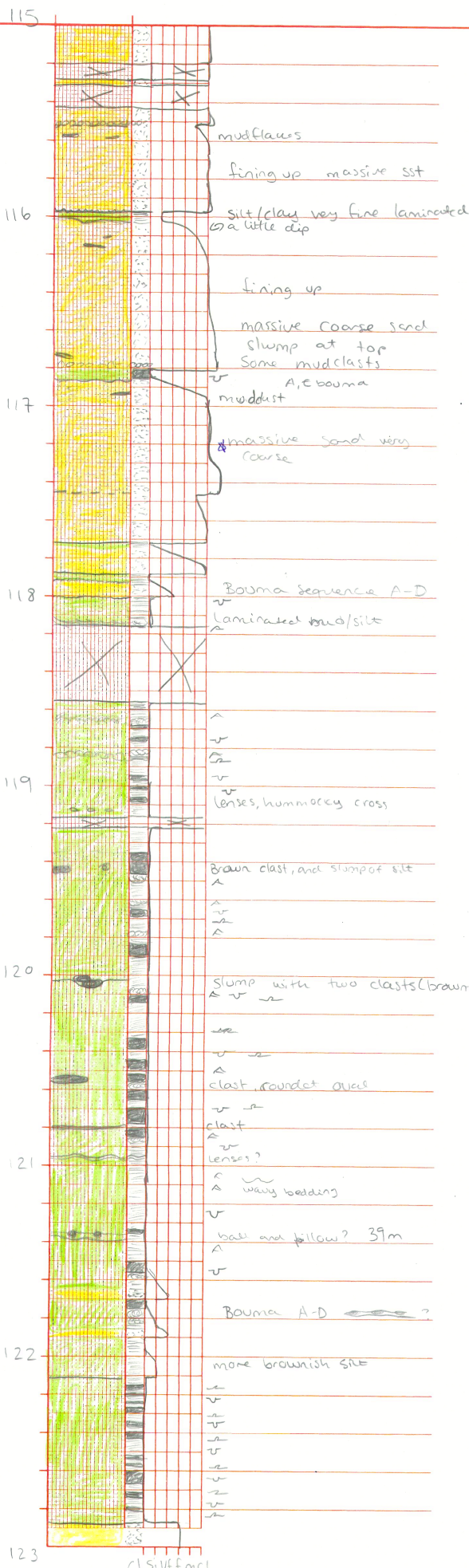
Cl silt f m c gl

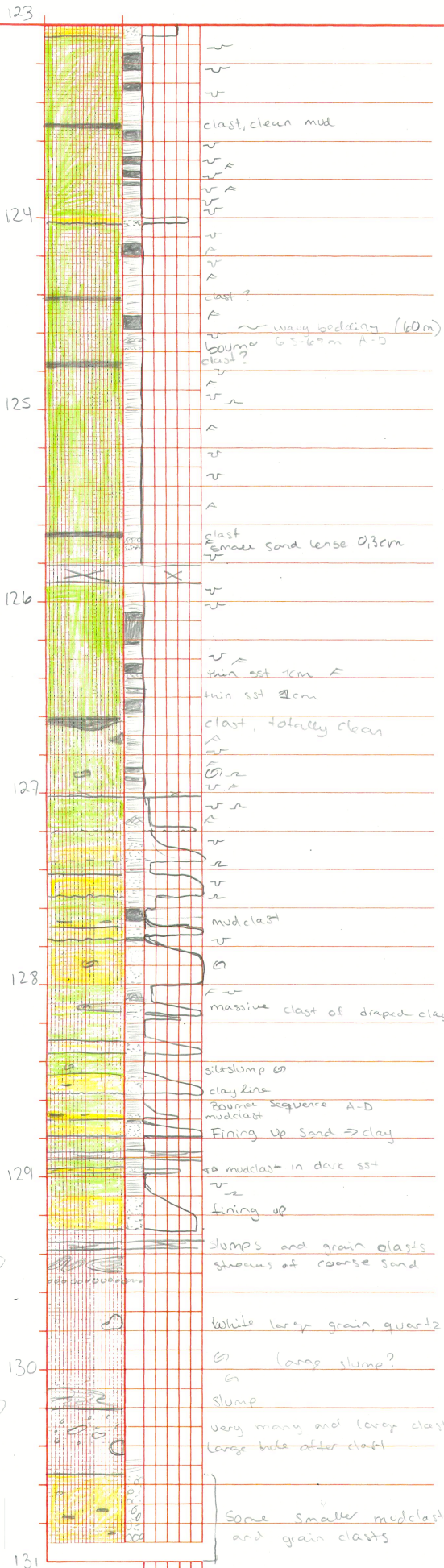




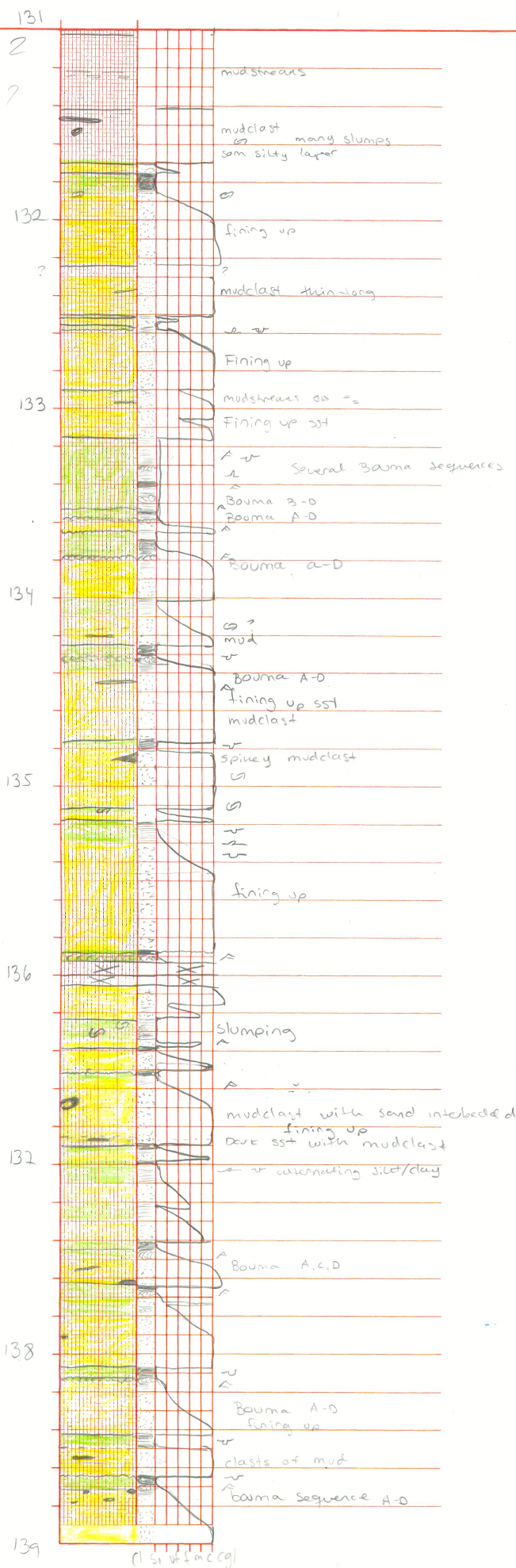




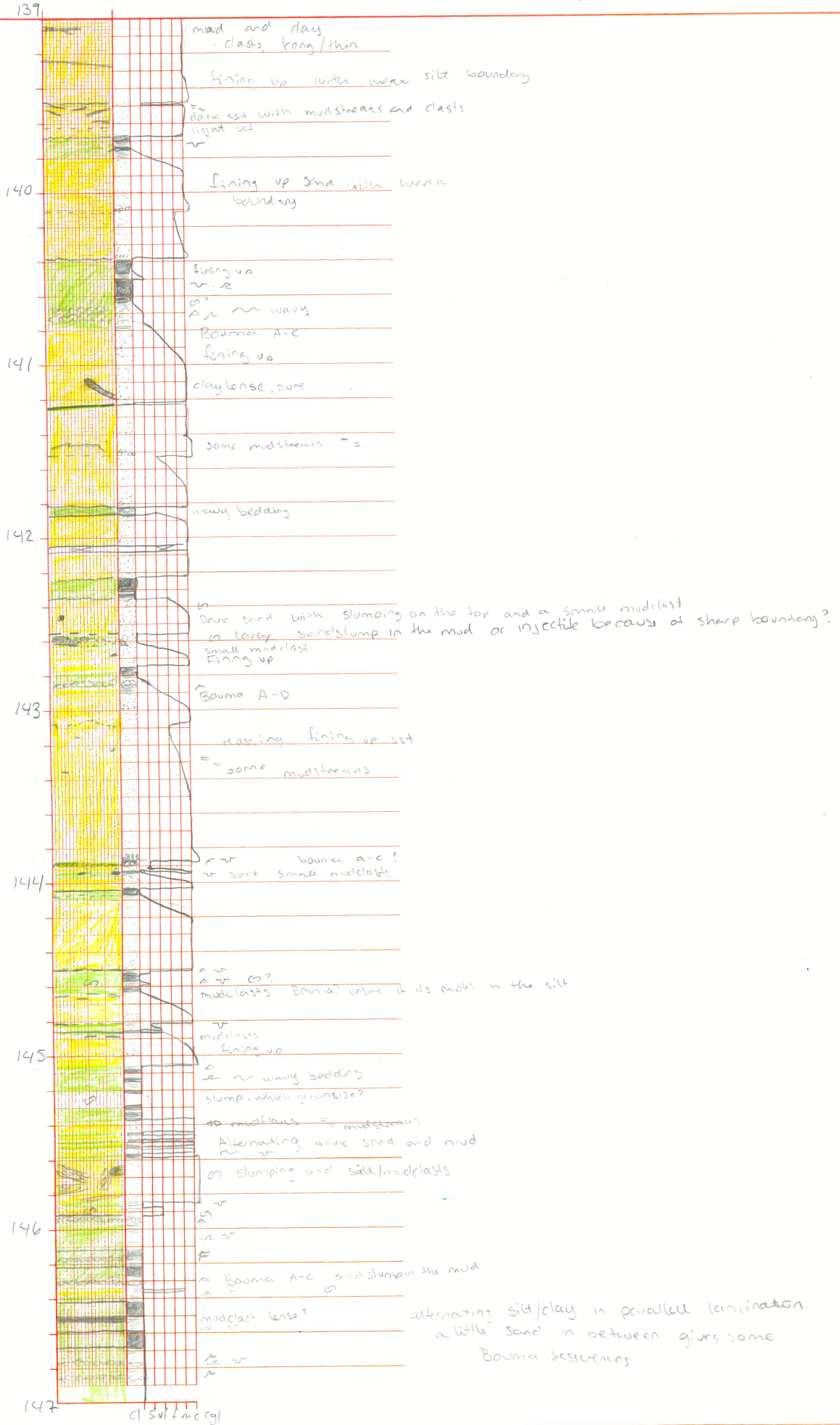




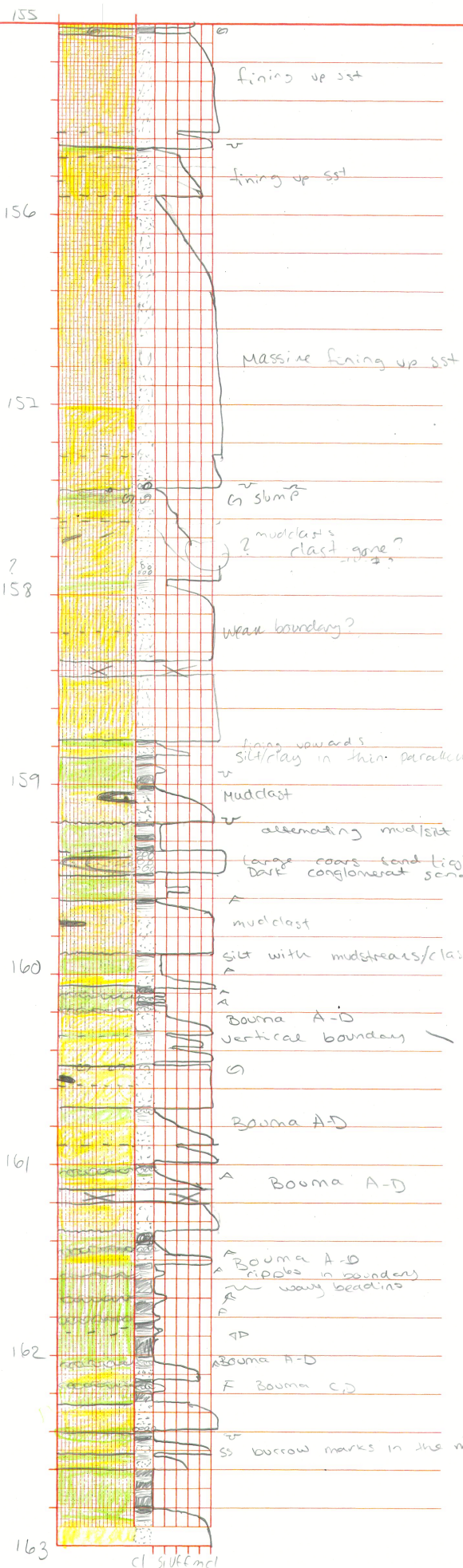
Must be very high energy to transport the grains











fining up sst

fining up sst

Massive fining up sst

cl silt/mcl

? mudclast  
clast zone?

wear boundary?

large voids  
silt/clay in thin parallel lamination

Mudclast

alternating mud/silt in parallel lamination

large coars sand light clast with mud  
dark conglomerate sand

mudclast

silt with mudstreaks/clasts?

Bouma A-D  
vertical boundary

Bouma A-D

Bouma A-D

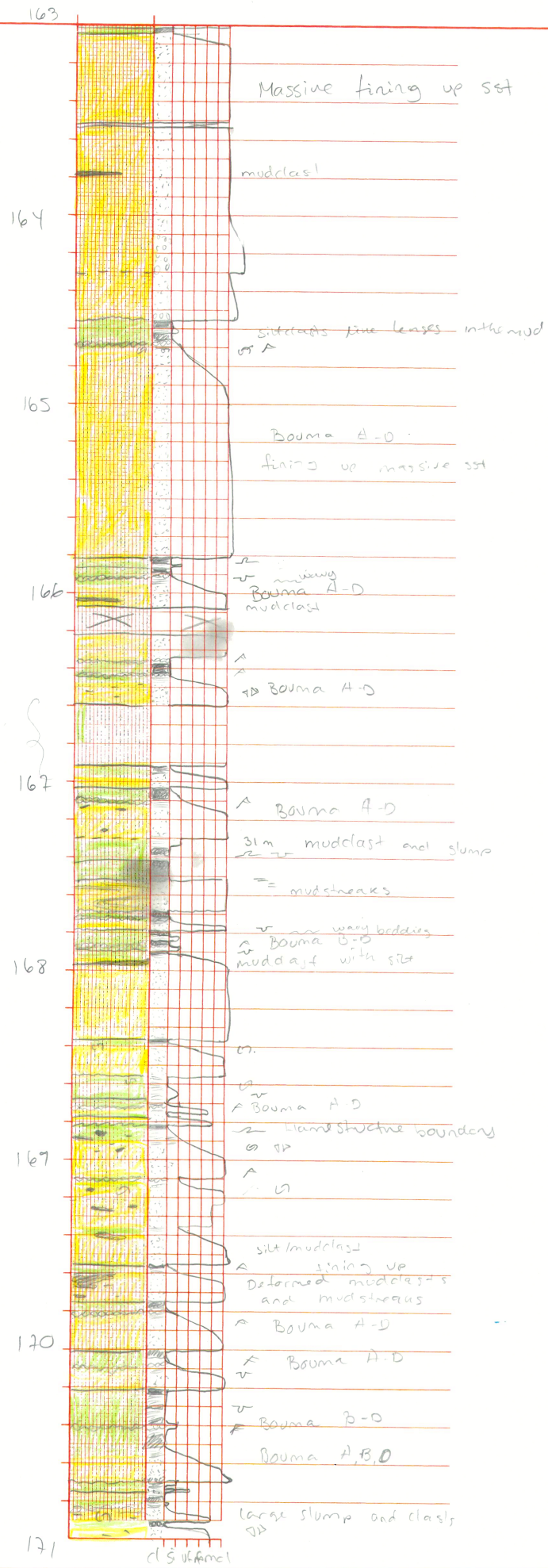
Bouma A-D  
ripples in boundary  
wavy bedding

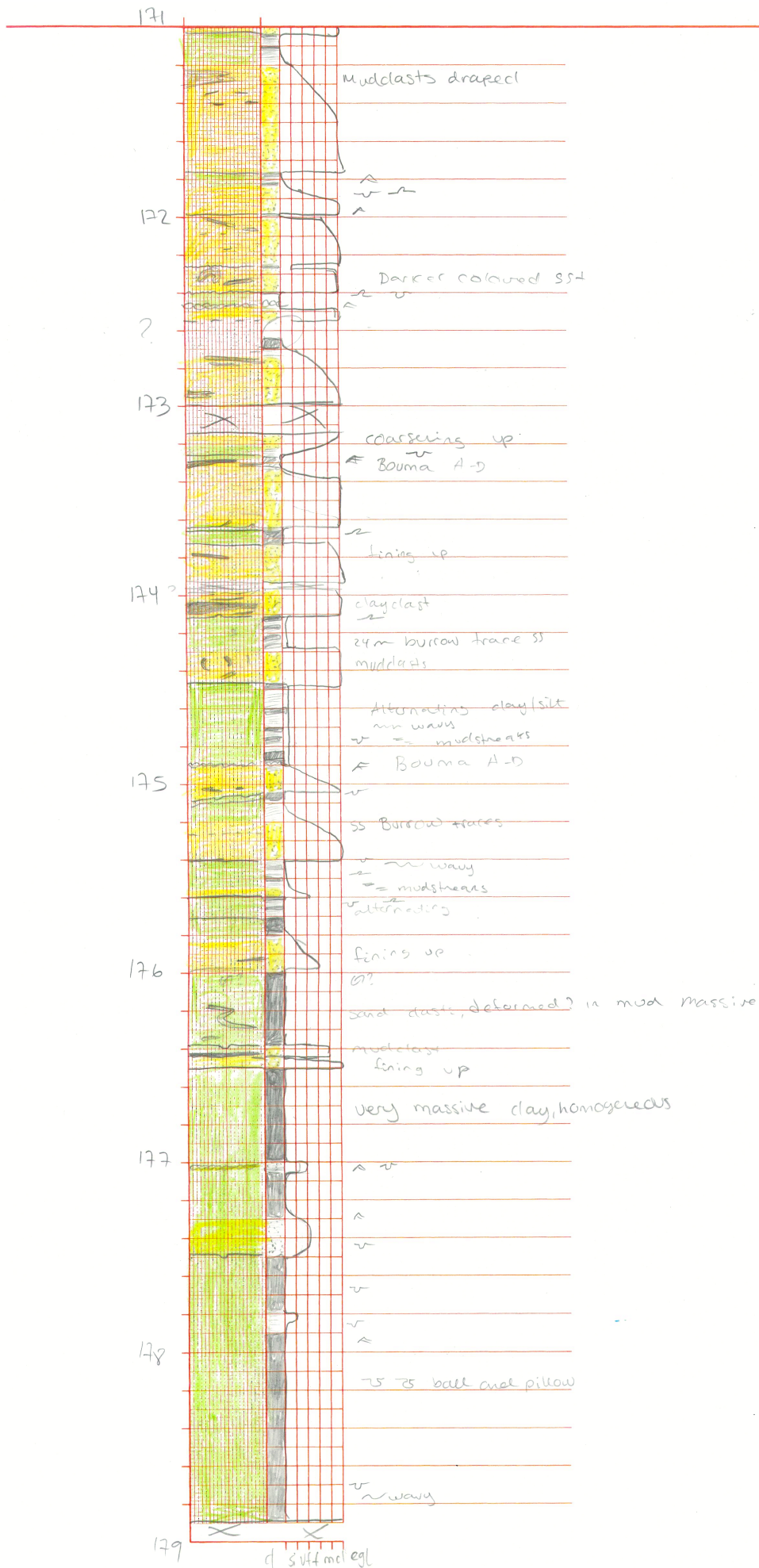
Bouma A-D

F Bouma C,D

ss burrow marks in the mud, vertical

cl silt/mcl





179

?

180

181

182

?

183

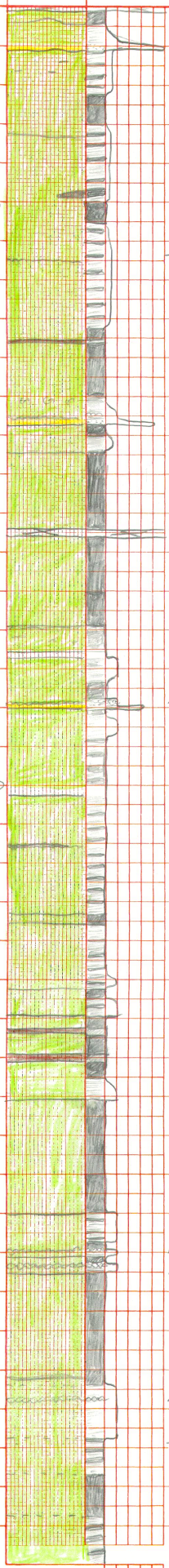
184

?

185

186

187



finings

clay streaks

siltclast

alternating silt/clay  
in parallel lamination

F Bouma A-C

clasts

Bouma A-C?

Ball and pillow

erosional surface with a brownish matrix

pillow

brownish clay section, brown mud

fining up

silt streaks

silt clasts? slump? insectile?

loading?

Bouma B-D

very massive uniform clay

some silt lines

some silt clasts

very thin silt lamination, parallel  
silt dominated

alternating clay and silt

massive homogeneous clay

cl silt m cgl



187

Homogeneous massive clay

188

lenses in the mud

from 17-26m more green silt/clay

189

coarse sand streaks

Burrow trace in brown clay?

190

GI amputation with a angle

flame structure in bounding

191

co soft red dirt?

Bouma A-C

Bouma A-D

192

12m some quartz streaks in the mud

Bouma A, C, D?

193

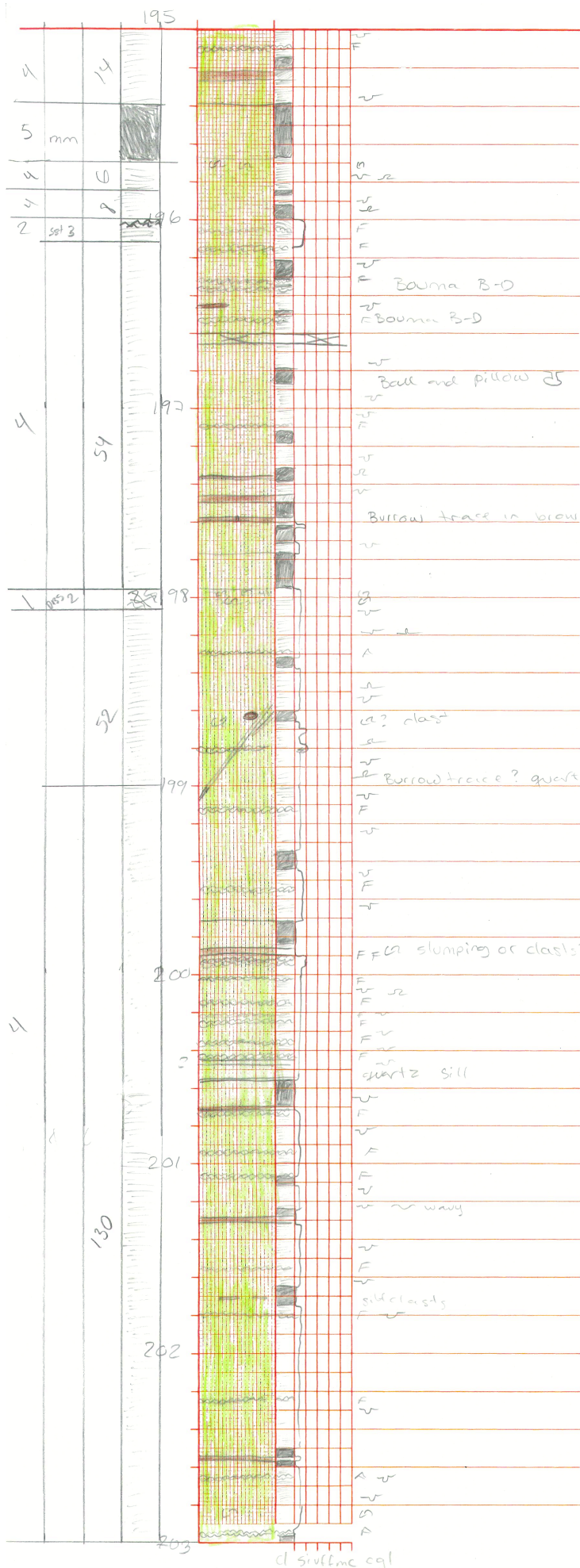
194

clast of

lens

195

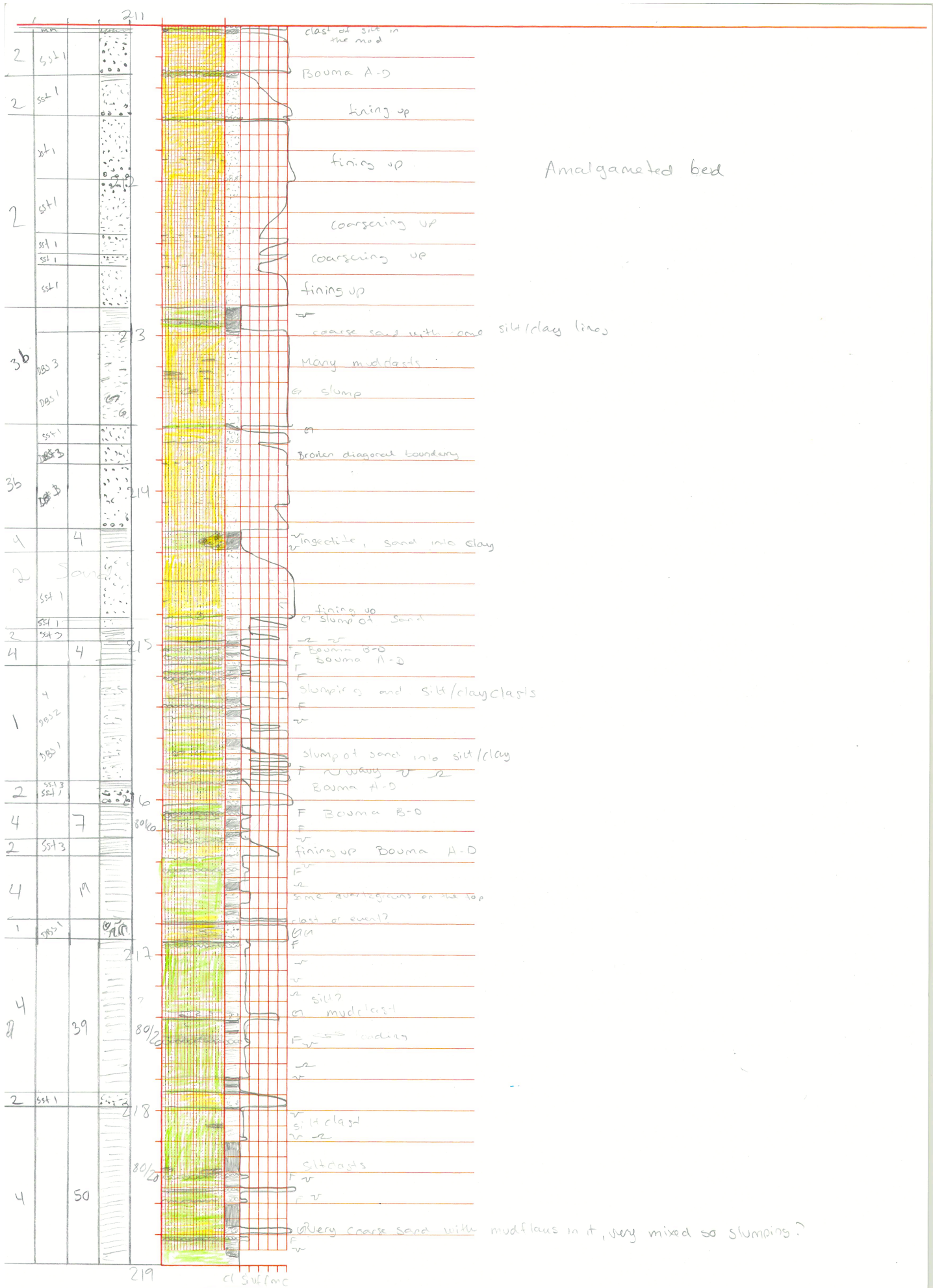
cl silt fine cgl



alternating clay/silt  
 in parallel lamination  
 from 177,5m - 209,5m







Amalgamated bed

coarse sand with some silt/clay lines

Injectite, sand into clay

fining up or slump of sand

Bouma B-D  
Bouma A-D

slumping and silt/clay clasts

slump of sand into silt/clay

Bouma A-D

Bouma B-D

fining up Bouma A-D

some overgrowths on the top

last of event?

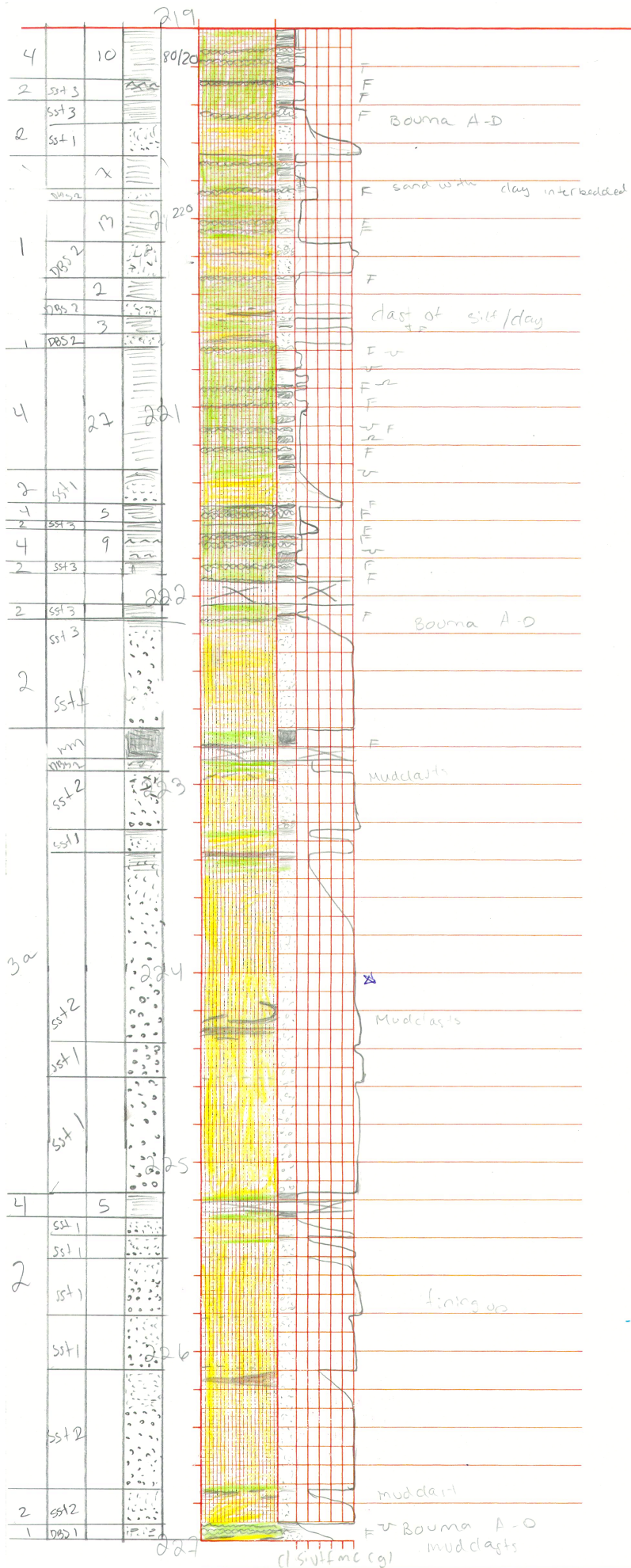
silt? mudclast

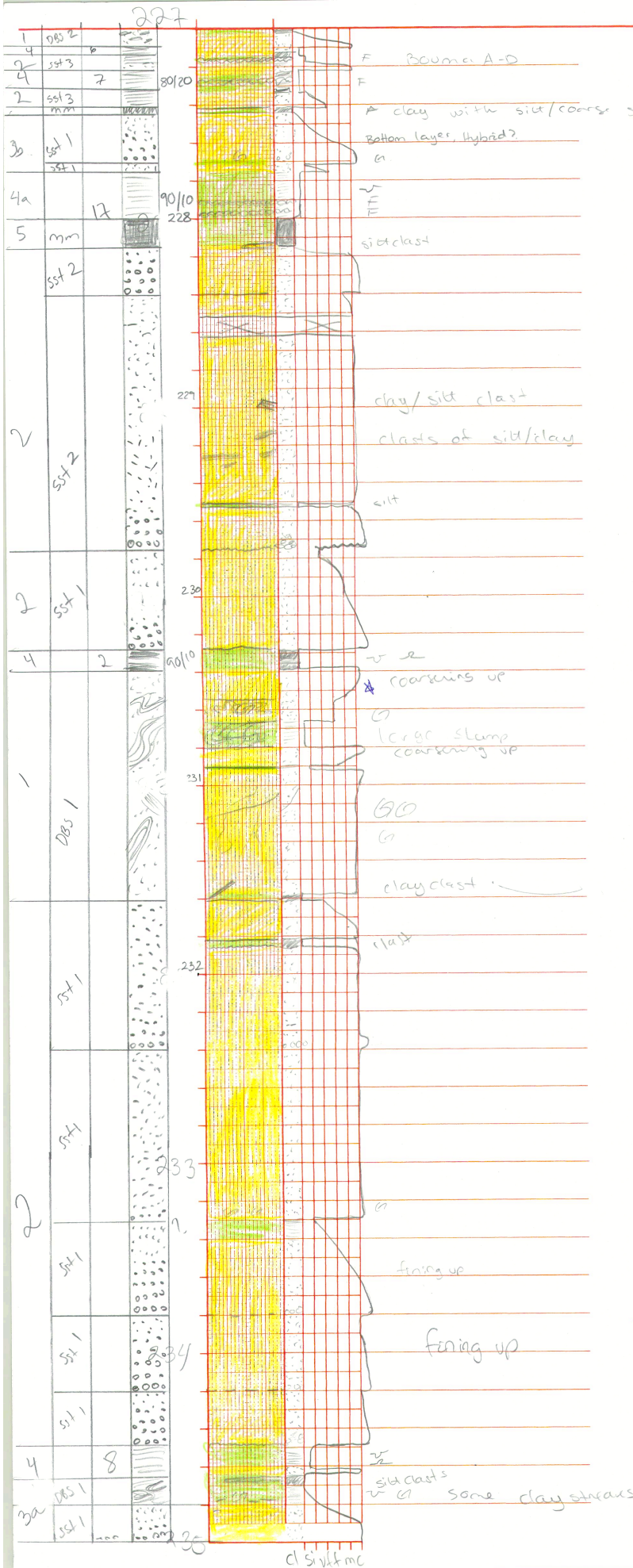
clast

silt/clast

silt clasts

very coarse sand with mudclasts in it, very mixed so slumping?





F BOUND A-D

F

A clay with silt/coarse sand clast with ripples

Bottom layer, Hybrid?

G

M

silt/clast

clay/silt clast

clasts of silt/clay

silt

coarsening up

large slump coarsening up

GO

clay/clast

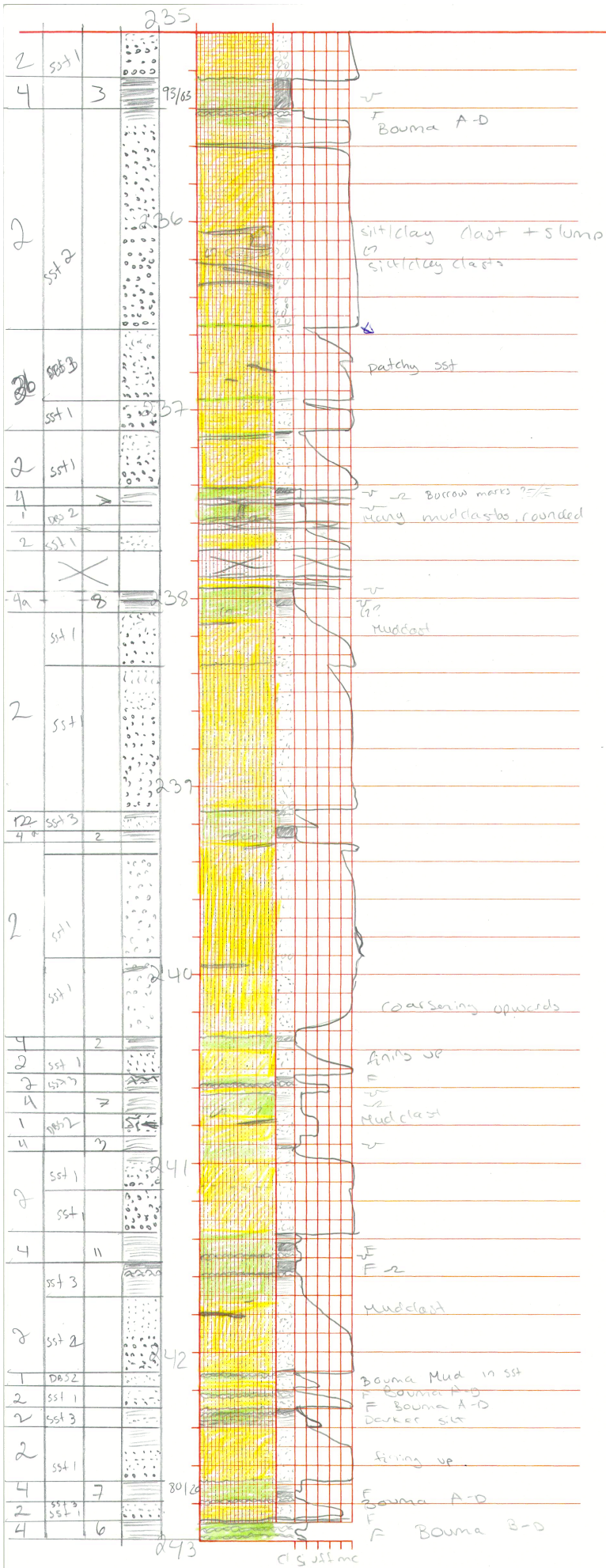
clast

fining up

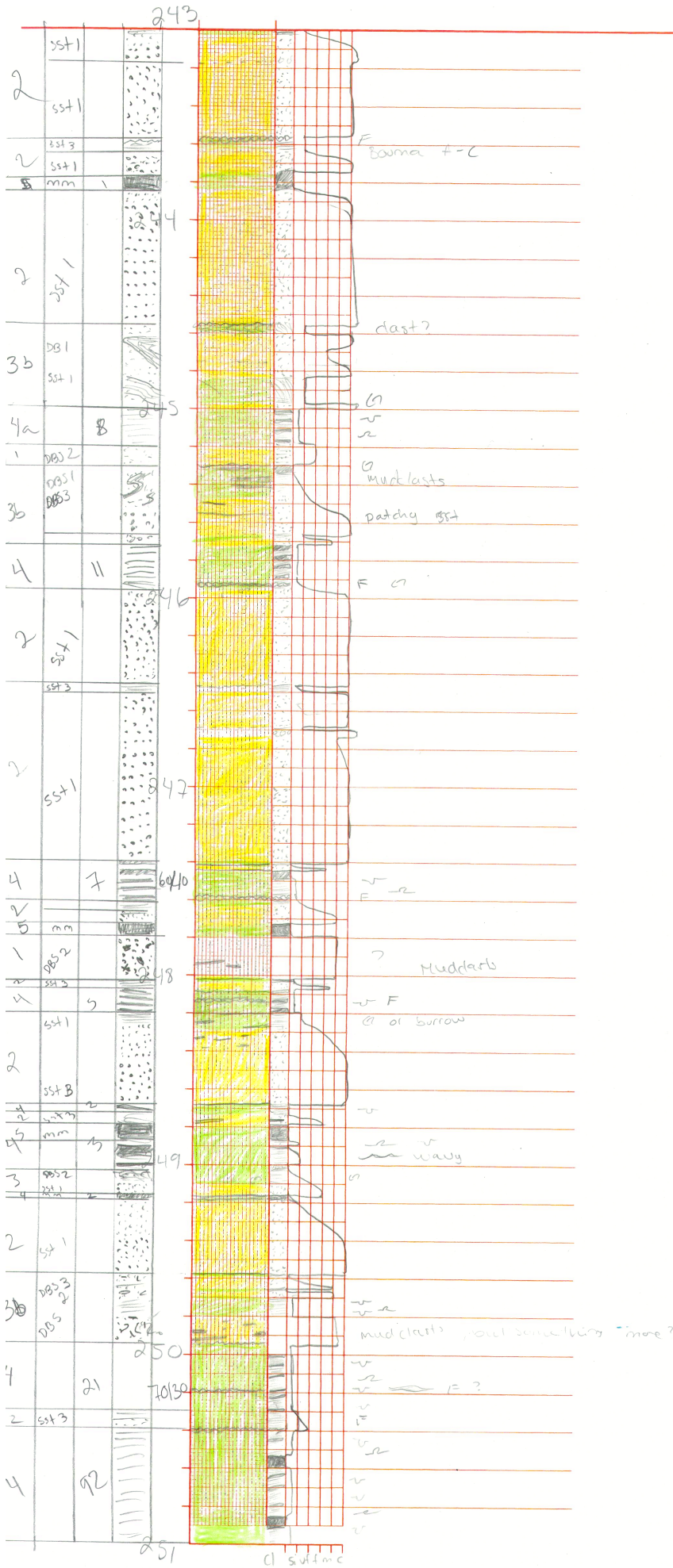
fining up

silt/clast

some clay streaks



LOCATION Well 09-U-02 SHEET NO. 23 DATE 02.10.17 SCALE 1:20 BY Karen

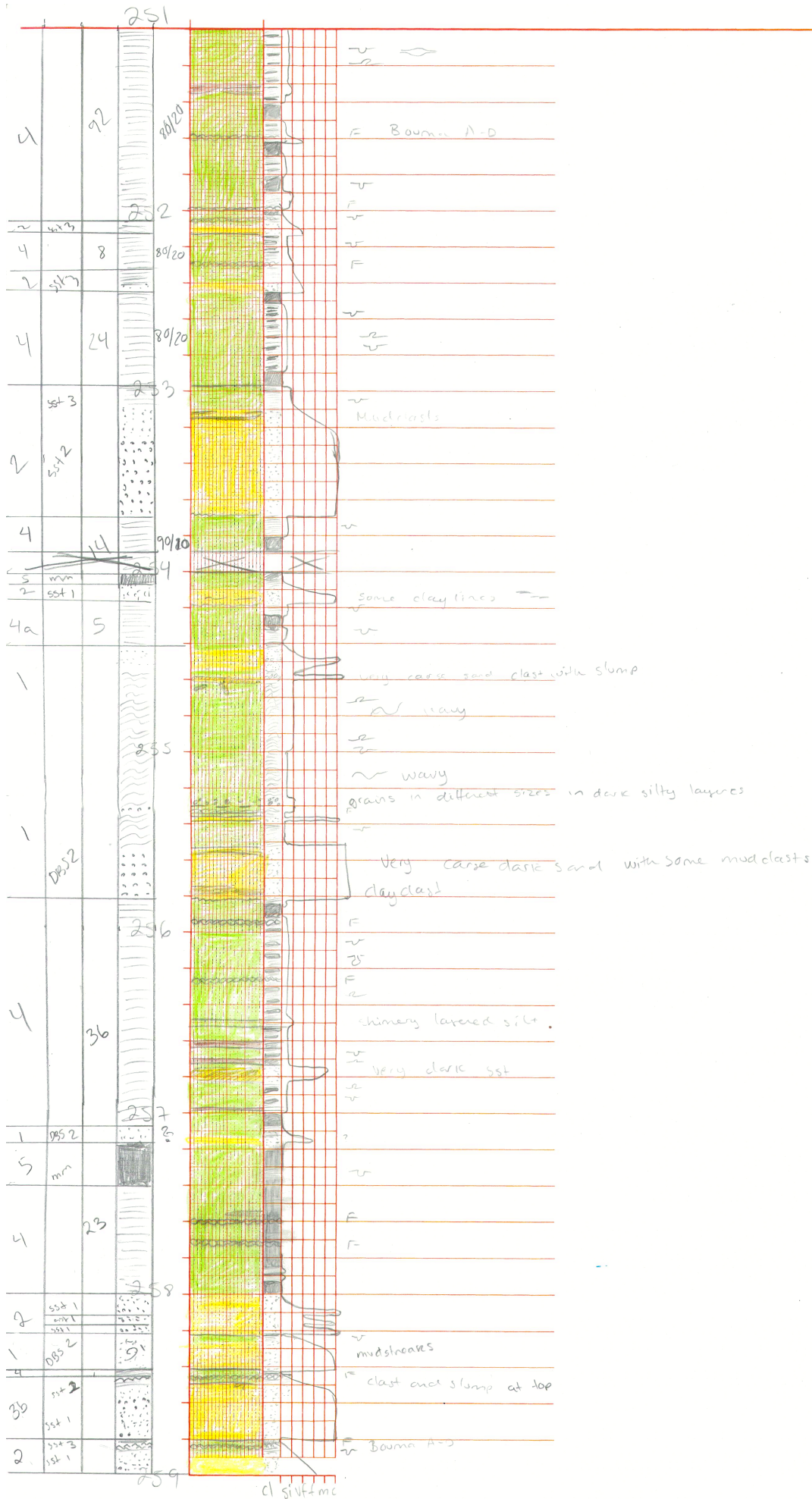


LOCATION 6611/09-U-02

SHEET NO. 24

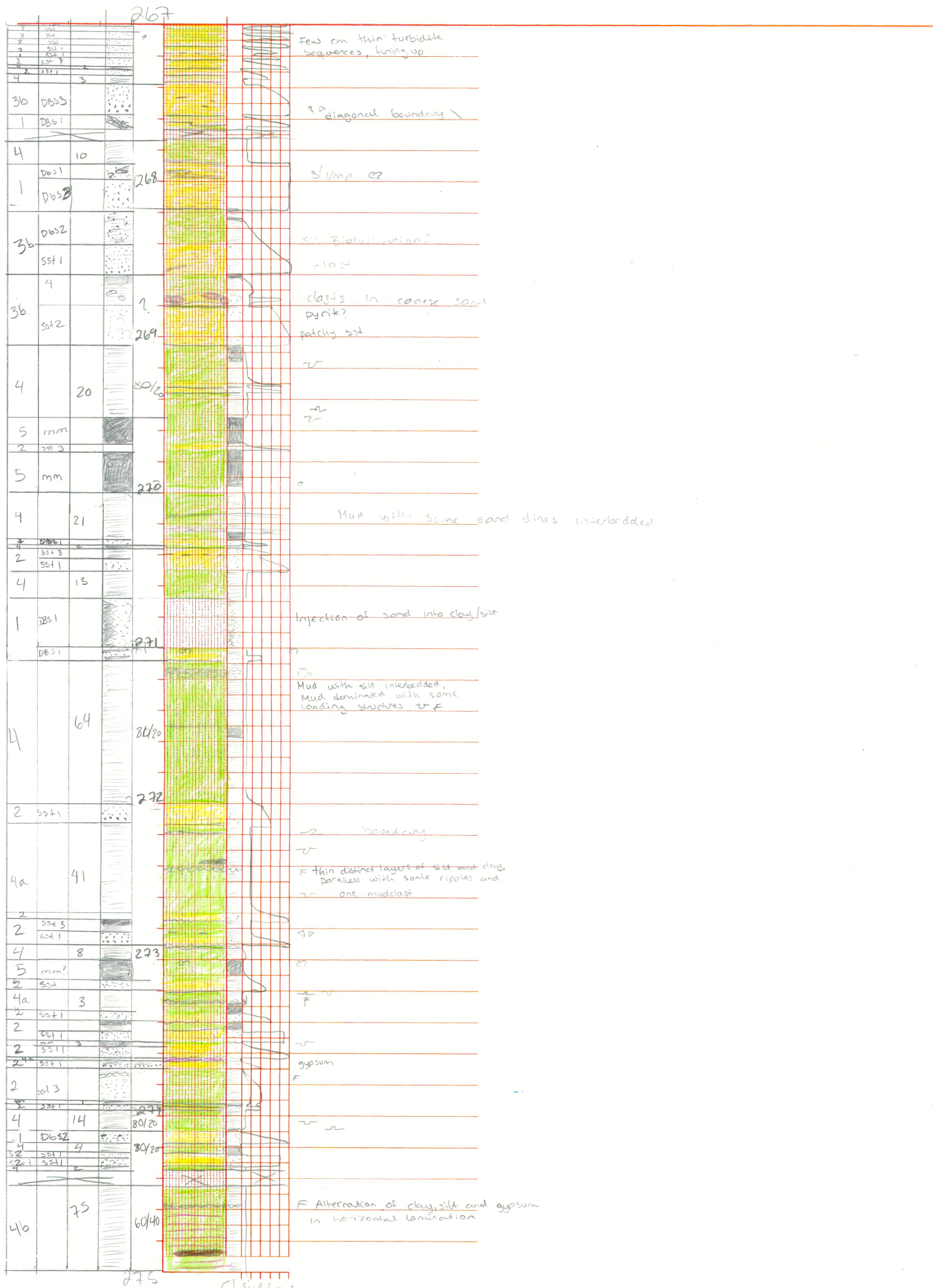
DATE 02/00-17 SCALE 1:20

BY Karen



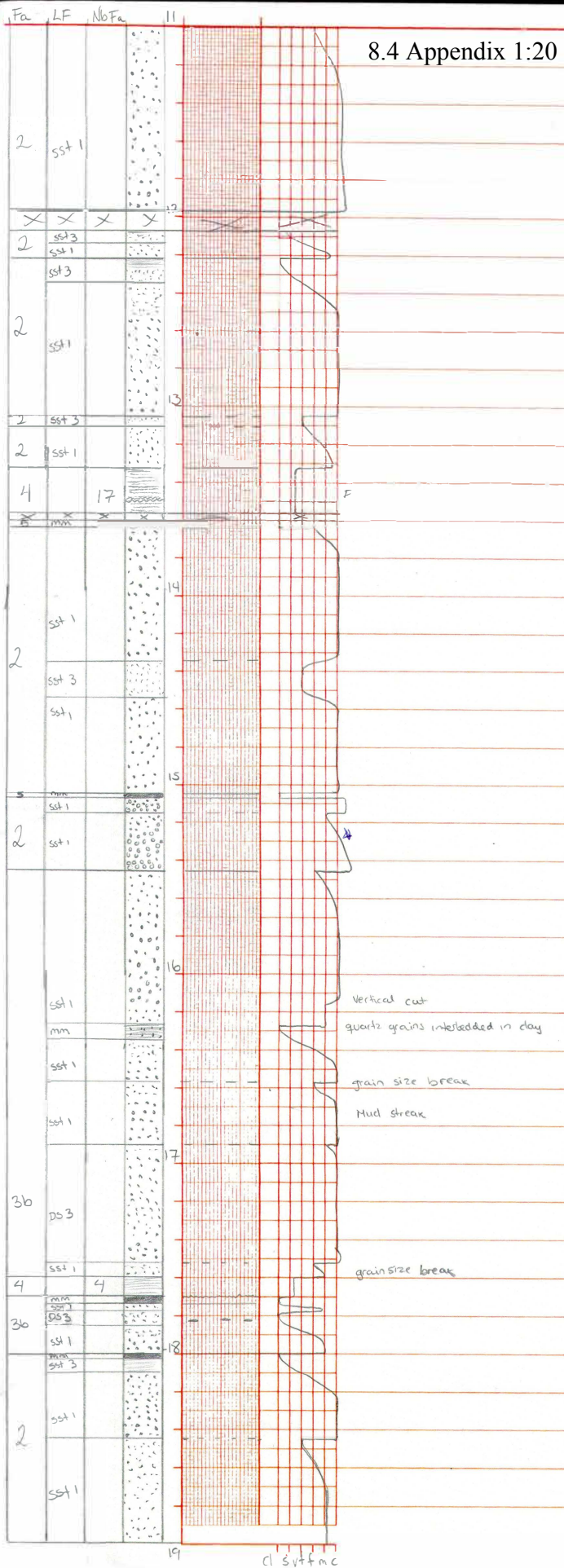








8.4 Appendix 1:20 Core 6611/09-U-01



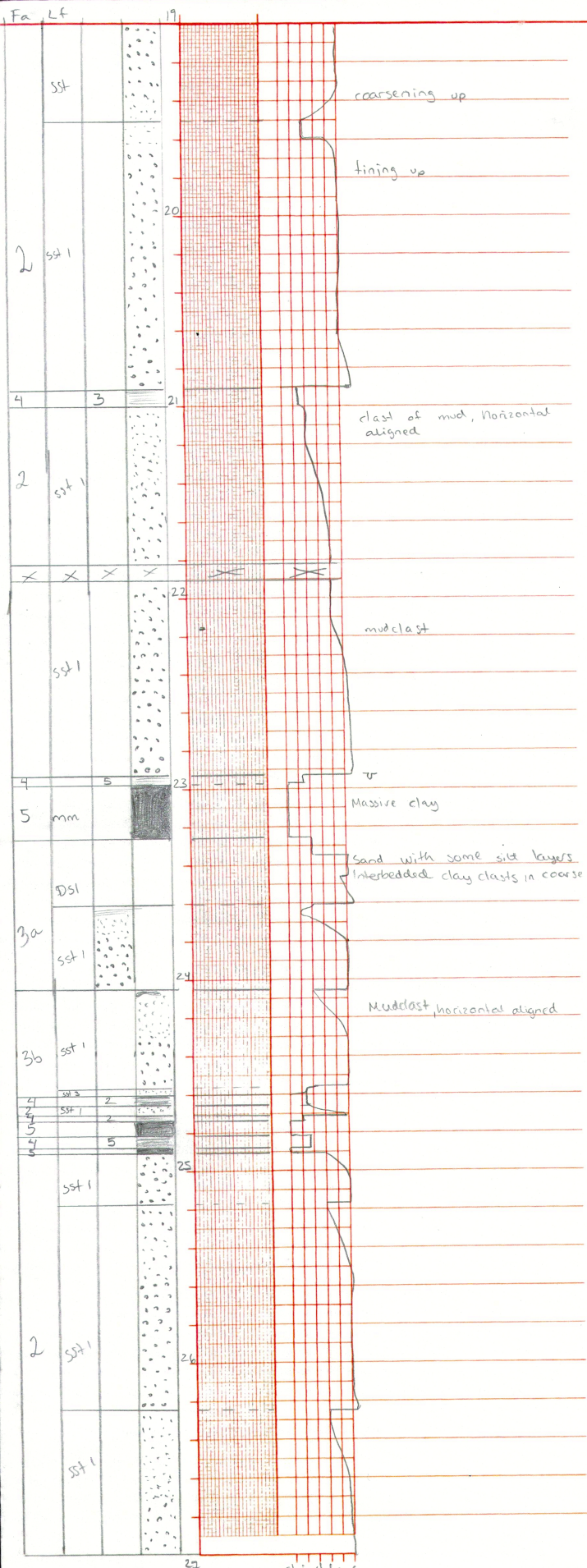
LOCATION 6611/09-U-01

SHEET NO. 1

DATE

SCALE 1:20

BY Karen M. Christensen



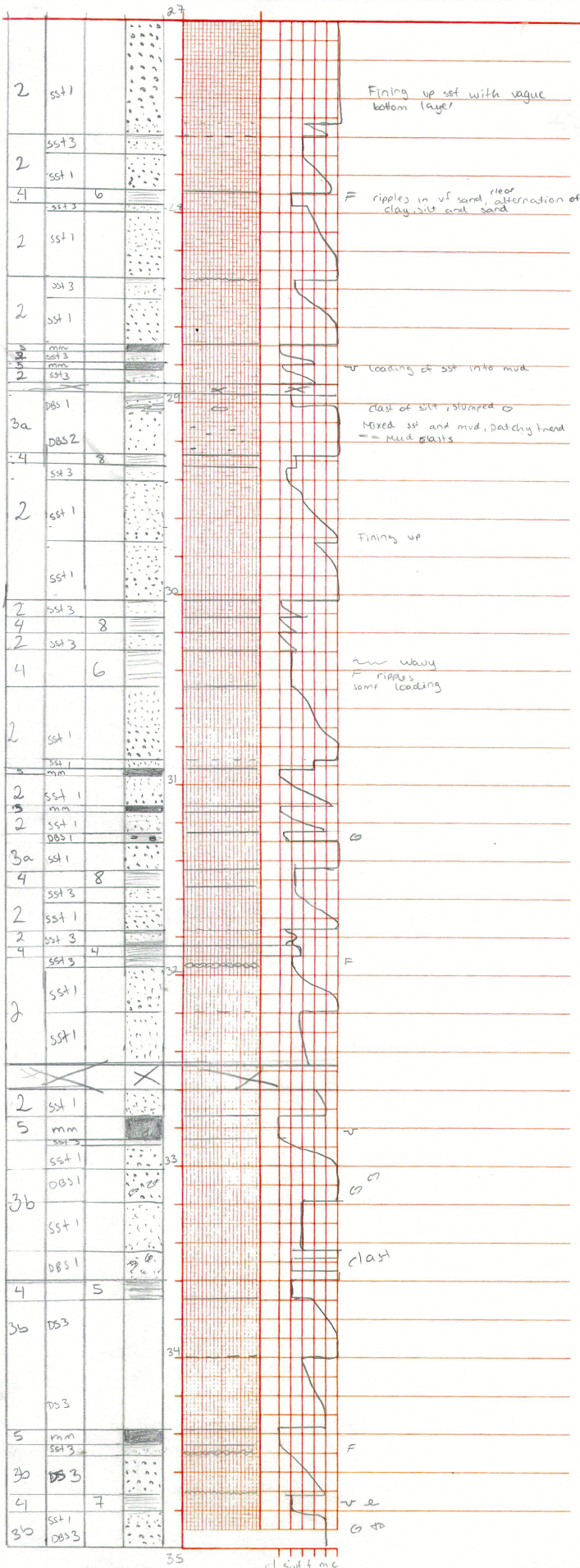
LOCATION 6611/09-U-01

SHEET NO. 2

DATE

SCALE

BY Karen M.L. Christensen



Fining up sst with vague bottom layer

F ripples in v of sand, clear alternation of clay, silt and sand

v loading of sst into mud

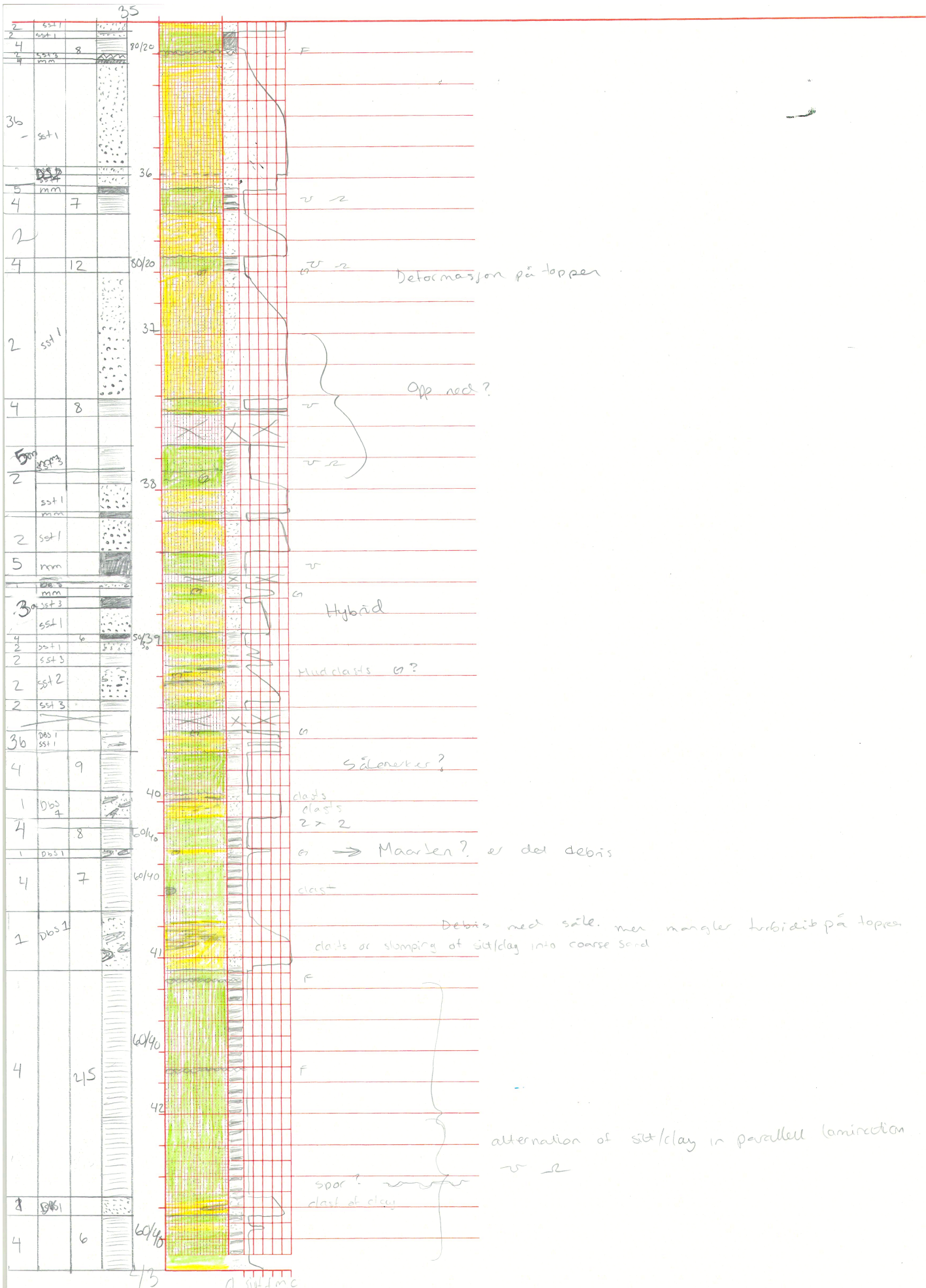
clast of silt, slumped  
Mixed sst and mud, patchy trend = Mud clasts

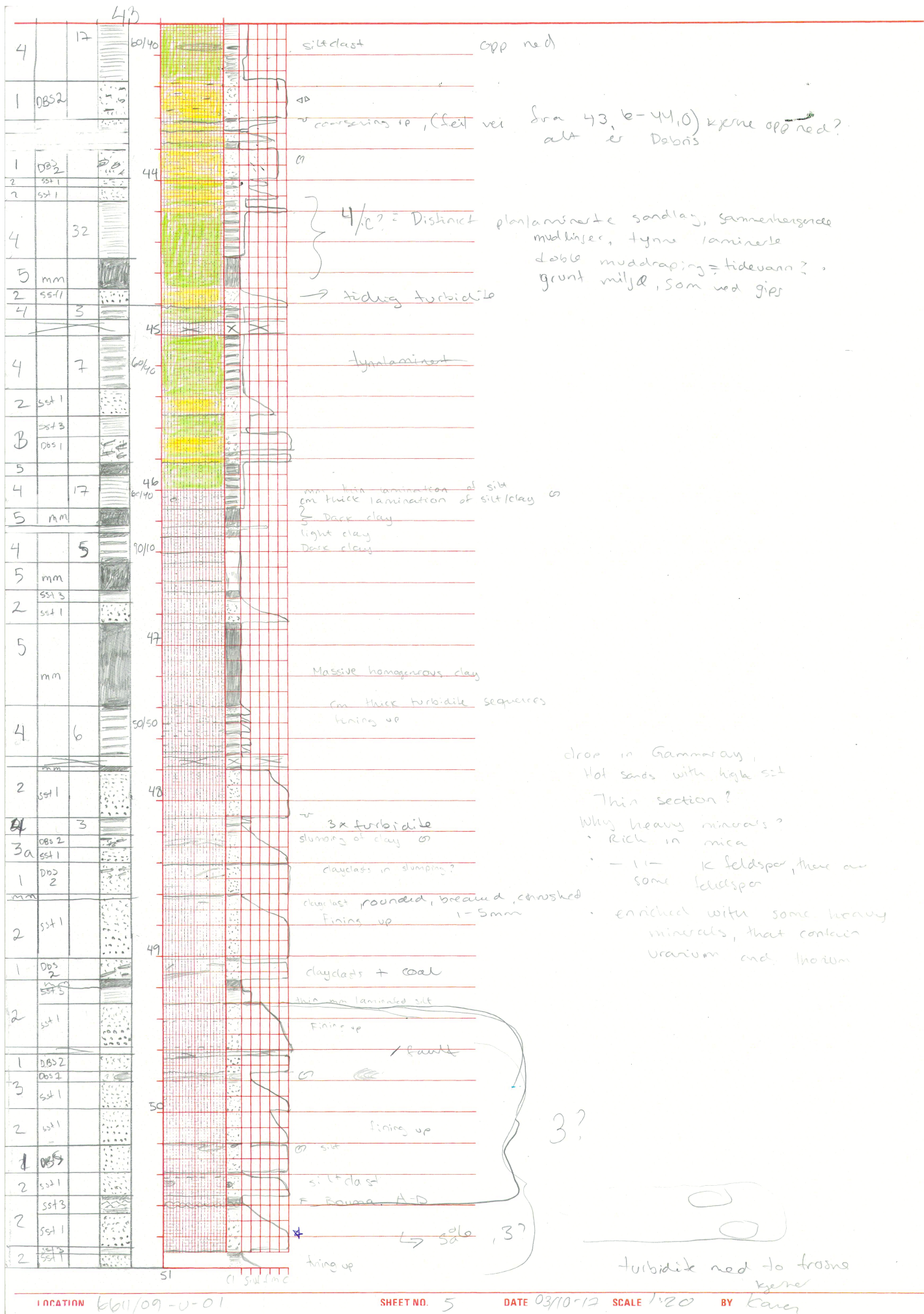
Fining up

wavy ripples some loading

clast

cl silt m c





Sira 43, b-44,0) kjerne opp ned?  
alt er Dobris

4/c? = Distinct planar-sorted sandlay, sammenhengende mulhiser, tyne laminerte doble muddraping = tidevann? grunt miljø, som ved gips

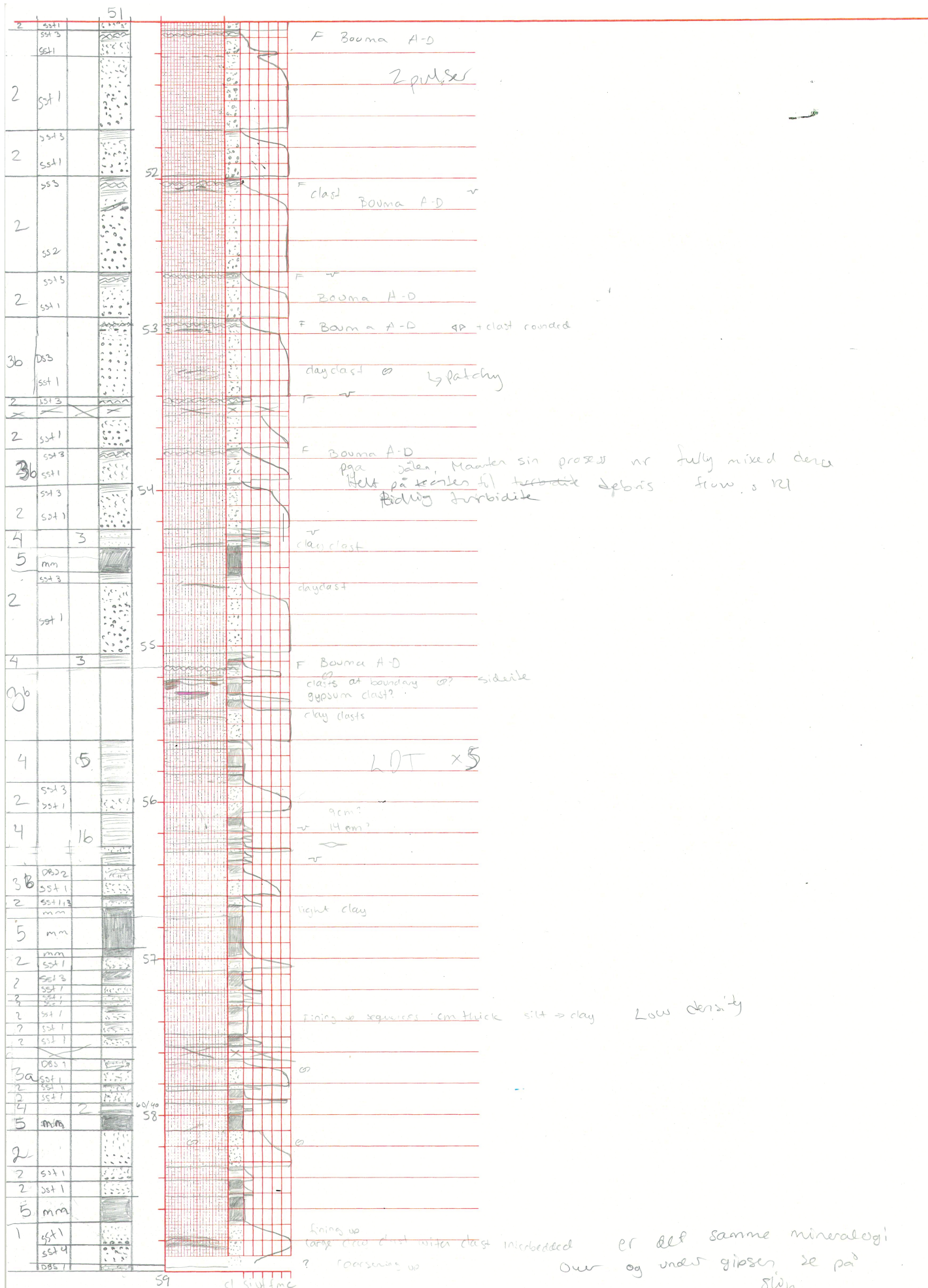
drop in Gamma-ray,  
Hot sands with high silt  
Thin section?

Why heavy minerals?  
Rich in mica  
- 11 - K feldspar, there are some feldspar  
enriched with some heavy minerals, that contain Uranium and Thorium

3?



turbidite need to freeze here



LOCATION 6611/09-U-01

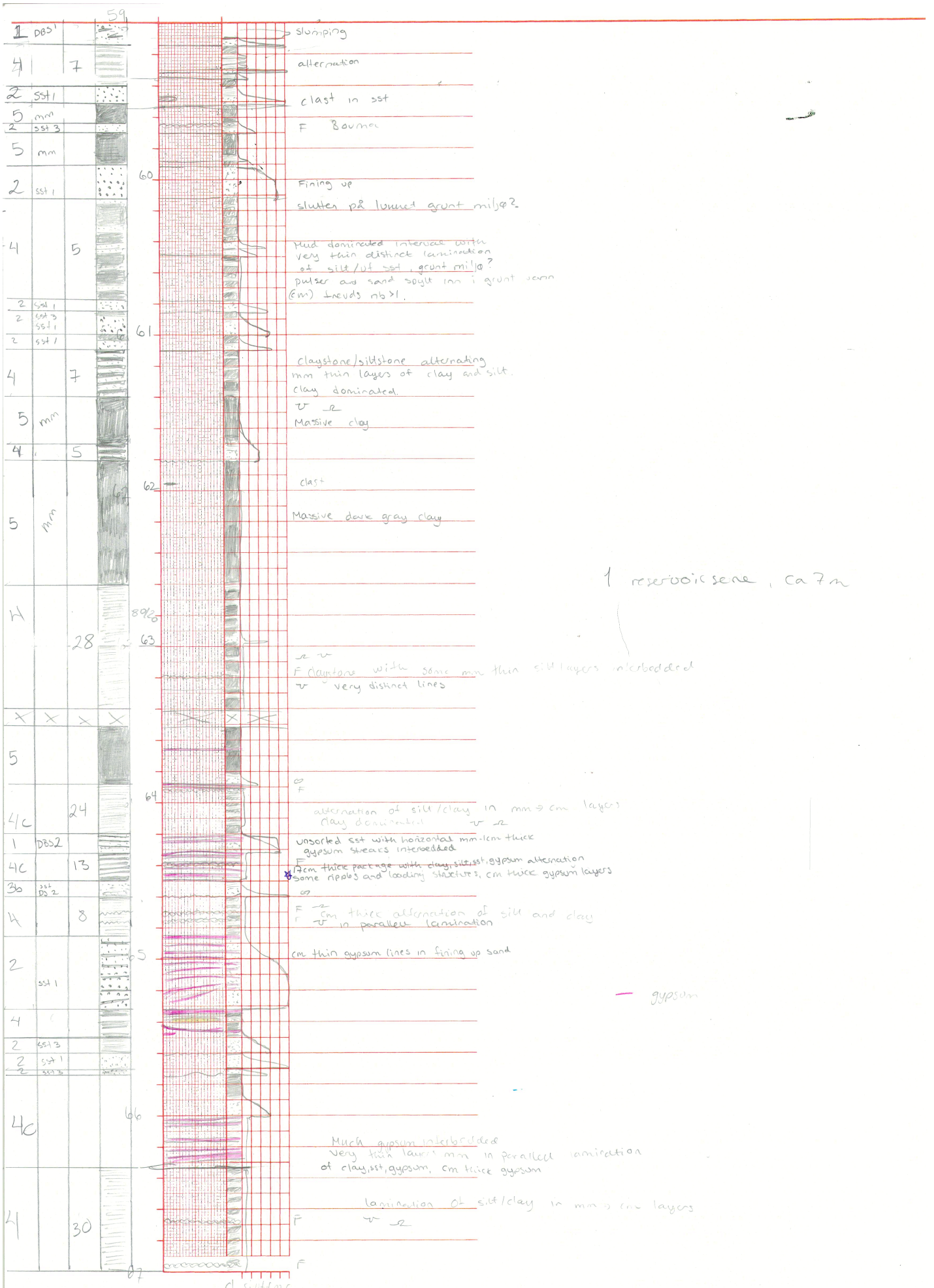
SHEET NO. 6

DATE 06/10-12

SCALE 1:20

BY Kaver



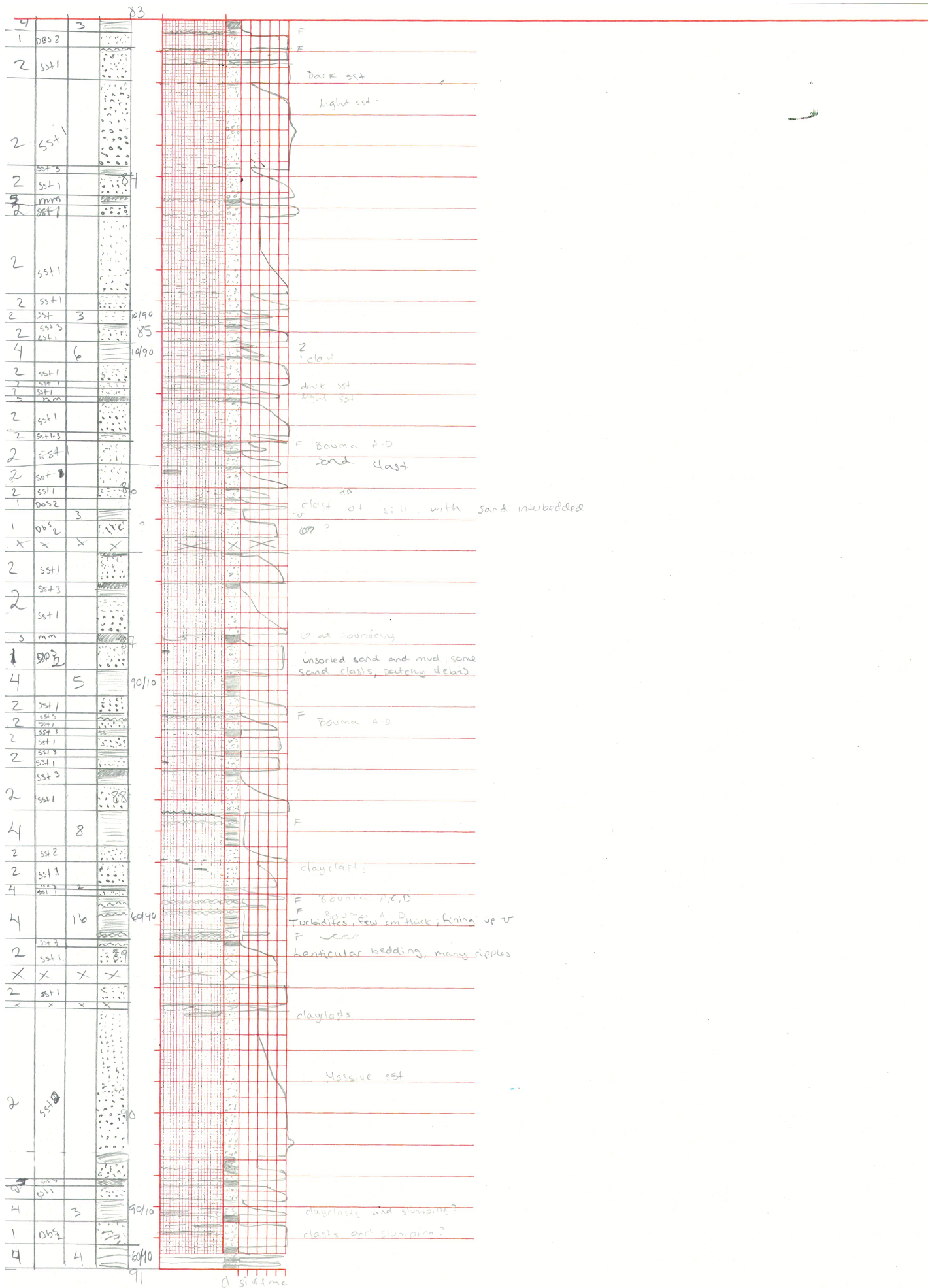


1 reservoiric zone, ca 7m

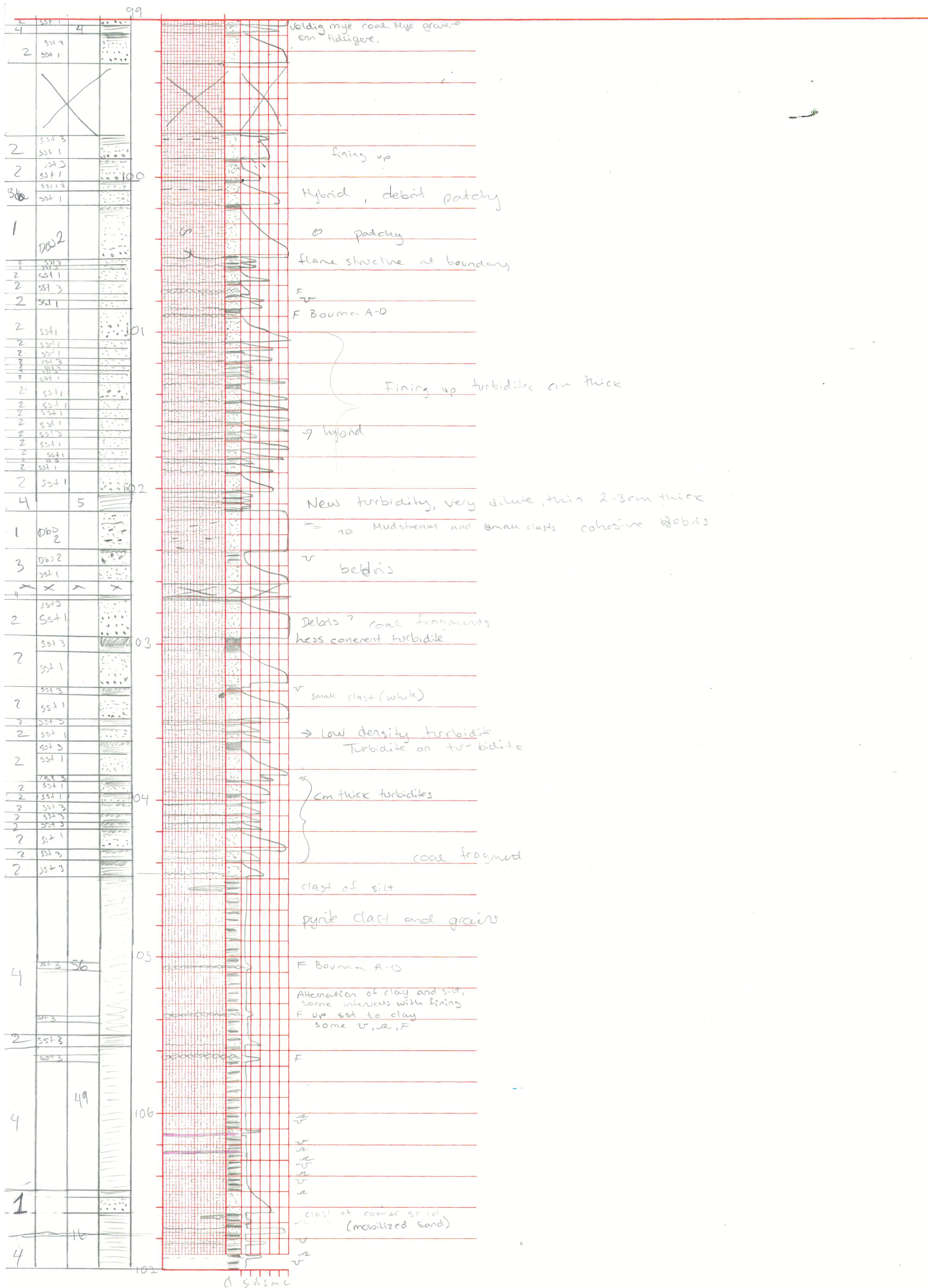
— gypsum













115

116

117

118

?

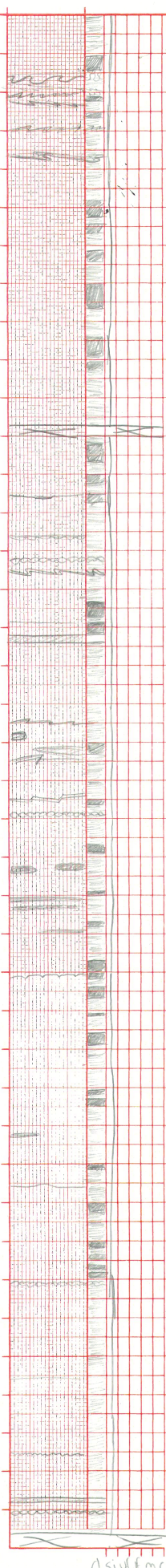
114

120

121

122

123



258

✓

Boundary with pink mineral, feldspar?

✓

F

white intervals, matte in colour

Microtautites

white clast, matte colour

Microtautites

F

clast of silt

clast clear mat. light

clast of silt

✓

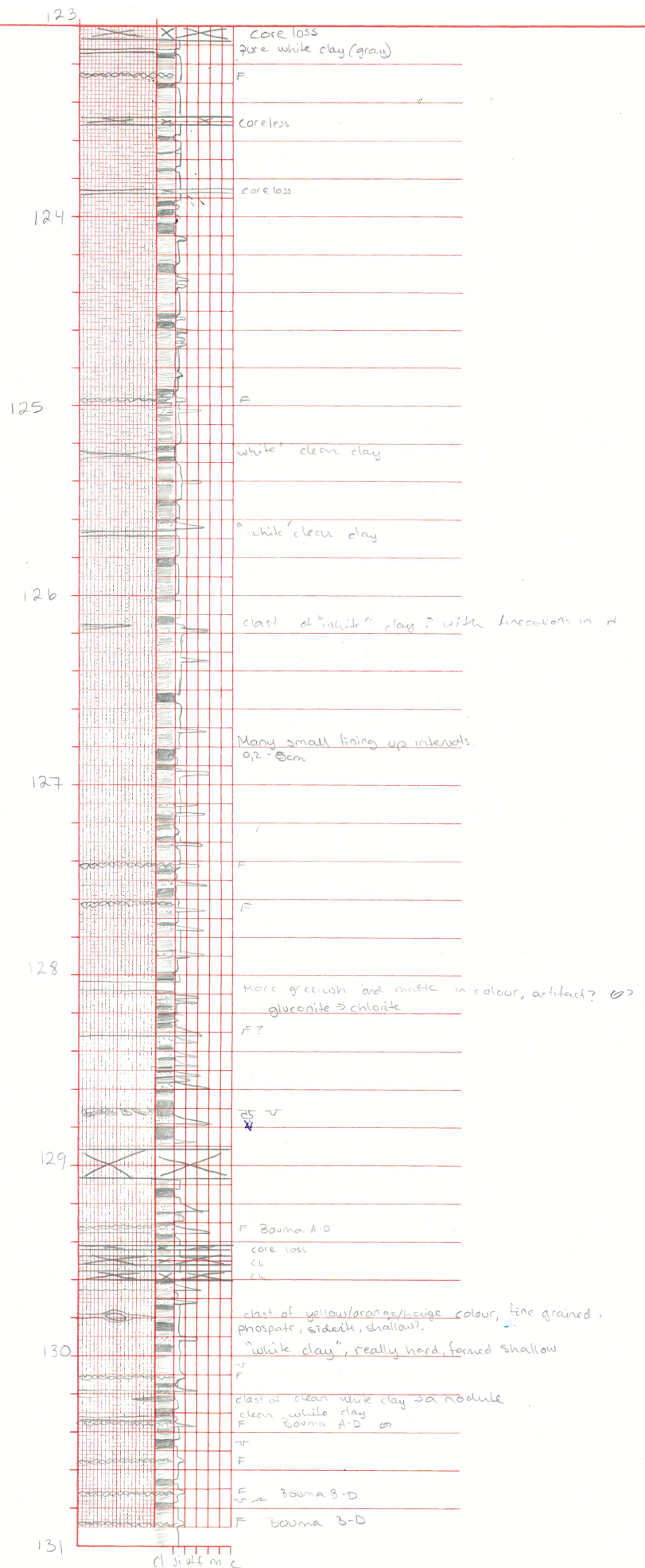
More greenish colour than above and below

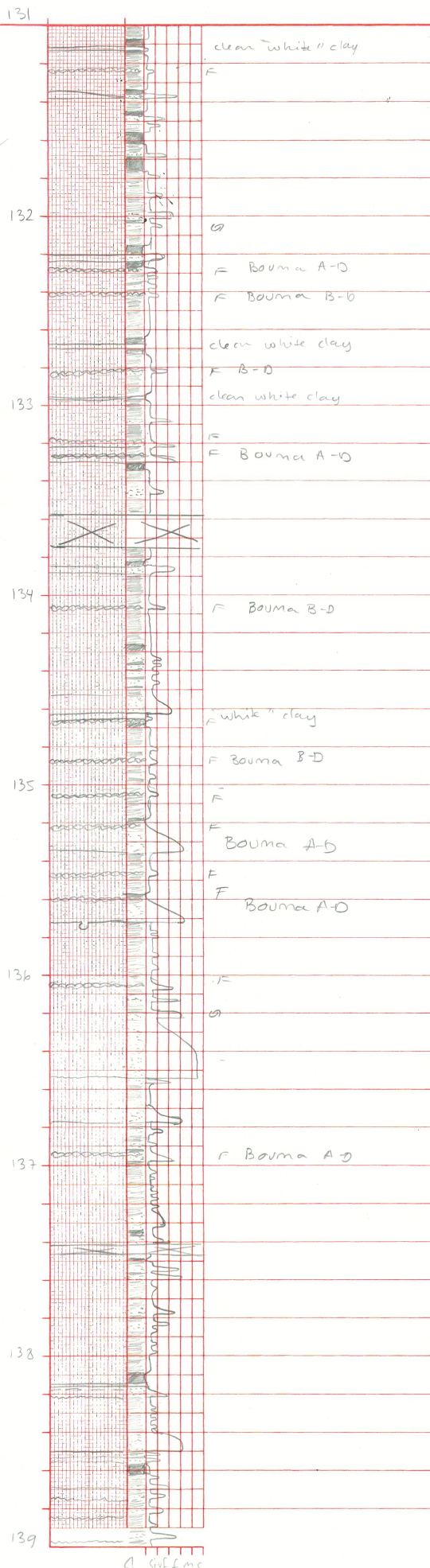
F

change in colour at 11cm from dark to white (pale)

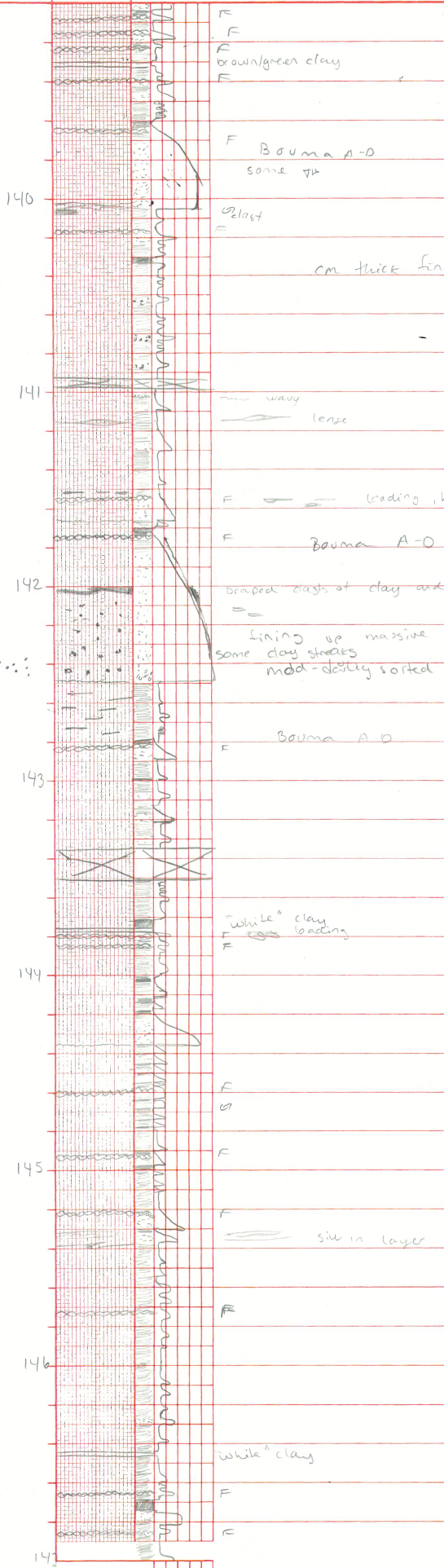
11 silt & mc





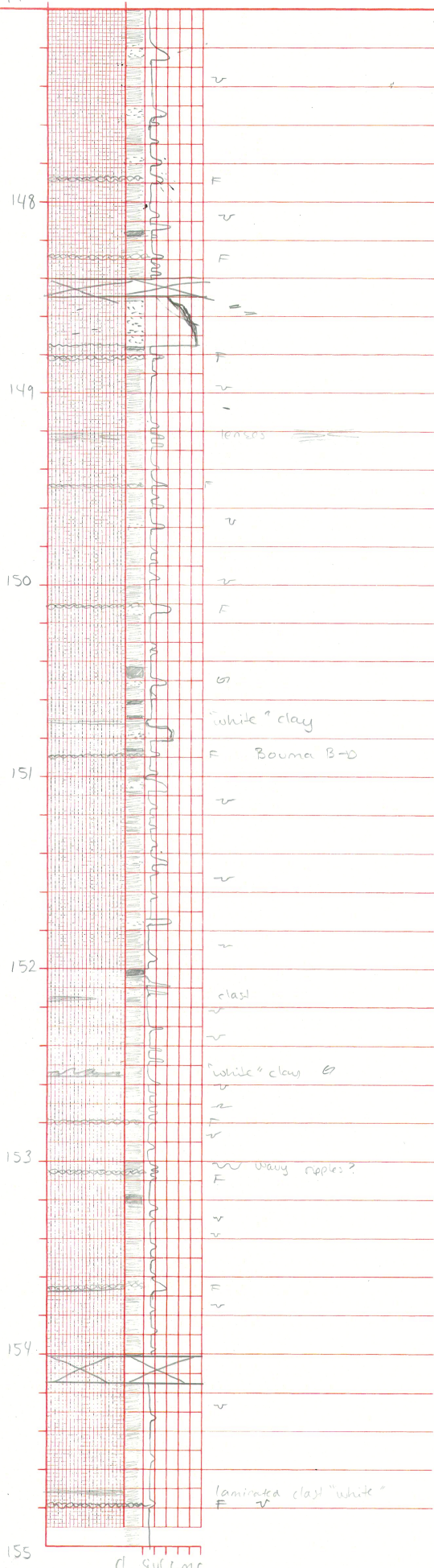


139

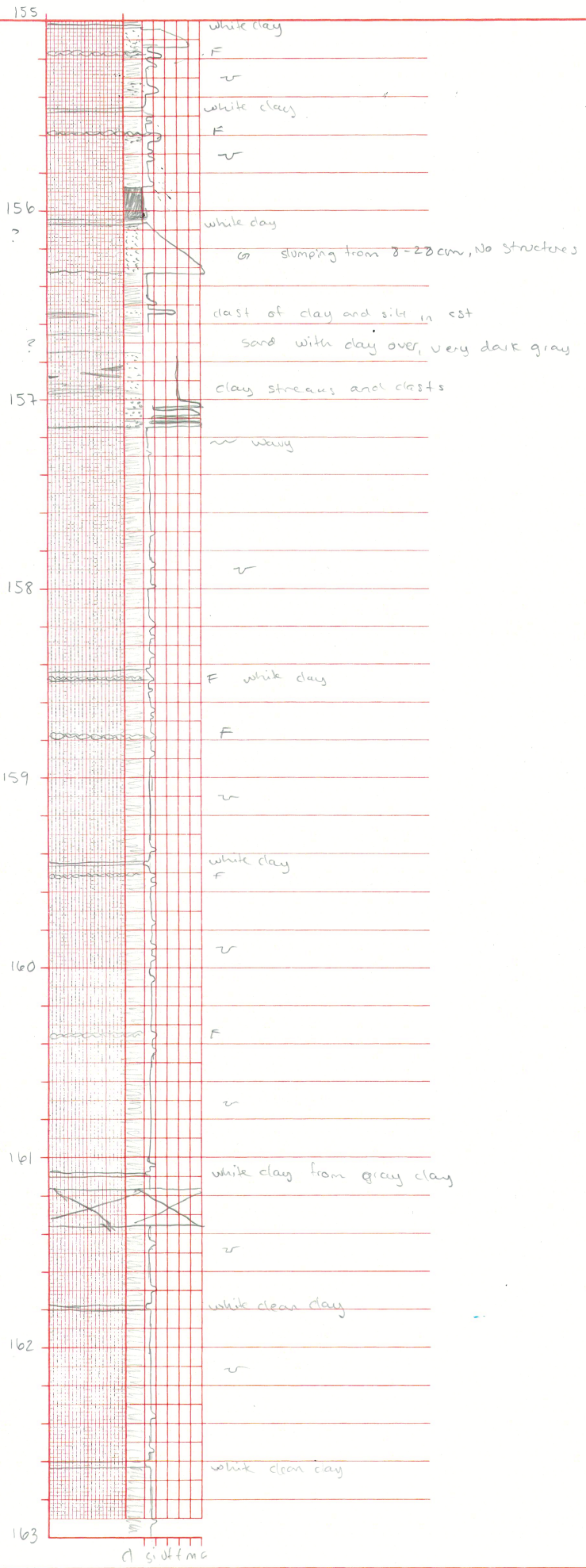


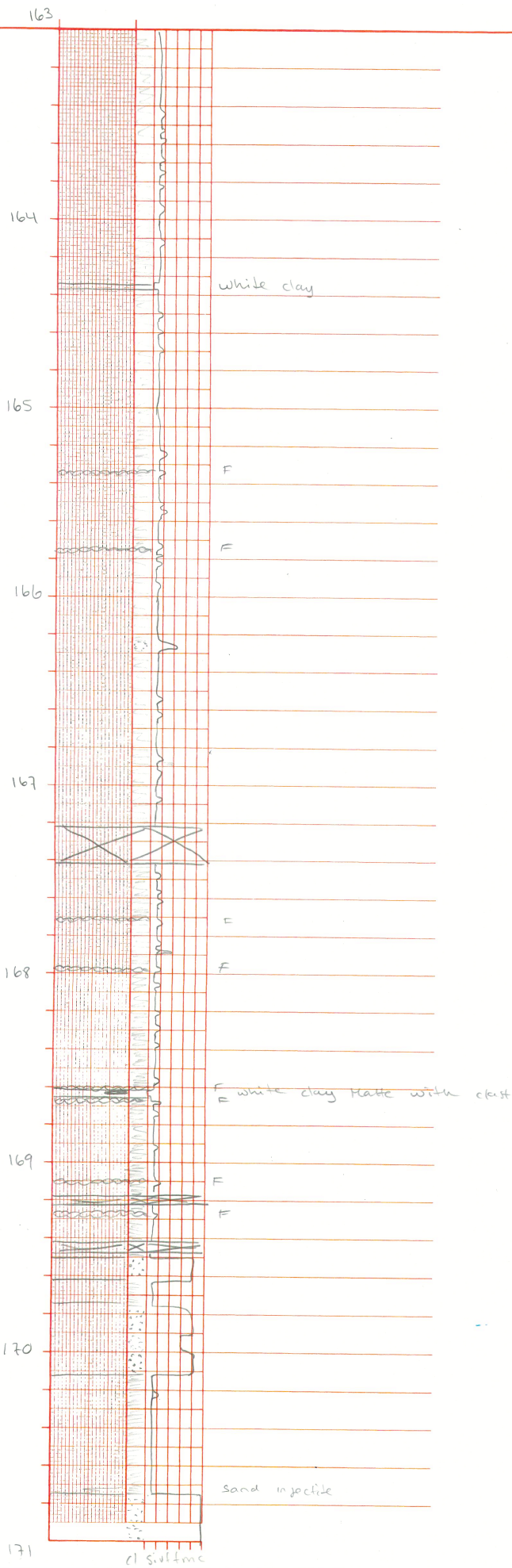
cl sieve mc

147



d' Sult mc





171

172

173

174

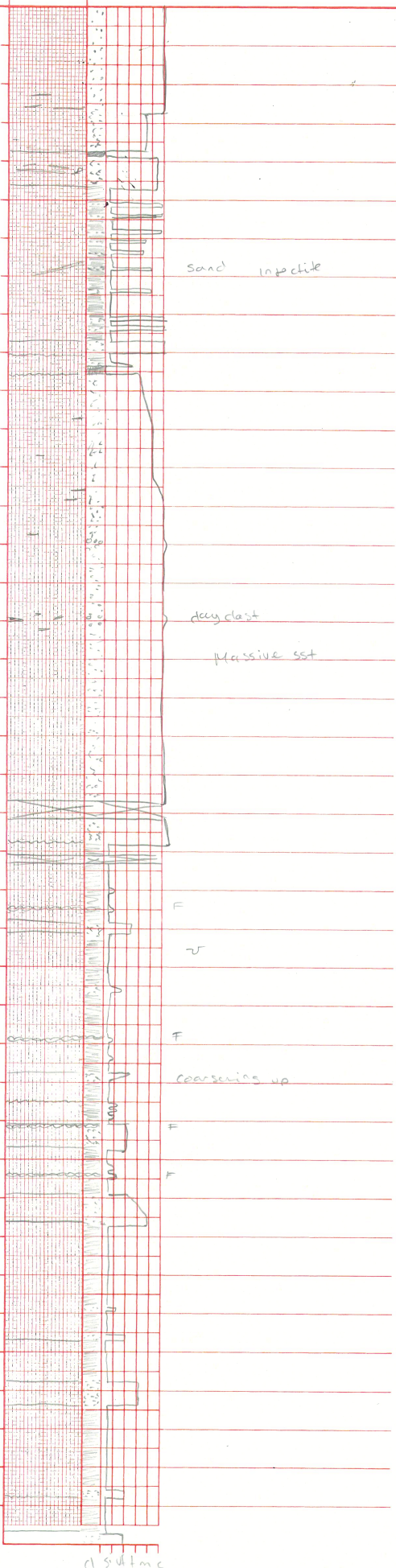
175

176

177

178

179



sand in part

fine clay

massive sst

F

~

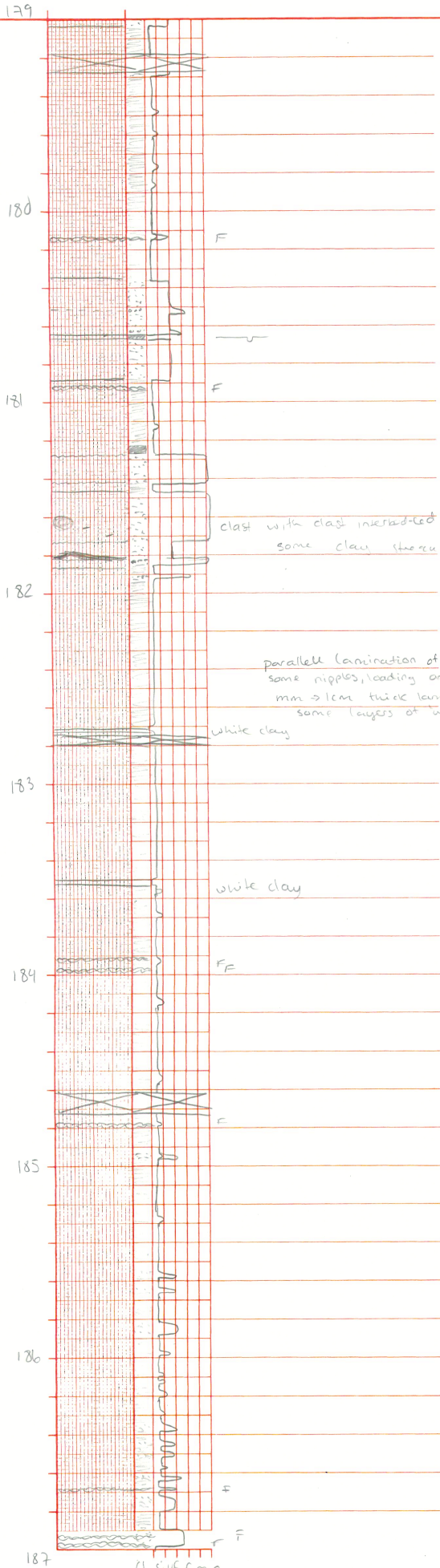
F

coarsening up

T

T

1/200 ft



clast with clast interbedded, white clay with mud brown?  
some clay streaks

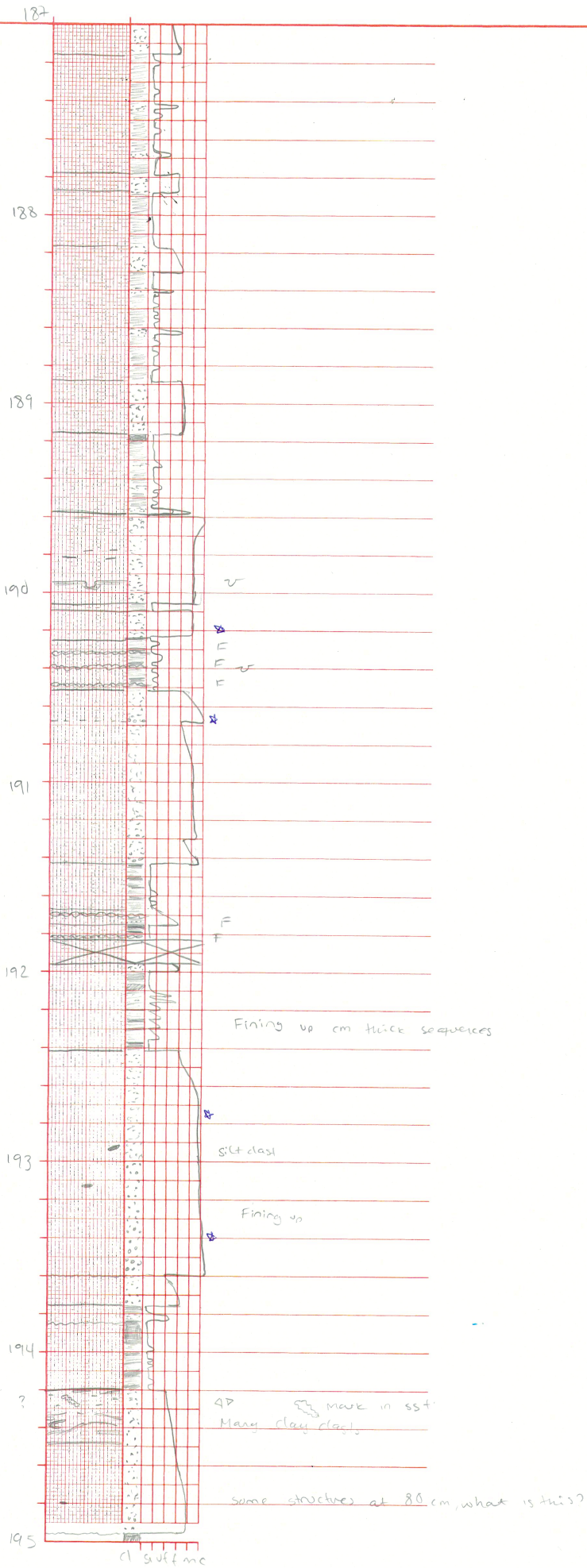
parallel lamination of silt, clay and sand.  
some ripples, loading and flame structures  
mm to cm thick lamination  
some layers of white clay

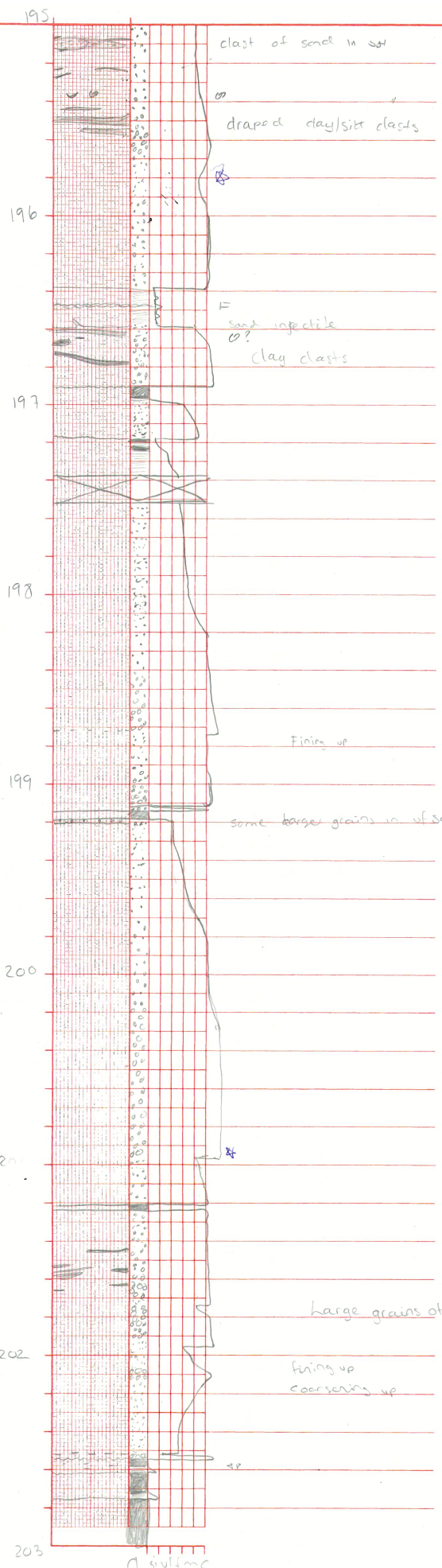
white clay

white clay

Cl silt fine







clast of sand in sst

draped clay/silt clasts

sand injectite  
clay clasts

fining up

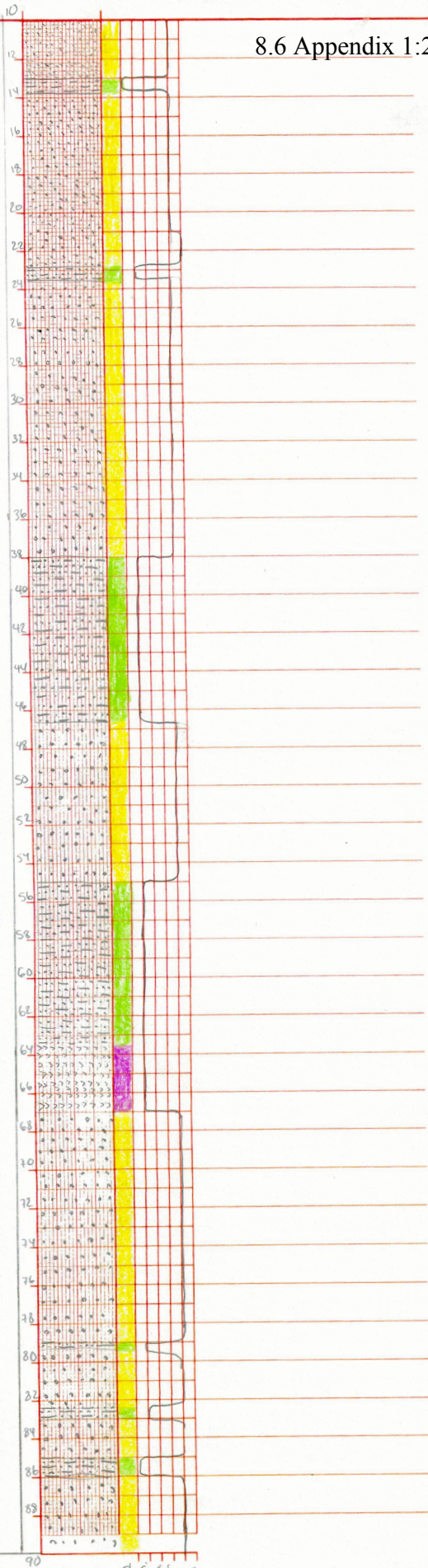
some larger grains in wf sand

large grains of

fining up  
coarsening up

quartz, calcid spar, 3 different types of clay (white, brown, gray)  
 Some grains with grains interbedded  
 grains up to 1.5cm in diameter  
 Very unsorted conglomerate with varies  
 degrees of roundness of the grains  
 Matrix is coarse sst

8.6 Appendix 1:200 Core 6611/09-U-02

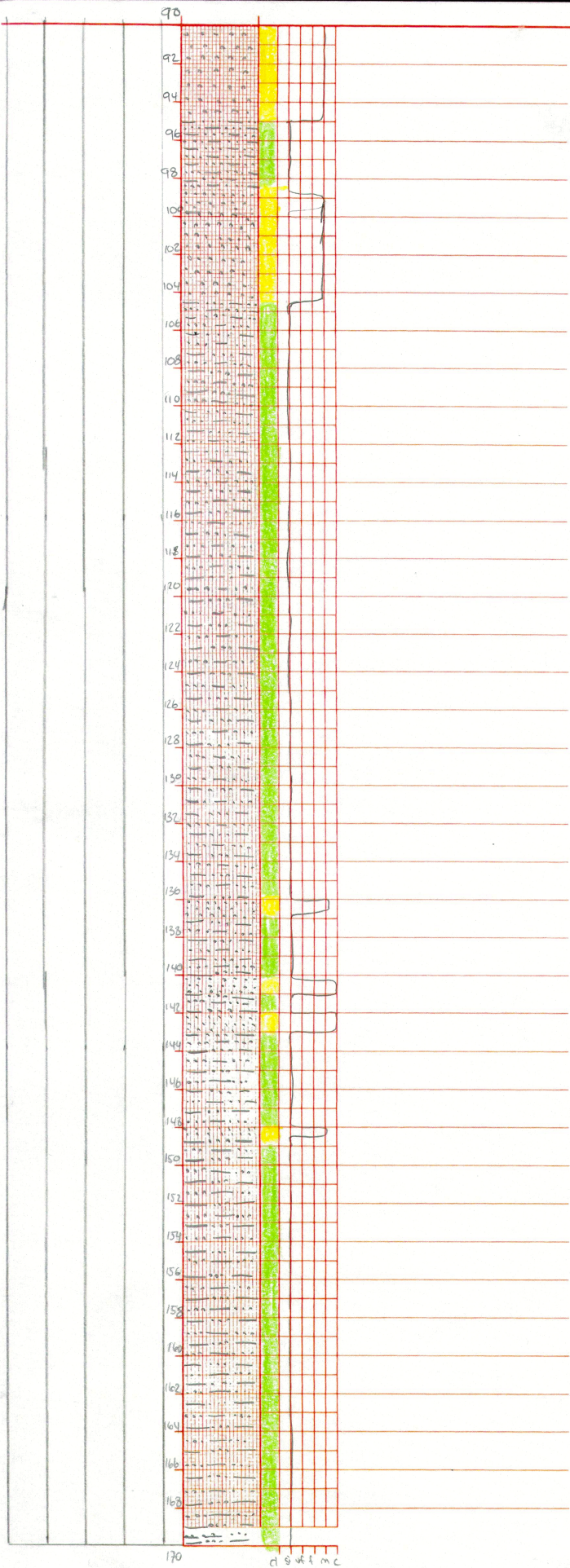


LOCATION 6611/09-U-01

SHEET NO. 1

DATE 17.06.2018 SCALE 1:200

BY Karen M.L. Christensen

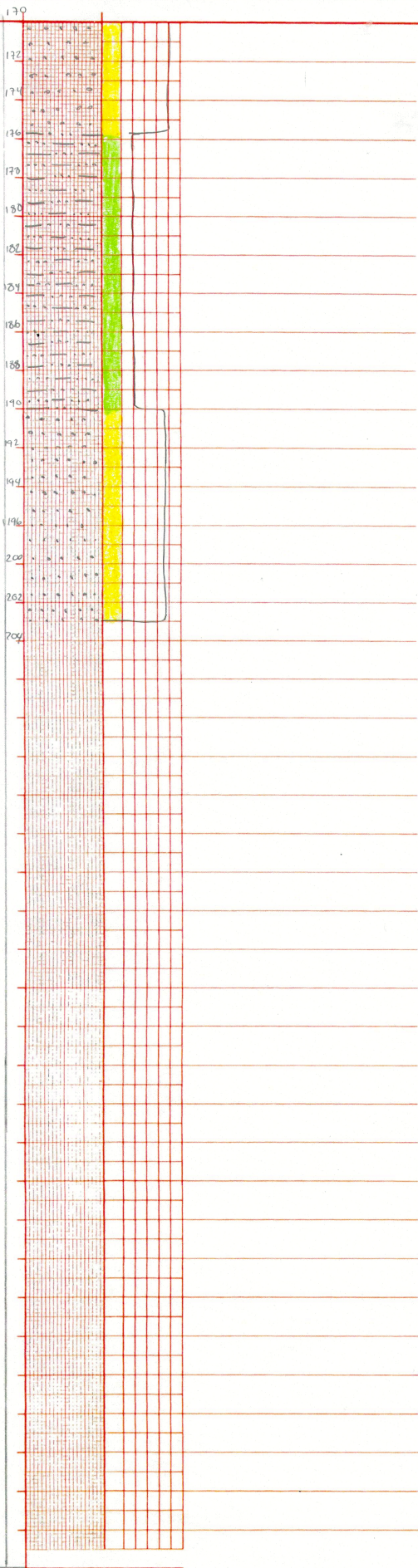


LOCATION 6611/09-U-01

SHEET NO. 2

DATE 17.06.2018 SCALE 1:200

BY Karen M.L. Christensen



d. b. v. f. m. c.

LOCATION 6611/09-U-01

SHEET NO. 3

DATE 17.06.2018 SCALE 1:200

BY Karen M. L. Christensen

266

267

269

266

268

270

272

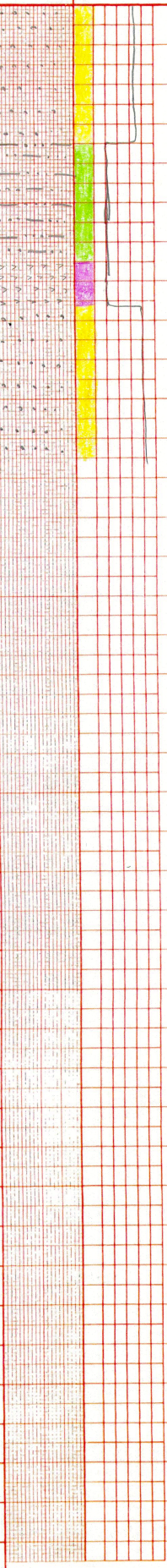
274

276

278

280

282



0 1 2 3 4 5 6 7 8 9 10 m

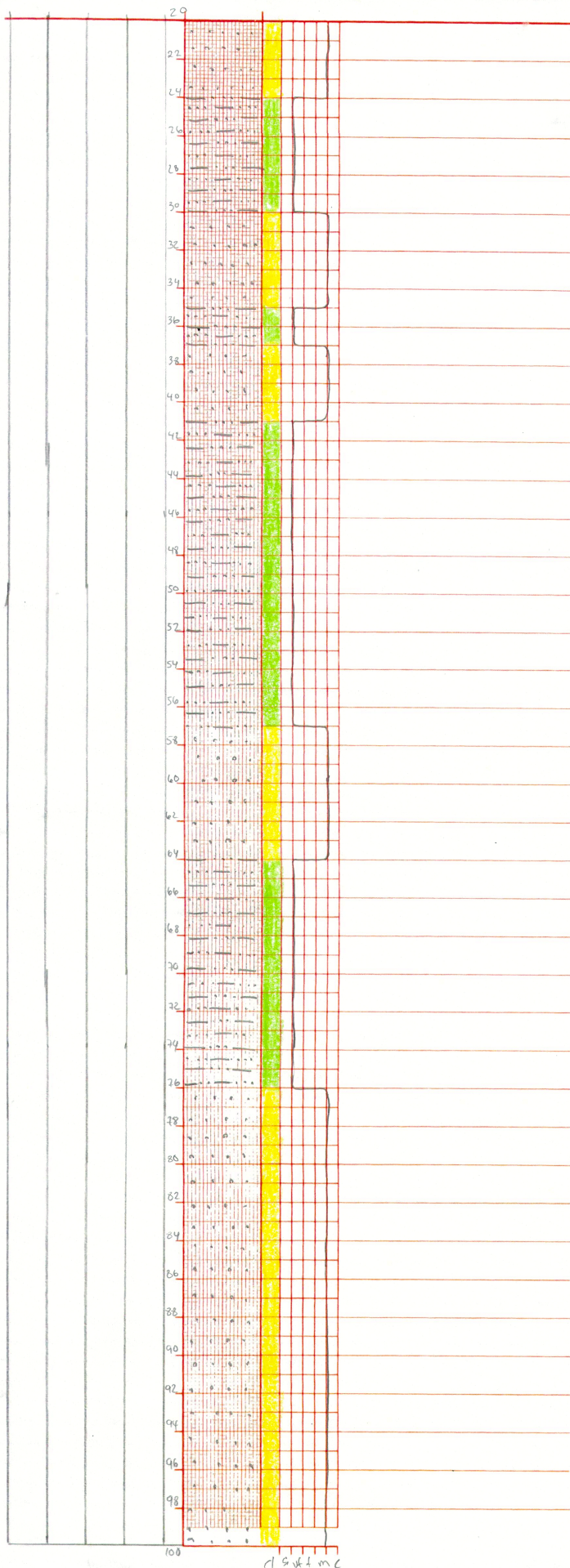
LOCATION 6611/09-U-02

SHEET NO. 4

DATE 17/06-18

SCALE 1:200

BY Karen M. L. Christensen



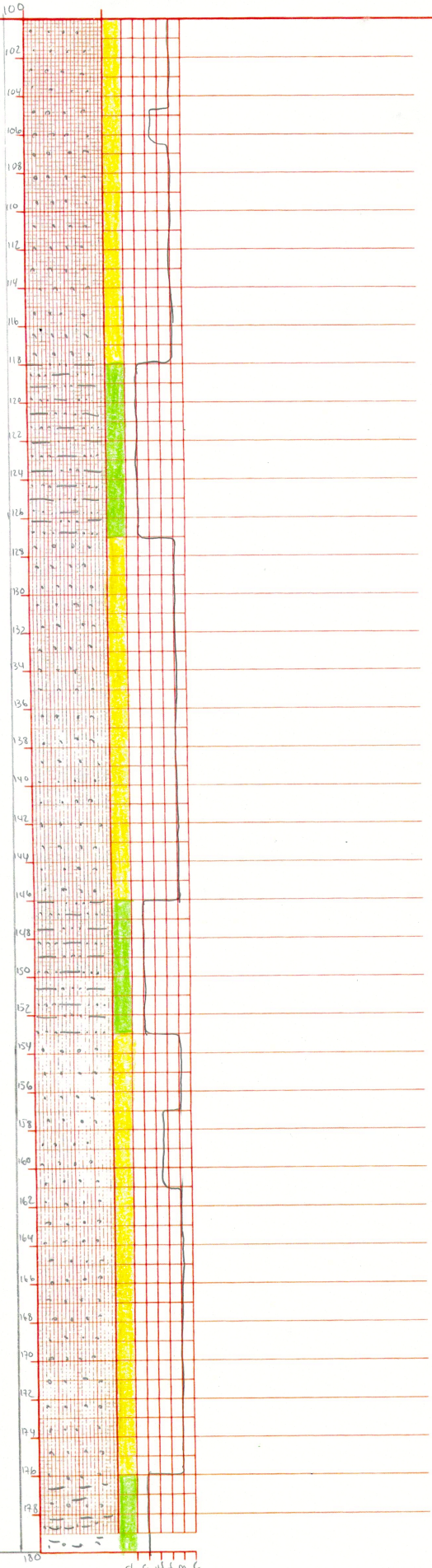
d 5 m t m c

LOCATION 6611/09-U-02

SHEET NO. 1

DATE 17.06.18 SCALE 1:200

BY Karen M L Christensen



1:50 44 m c

LOCATION 6611/09-U-02

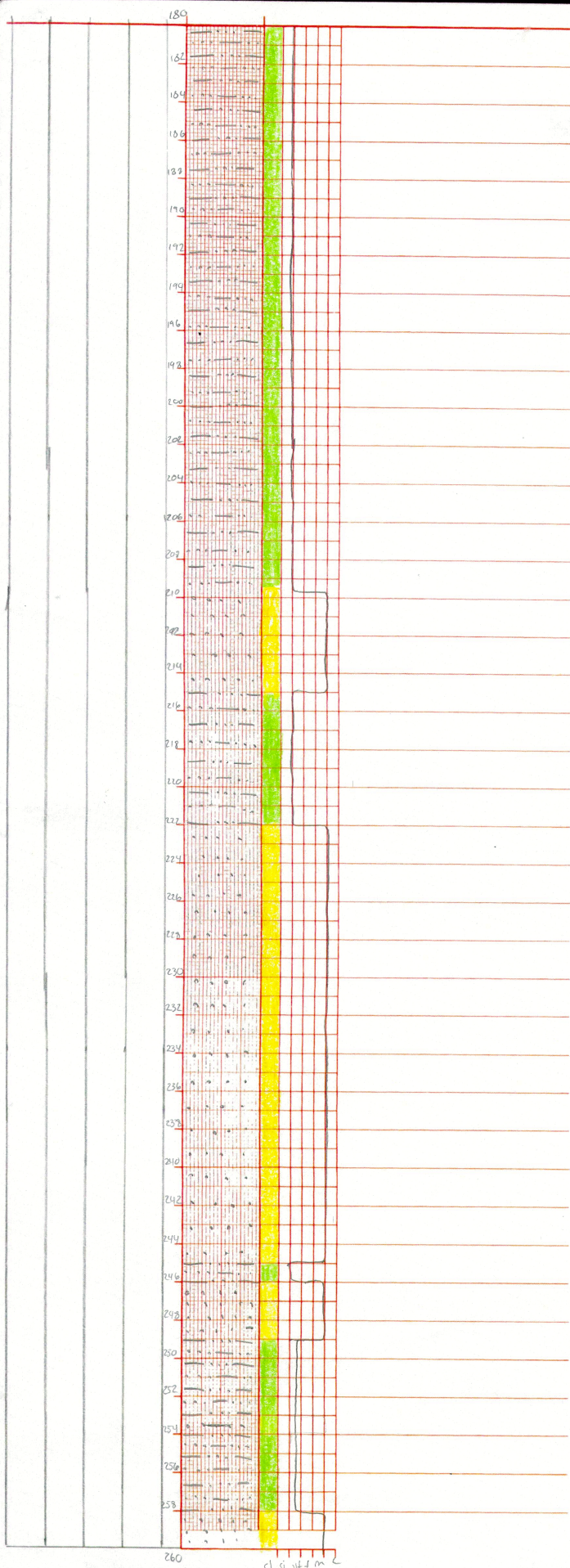
SHEET NO. 2

DATE 17.06.18

SCALE 1:200

BY Karen M.L. Christensen





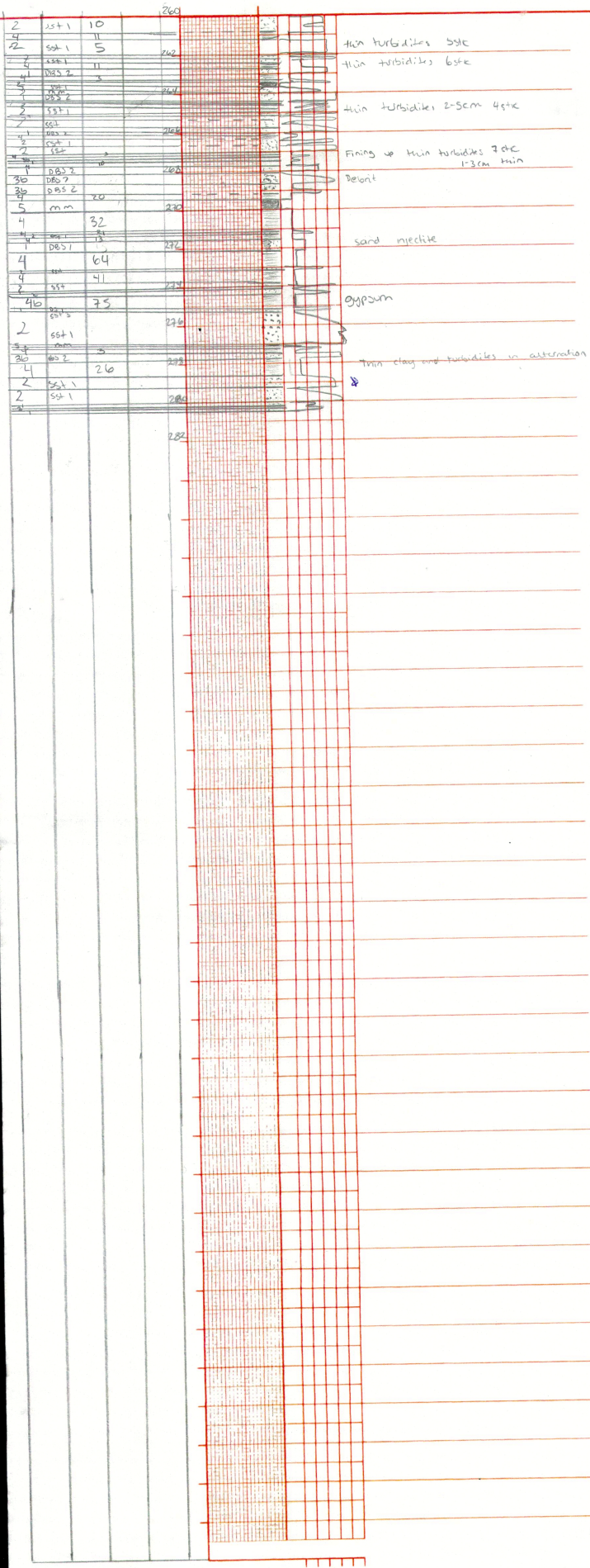
LOCATION 6611/09-U-02

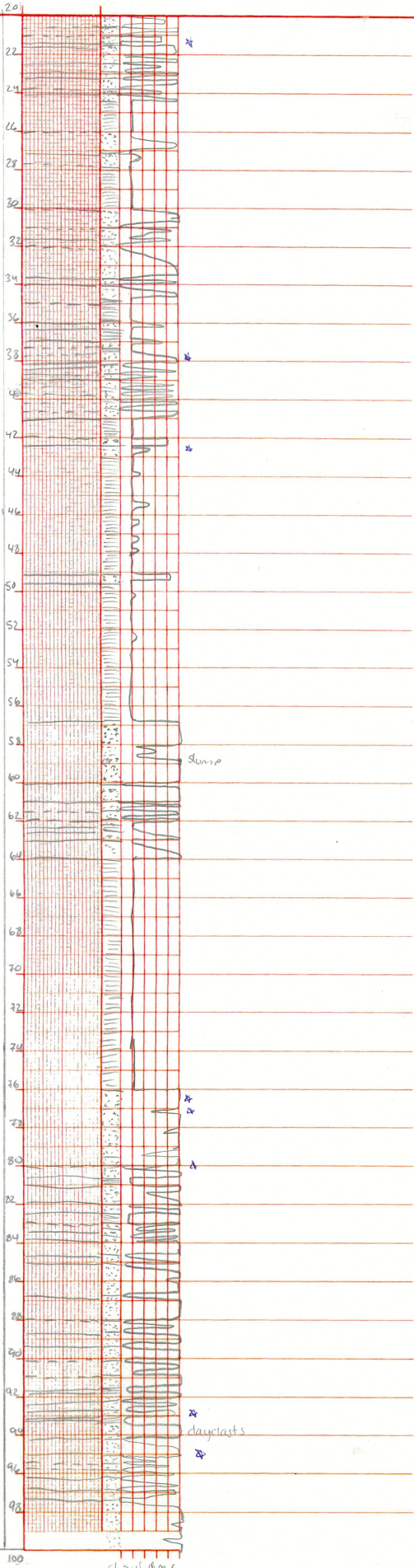
SHEET NO. 3

DATE 17.06.12

SCALE 1:200

BY Karen M.L. Christensen





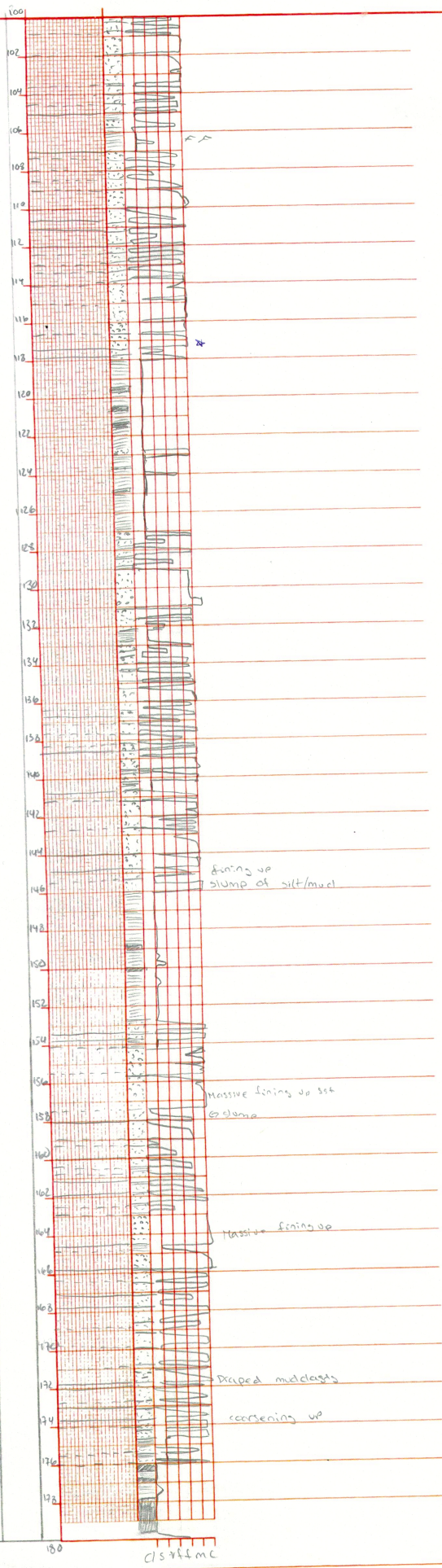
LOCATION 6611/09-U-02

SHEET NO. 1

DATE 28.05.18

SCALE 1:200

BY Karen M L Christensen



cls 764 mc

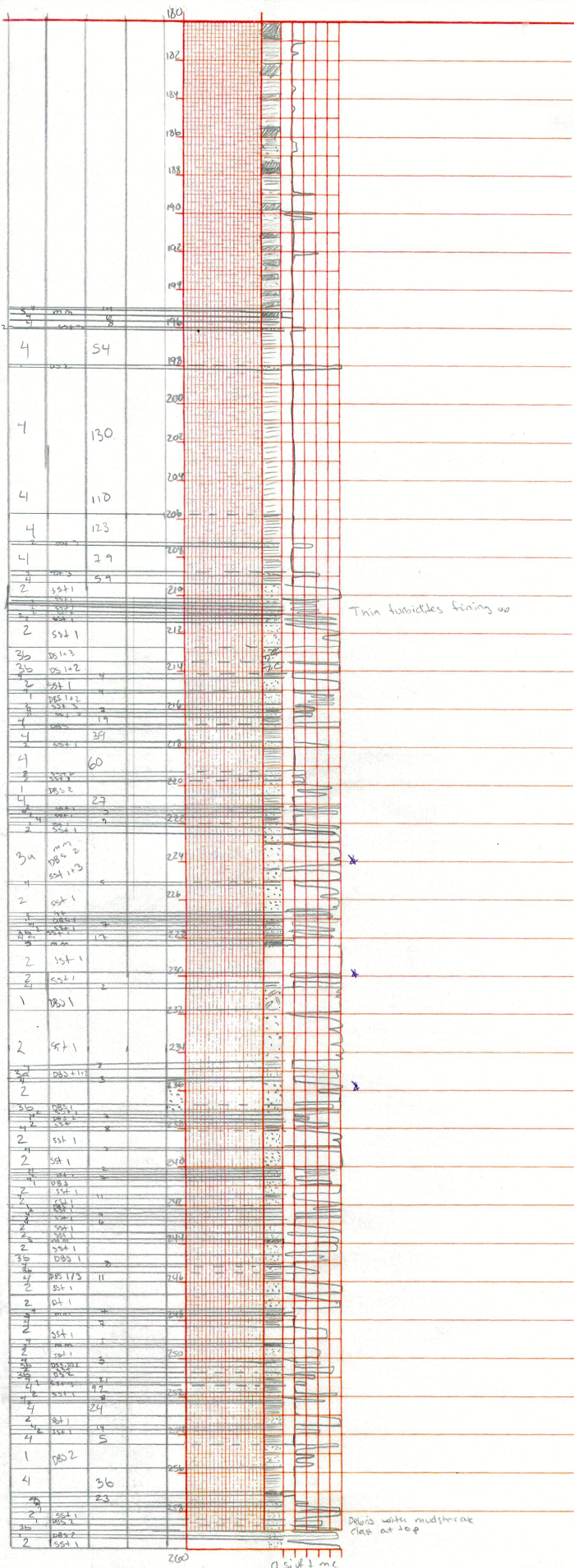
LOCATION 6611/09-U-02

SHEET NO. 2

DATE 28.05.18

SCALE 1:200

BY Karen M.L. Christensen



LOCATION 6611/09-U-02

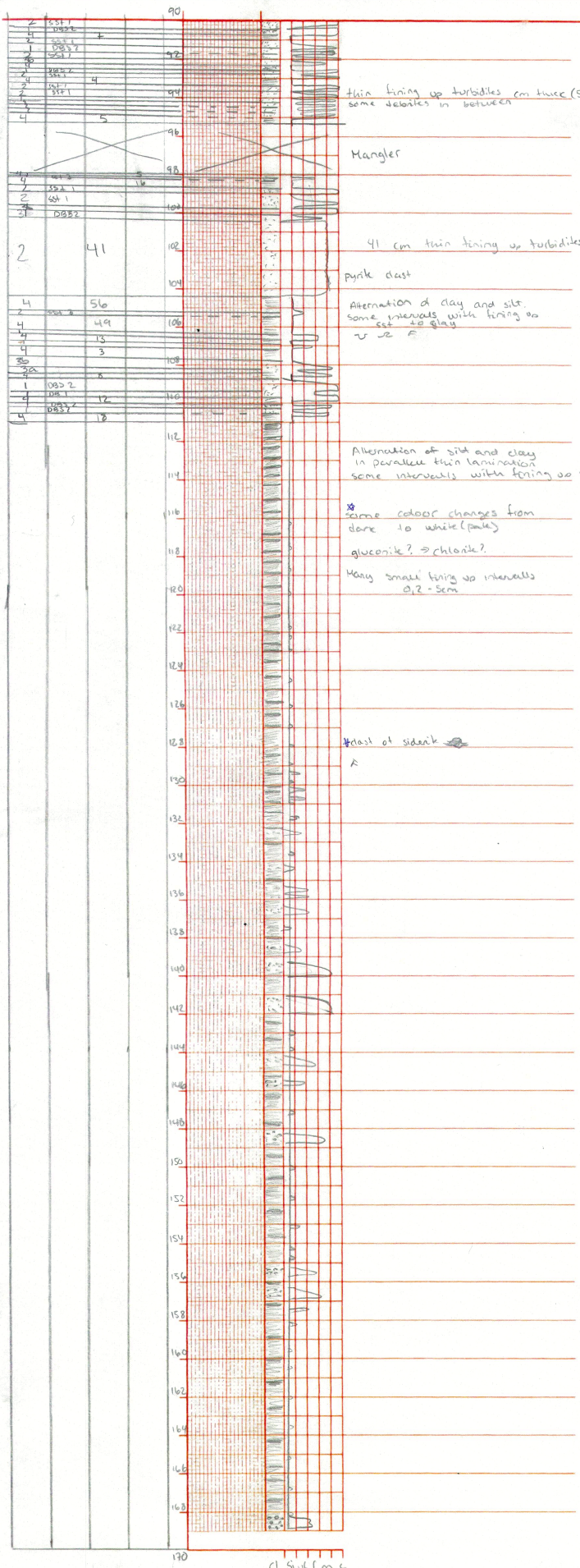
SHEET NO. 3

DATE 28.05.18

SCALE 1:200

BY Karen M.L. Christensen





thin lining up turbidites cm thick (5-10cm)  
some debrites in between

Mangler

41 cm thin lining up turbidites

pyrite dust

Alternation of clay and silt  
some intervals with lining up  
sst to clay

Alternation of silt and clay  
in parallel thin lamination  
some intervals with lining up sst

\* some colour changes from  
dark to white (pale)

glauconite? -> chlorite?

Many small lining up intervals  
0,2-5cm

thrust of siderite

170

172

174

176

178

180

182

184

186

188

190

192

194

196

198

200

202

204

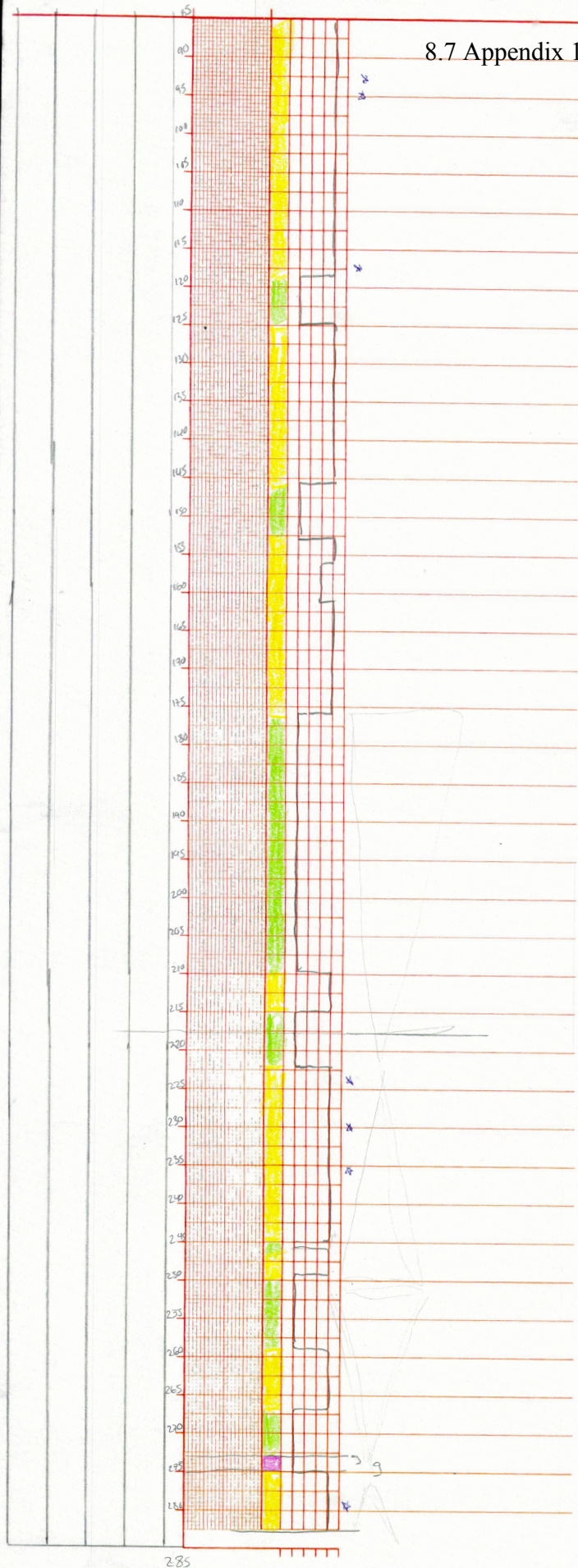
sand injectite?

thick turbidites lining up

Very unsorted conglomerate with large grains of quartz, some boulders up to 1.5cm  
fining and coarsening up



8.7 Appendix 1:500 Core 6611/09-U-02



LOCATION 6611/09-U-02

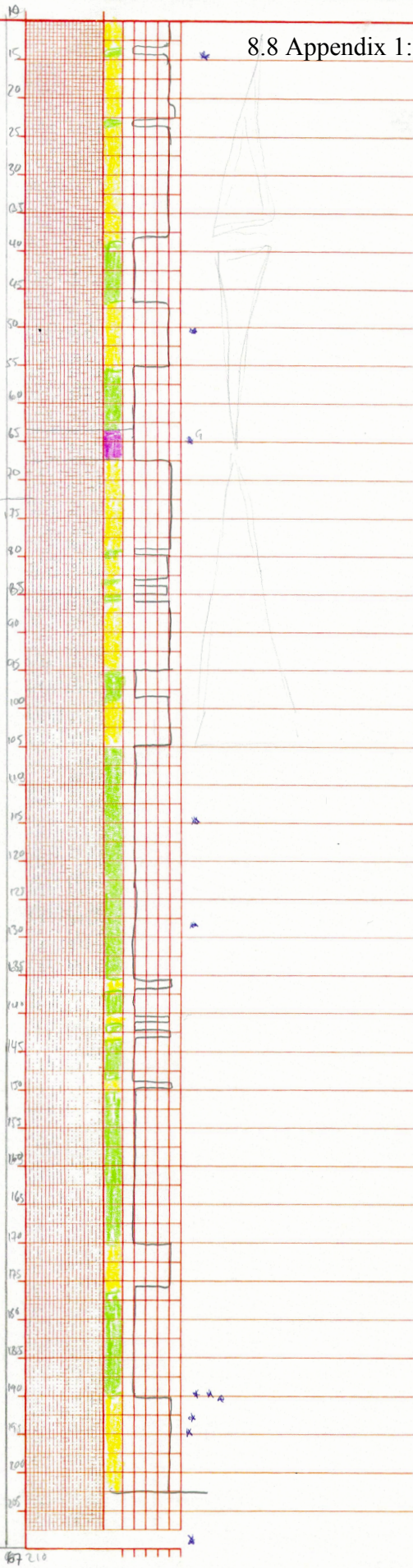
SHEET NO.

DATE

SCALE 1:500

BY Karen M.L. Christensen

8.8 Appendix 1:500 Core 6611/09-U-01



LOCATION 6611/09-U-01

SHEET NO.

DATE

SCALE 1:500

BY Karen M. L. Christensen